

DEVELOPMENT OF HIGH TEMPERATURE  
SILICONE ADHESIVE FORMULATIONS FOR  
THERMAL PROTECTION SYSTEM APPLICATIONS

NASA-CR-124389) DEVELOPMENT OF HIGH  
TEMPERATURE SILICONE ADHESIVE FORMULATIONS  
FOR THERMAL PROTECTION SYSTEM APPLICATIONS  
Final Report, 12 Jan. 1972 - (General  
Electric Co.)

N73-31533

CSSL 11A

G3/18

Unclas  
17921

117

General Electric Company  
Re-Entry and Environmental Systems Division  
P.O. Box 8555  
Philadelphia, Pennsylvania 19101

Final Report

May 1973



Prepared for the Marshall Space Flight Center  
NASA Contract Number NAS8-28113  
DCN 1-2-50-23534

**DEVELOPMENT OF HIGH TEMPERATURE  
SILICONE ADHESIVE FORMULATIONS FOR  
THERMAL PROTECTION SYSTEM APPLICATIONS**

General Electric Company  
Re-Entry and Environmental Systems Division  
P.O. Box 8555  
Philadelphia, Pennsylvania 19101

Final Report  
May 1973

Prepared By: *Ralph R. Hockridge*  
Ralph R. Hockridge  
Project Manager

Prepared for the Marshall Space Flight Center  
NASA Contract Number NAS8-28113  
DCN 1-2-50-23534

## TABLE OF CONTENTS

| Section |  | Page |
|---------|--|------|
| 1       | INTRODUCTION AND SUMMARY .....                     | 1-1  |
| 1.1     | Introduction .....                                 | 1-1  |
| 1.2     | Summary and Conclusions .....                      | 1-1  |
| 2       | ADHESIVE SYSTEM REQUIREMENTS (TASK 1) .....        | 2-1  |
| 2.1     | General .....                                      | 2-1  |
| 2.2     | Design .....                                       | 2-1  |
| 2.3     | Mechanical .....                                   | 2-3  |
| 2.4     | Weight .....                                       | 2-6  |
| 2.5     | Thermal .....                                      | 2-6  |
| 2.6     | References .....                                   | 2-7  |
| 3       | POLYMER RESEARCH AND DEVELOPMENT (TASK 2) .....    | 3-1  |
| 3.1     | Candidate Polymer/Adhesive Selection .....         | 3-1  |
| 3.1.1   | GE PD-200 (Base) .....                             | 3-1  |
| 3.1.2   | GE PD-200 .....                                    | 3-1  |
| 3.1.3   | PD-200 (Modified) .....                            | 3-3  |
| 3.2     | Evaluation of Candidate Commercial Materials ..... | 3-4  |
| 3.2.1   | Permacel ES-5168 Rubber Film .....                 | 3-4  |
| 3.2.2   | CHR R-10480 .....                                  | 3-5  |
| 3.2.3   | Raybestos-Manhattan Silicone Sponge .....          | 3-8  |
| 3.3     | Silicone Blends .....                              | 3-13 |
| 3.4     | Developmental Polymers .....                       | 3-13 |
| 3.5     | References .....                                   | 3-15 |
| 4       | ADVANCED ADHESIVE DEVELOPMENT (TASK 3) .....       | 4-1  |
| 4.1     | General .....                                      | 4-1  |
| 4.2     | Formulation Studies .....                          | 4-1  |
| 4.2.1   | Fybex® Fiber Addition .....                        | 4-1  |
| 4.2.2   | Nucleation Site Investigation .....                | 4-2  |
| 4.2.2.1 | Microballoons .....                                | 4-2  |
| 4.2.2.2 | Carbon Black .....                                 | 4-2  |
| 4.2.3   | Density Reduction of PD-200 .....                  | 4-9  |
| 4.2.4   | Post-Cure Evaluation of PD 200-16 .....            | 4-9  |
| 4.2.5   | Current Process Flow Plan .....                    | 4-15 |
| 4.3     | Mechanical Properties .....                        | 4-15 |
| 4.3.1   | Tension Tests .....                                | 4-16 |
| 4.3.1.1 | Experimental Procedure .....                       | 4-16 |
| 4.3.1.2 | Results and Discussion .....                       | 4-18 |
| 4.3.2   | Shear Tests .....                                  | 4-25 |
| 4.3.2.1 | Experimental Procedure .....                       | 4-25 |
| 4.3.2.2 | Results and Discussion .....                       | 4-25 |

## TABLE OF CONTENTS (Cont)

| Section |   | Page |
|---------|---|------|
|         | 4.3.3 Thermal Expansion .....   | 4-30 |
|         | 4.3.3.1 Experimental Procedure .....  | 4-30 |
|         | 4.3.3.2 Results and Discussion .....  | 4-30 |
|         | 4.3.4 Tensile-Stress Relaxation .....   | 4-30 |
| 4.4     | Thermal Properties .....  | 4-31 |
|         | 4.4.1 Thermal Conductivity .....  | 4-31 |
|         | 4.4.1.1 Mercury Intrusion Porosity<br>Measurements .....                        | 4-33 |
|         | 4.4.2 Specific Heat .....   | 4-34 |
|         | 4.4.3 TGA .....   | 4-34 |
|         | 4.4.4 Thermal Cycling (Low Temperature) .....                                   | 4-38 |
|         | 4.4.5 Effect of Long Term Cold Soak on Tensile<br>Properties of PD 200-16 ..... | 4-41 |
|         | 4.4.6 Arc Test .....  | 4-42 |
| 4.5     | Ceramic Adherends .....   | 4-44 |
| 4.6     | References .....  | 4-44 |
| 5       | APPLICATIONS DEVELOPMENT (TASK 4) .....   | 5-1  |
| 5.1     | General .....   | 5-1  |
| 5.2     | Primer Study .....  | 5-1  |
| 5.3     | Application Studies .....   | 5-2  |
|         | 5.3.1 Plane Surfaces .....  | 5-3  |
|         | 5.3.2 Simulated Air Frame .....   | 5-7  |
|         | 5.3.2.1 First Trial Series .....  | 5-8  |
|         | 5.3.2.2 Second Trial Bonding Series .....                                       | 5-11 |
|         | 5.3.2.3 Third Trial Bonding Series .....  | 5-11 |
|         | 5.3.2.4 Adhesive Applications-General<br>Procedure .....                        | 5-11 |
| 5.4     | Simulated Service Tests .....   | 5-14 |
| 5.5     | References .....  | 5-14 |
|         | Appendix A-1. ....  | A-1  |
|         | Appendix A-2. ....  | A-5  |
|         | Appendix A-3. ....  | A-11 |



# LIST OF ILLUSTRATIONS

| Figure |   | Page |
|--------|---|------|
| 2-1    | TPS Diagram Requirements . . . . .  | 2-2  |
| 2-2    | TPS Installation . . . . .  | 2-2  |
| 2-3    | Variation Of Bond Stress With Soak Temperature . . . . .                        | 2-4  |
| 2-4    | Bond Tensile Stress Histories . . . . .   | 2-4  |
| 2-5    | Area 1 Prototype Panel Temperature Histories . . . . .                          | 2-5  |
| 2-6    | Area 2 Prototype Panel Temperature Histories . . . . .                          | 2-6  |
| 2-7    | Bond Stress Distribution - Post Entry Maneuver/<br>Cool Down . . . . .          | 2-8  |
| 2-8    | Approximate Time Required To Soak To Maximum<br>Substrate Temperature . . . . . | 2-8  |
| 2-9    | REI-Bondline Soak-Out Effects . . . . .   | 2-9  |
| 3-1    | Effect of Varying PD 200-F28 Thickness, Area 2<br>Perturbed . . . . .           | 3-3  |
| 3-2    | Butt Tensile Specimens . . . . .  | 3-4  |
| 3-3    | Cohrlastic R-10480, Cross-Section, 4.5X . . . . .                               | 3-6  |
| 3-4    | Cohrlastic R-10480, Cross-Section, 10X . . . . .                                | 3-6  |
| 3-5    | Cohrlastic R-10480, As Cut From Panel . . . . .                                 | 3-7  |
| 3-6    | Cohrlastic R-10480, After Reduced Pressure . . . . .                            | 3-7  |
| 3-7    | Raybestos-Manhattan RL-2822, Cross-Section, 10X . . . . .                       | 3-8  |
| 3-8    | Raybestos-Manhattan RL-1973, Cross-Section, 10X . . . . .                       | 3-9  |
| 3-9    | Raybestos-Manhattan RL-1973, As Cut From Panel . . . . .                        | 3-10 |
| 3-10   | Raybestos-Manhattan RL-1973, After Reduced Pressure. . . . .                    | 3-11 |
| 3-11   | Raybestos-Manhattan RL-2822, As Cut From Panel . . . . .                        | 3-11 |
| 3-12   | Raybestos-Manhattan RL-2822, After Reduced Pressure. . . . .                    | 3-12 |
| 3-13   | PD 200-16 Comparison Specimen . . . . .   | 3-12 |
| 3-14   | Dimensional Stability of Strain Isolator Materials . . . . .                    | 3-13 |
| 3-15   | Compressive Modulus of Modified RTV 630. . . . .                                | 3-14 |
| 4-1    | PD-200 Modified With 3.5% Titanate Fibers, Cross-Section,<br>10X . . . . .      | 4-3  |
| 4-2    | PD-200 Modified With 3.5% Titanate Fibers, Cross-Section,<br>4.5X . . . . .     | 4-3  |
| 4-3    | PD-200, Cross-Section, 10X . . . . .  | 4-4  |
| 4-4    | PD-200, Cross-Section, 4.5X . . . . .   | 4-4  |
| 4-5    | PD-200 Modified With 5% Microballoons, Cross-Section,<br>4.5X . . . . .         | 4-5  |
| 4-6    | PD-200 Modified With 5% Microballoons, Cross-Section,<br>10X . . . . .          | 4-5  |
| 4-7    | PD-200 Modified With 5% Microballoons, Cross-Section,<br>22X . . . . .          | 4-6  |
| 4-8    | PD-200 Modified With 5% Microballoons, Cross-Section,<br>4.5X . . . . .         | 4-6  |
| 4-9    | PD-200 Modified with 5% Microballons, Cross-Section<br>10X . . . . .            | 4-7  |

## LIST OF ILLUSTRATIONS (Cont)

| Figure |  | Page |
|--------|--|------|
| 4-10   | PD-200 Modified With 5% Microballoons, Cross-Section, 22X . . . . .                        | 4-7  |
| 4-11   | PD-200 (Modified), Cross-Section, 4.5X . . . . .   | 4-10 |
| 4-12   | PD-200 (Modified), Cross-Section, 10X . . . . .  | 4-10 |
| 4-13   | PD-200 (Modified), Cross-Section, 4.5X . . . . .   | 4-11 |
| 4-14   | PD-200 (Modified), Cross-Section, 10X . . . . .  | 4-11 |
| 4-15   | PD-200 Mod (Lot 618) Shrinkage vs Post-Cure Temp. . . . .                                  | 4-12 |
| 4-16   | PD-200 Mod Post-Cure Temperature vs Density Change (Lot 618) . . . . .                     | 4-12 |
| 4-17   | Room Temperature Tensile Strength PD-200 (Mod) vs Post-Cure Temperature . . . . .          | 4-15 |
| 4-18   | PD-200 Manufacture Flow Plan . . . . .   | 4-16 |
| 4-19   | Tensile Specimen PD-200-16 . . . . .   | 4-17 |
| 4-20   | Tensile Stress-Strain Behavior For PD 200-16 (XY Direction) at 116°K . . . . .             | 4-19 |
| 4-21   | Tensile Stress-Strain Behavior For PD 200-16 (Z Direction) at 116°K . . . . .              | 4-19 |
| 4-22   | Tensile Stress-Strain Behavior For PD 200-16 (XY Direction) at 178°K . . . . .             | 4-20 |
| 4-23   | Tensile Stress-Strain Behavior For PD 200-16 (Z Direction) at 178°K . . . . .              | 4-20 |
| 4-24   | Tensile Stress-Strain Behavior For PD 200-16 (XY Direction) at 297°K . . . . .             | 4-21 |
| 4-25   | Tensile Stress-Strain Behavior For PD 200-16 (Z Direction) at 297°K . . . . .              | 4-21 |
| 4-26   | Tensile Stress-Strain Behavior For PD 200-16 (XY Direction) at 478°K . . . . .             | 4-22 |
| 4-27   | Tensile Stress-Strain Behavior For PD 200-16 (Z Direction) at 478°K . . . . .              | 4-22 |
| 4-28   | Tensile Stress-Strain Behavior For PD 200-16 (XY Direction) at 589°K . . . . .             | 4-23 |
| 4-29   | Tensile Stress-Strain Behavior For PD 200-16 (Z Direction) at 589°K . . . . .              | 4-23 |
| 4-30   | Tensile Strength of PD 200-16 . . . . .  | 4-24 |
| 4-31   | Initial Tensile Modulus of PD 200-16 . . . . .   | 4-24 |
| 4-32   | Shear Deformation Measurement Scheme . . . . .   | 4-26 |
| 4-33   | Torsional Shear Specimen, Post Test . . . . .  | 4-27 |
| 4-34   | Shear Strength of PD 200-16 . . . . .  | 4-27 |
| 4-35   | Shear Stress-Strain Curves For PD 200-16 at 116°K . . . . .                                | 4-28 |
| 4-36   | Typical Shear Stress-Strain Behavior Of PD 200-16 From Glass Transition to 589°K . . . . . | 4-28 |

# LIST OF ILLUSTRATIONS (Cont)

| Figure |   | Page |
|--------|---|------|
| 4-37   | Thermal Expansion of PD 200-16 . . . . .                                      | 4-31 |
| 4-38   | Thermal Conductivity of PD 200-16 . . . . .                                   | 4-33 |
| 4-39   | Pressure Dependence Of The Thermal Conductivity Of<br>PD 200-16 . . . . .     | 4-34 |
| 4-40   | Macro-Porosimeter Test, Lot #622 Untested . . . . .                           | 4-36 |
| 4-41   | Macro-Porosimeter Test, Lot #622 Tested . . . . .                             | 4-37 |
| 4-42   | Macro-Porosimeter Test, Lot #602 . . . . .                                    | 4-38 |
| 4-43   | Pore Size Vs Percent Pore Distribution . . . . .                              | 4-39 |
| 4-44   | Specific Heat Of PD-200 . . . . .   | 4-40 |
| 4-45   | Thermogravimetric Analysis Of PD 200 Cured At<br>450°K For 15 Hours . . . . . | 4-42 |
| 4-46   | PD 200-16 Arc Test . . . . .  | 4-46 |
| 4-47   | Typical Failed Specimens . . . . .  | 4-47 |
| 5-1    | Lap Shear Configuration . . . . .   | 5-2  |
| 5-2    | Simulated Airframe . . . . .  | 5-8  |
| 5-3    | Series 1 Rivet Head Bonding . . . . .   | 5-10 |
| 5-4    | Series 2 Rivet Head Bonding . . . . .   | 5-12 |
| 5-5    | Series 3 Rivet Head Bonding . . . . .   | 5-13 |
| 5-6    | Simulated Structure . . . . .   | 5-15 |
| 5-7    | Adhesive Application To Rivet Heads . . . . .                                 | 5-15 |
| 5-8    | Adhesive Application . . . . .  | 5-16 |
| 5-9    | Applied Adhesive, Showing "Texture" Finish . . . . .                          | 5-16 |
| 5-10   | PD 200 Foam Applied To Adhesive . . . . .                                     | 5-17 |
| 5-11   | Application Of Vacuum "Bleeder" Material . . . . .                            | 5-17 |
| 5-12   | Completed Vacuum Bag Assembly . . . . .                                       | 5-18 |
| 5-13   | REI/PD 200 Bonding Flow Plan . . . . .  | 5-18 |
| 5-14   | RSI Tensile Test Model . . . . .  | 5-19 |
| A-1.1  | Ultimate Strength Of PD-200 (Base) . . . . .                                  | A-3  |
| A-1.2  | Elastic Moduli Of PD-200 (Base) . . . . .                                     | A-3  |
| A-1.3  | TGA Analysis of PD-200 (Base) . . . . .                                       | A-3  |
| A-1.4  | Thermal Conductivity of PD-200 (Base) . . . . .                               | A-3  |
| A-2.1  | Tensile Strength of PD-200 . . . . .  | A-4  |
| A-2.2  | Shear Strength of PD-200 . . . . .  | A-6  |
| A-2.3  | Tensile Modulus of PD-200 . . . . .   | A-6  |
| A-2.4  | Shear Modulus of PD-200 . . . . .   | A-7  |
| A-2.5  | Low Temperature Modulus of PD-200 . . . . .                                   | A-7  |
| A-2.6  | TGA of PD-200 . . . . .   | A-8  |
| A-2.7  | Specific Heat of PD-200 . . . . .   | A-8  |
| A-2.8  | Thermal Conductivity of PD-200 . . . . .                                      | A-9  |
| A-2.9  | Thermal Expansion of PD-200 . . . . .   | A-9  |

## LIST OF TABLES

| Table |   | Page |
|-------|---|------|
| 3-1   | RTV Silicone Adhesive Candidates . . . . .  | 3-2  |
| 4-1   | Room Temperature Tensile Properties of PD-200<br>(Mod) Foam . . . . .                                   | 4-8  |
| 4-2   | Foam Density Evaluation . . . . .   | 4-13 |
| 4-3   | PD-200 Density Data . . . . .   | 4-14 |
| 4-4   | Torsional Shear Test Data For PD 200-16 . . . . .   | 4-29 |
| 4-5   | Summary of Stress Relaxation Data on PD 200-16 . . . . .  | 4-31 |
| 4-6   | Calculated Pore Distribution For Samples of<br>PD 200 . . . . .   | 4-41 |
| 4-7   | Tension Test Results on PD 200-16 Specimens<br>Tested at Various Temperatures and Conditions . . . . .  | 4-44 |
| 4-8   | Experimental Matrix For Evaluation of Selected<br>Adhesive System . . . . .                             | 4-46 |
| 4-9   | Butt Tensile Test Results . . . . .   | 4-47 |
| 5-1   | Qualitative Bond Results, SS-4155 Primer . . . . .  | 5-3  |
| 5-2   | Aluminum/PD-200/Aluminum Lap Shear Data . . . . .   | 5-4  |
| 5-3   | Titanium/PD-200/Titanium Lap Shear Data . . . . .   | 5-5  |
| 5-4   | Weight Pick-Up, PD-200 (0.37 gm/cc, 23 pcf) . . . . .   | 5-9  |
| A-2.1 | Room Temperature Lap Shear Strength of PD-200<br>Adhesive After 16 Hour Thermal Soak Exposures. . . . . | A-10 |

## FORWARD

This final report was prepared by the General Electric Company, Re-Entry and Environmental Systems Division (GE-RESD) for NASA/MSFC contract NAS8-28113, "Development of High Temperature Silicone Adhesive Formulations for Thermal Protection System Applications" Program. This work was performed under the direction of the Astronautics Laboratory with Dr. W. E. Hill as the Contracting Officer's Representative.

This report covers the work conducted from January 12, 1972, through March 12, 1973, at RESD's Materials and Structures Laboratory under the management of Mr. V. N. Saffire. Dr. A. A. Hiltz acted as Project Manager from January 12, 1972, through April 1, 1972, and provided consultation services throughout the program. Mr. R. R. Hockridge acted as Project Manager from April 1, 1972, and compiled the Final Report.

This report is arranged in accordance with the major Tasks performed under this contract. Where appropriate, other contract and GE-RESD funded work is included and identified as such.

The author wishes to acknowledge the contributions of the following individuals who were responsible for performing program tasks, and in the preparation of data for this final report: F. Curtis, Dr. A. Hiltz, J. Kreitz, and H. Thibault (Composites and Plastics Laboratory), K. Bleiler, J. Brazel, J. Konell and D. Lowe (Materials Performance Laboratory), W. Staley (Metallurgy and Ceramics Laboratory), and B. Zabolski (Manufacturing Engineering). Lastly, the assistance of Mrs. D. Larson in typing, copying and collating is gratefully acknowledged.

## NOMENCLATURE

|                         |   |
|-------------------------|---|
| Adhesive Failure        | Failure of the Adhesive at the Adhesive/substrate Interface                       |
| B-Staged                | An Intermediate Stage in the Process of Conversion of a Resin to a Solid Material |
| Cohesive Failure        | Failure by Cleavage Within the Adhesive Mass                                      |
| $\delta$                | Strain ( $\Delta L/L$ )   |
| E                       | Initial Tangent Modulus of Elasticity   |
| $E_C$                   | Compressive Modulus   |
| $E_S$                   | Secant Tensile Modulus at Failure   |
| $\epsilon_u$            | Ultimate Elongation   |
| ESM                     | General Electric Elastomeric Shield Material                                      |
| FS                      | Factor of Safety  |
| $G_I$                   | Initial Tangent Shear Modulus   |
| $G_S$                   | Secant Shear Modulus at Failure   |
| $\Delta L$              | Change in Length (Deformation)  |
| LVDT                    | Linear Variable Differential Transformer  |
| Nuocure 28 <sup>®</sup> | Tin Octoate, Tenneco Chemicals Inc., Nuodex Division                              |
| pcf                     | Pounds per cubic foot   |
| PPH                     | Parts per Hundred   |
| $\sigma_u$              | Ultimate Strength   |
| $\rho$                  | Density   |
| REI                     | General Electric Reusable External Insulation                                     |
| RIC                     | Rockwell International Corporation  |
| RH                      | Relative Humidity   |
| RSI                     | Reusable Surface Insulation   |
| RTV                     | Room Temperature Vulcanizing Silicone Rubber                                      |
| SNAP-27                 | Space Nuclear Auxiliary Power Unit  |
| SPBD                    | General Electric Silicone Products Business Department                            |
| $\tau_u$                | Ultimate Shear Stress   |

## NOMENCLATURE (Cont.)

|              |   |
|--------------|---|
| $T_g$        | Glass Transition Temperature              |
| T-12         | Dibutyl tin dilaurate, M&T Chemical Corp. |
| TGA          | Thermogravimetric Analysis                |
| TPS          | Thermal Protection System                 |
| $\bar{X}$    | Average Value                             |
| XY Direction | In-Plane Direction                        |
| Z Direction  | Through-The-Thickness                     |

## **SECTION 1**

### **INTRODUCTION AND SUMMARY**

#### **1.1 INTRODUCTION**

This final report describes the work performed on NASA Contract NAS 8-28113, "Development of High Temperature Silicone Adhesive Formulations for Thermal Protection Systems Applications". The overall objectives of this program have been to (1) identify adhesives suitable for attachment of light-weight ceramic insulations to rigid substrates for Space Shuttle RSI (reusable surface insulation) application, (2) conduct polymer research and development studies to select and evaluate candidate commercially available silicone polymer systems, (3) formulate and/or modify the silicone polymers as adhesive systems and conduct property evaluation tests over the temperature range 200° K to 616° K (-100°F to +650°F) on metallic and ceramic adherends, and (4) conduct fabrication studies utilizing the best system from the earlier phases of the program, and conduct thermal tests simulating the service life of the vehicle.

In meeting the objectives of the program, GE-RESD has conducted trade-off studies and screening evaluations of commercial polymers and silicone foam sheet stock, and has developed a low modulus, low density 0.26 gm/cc (16 pcf) modification of the GE-RESD PD-200 based upon GE RTV-560 silicone polymer.

The PD-200-16 elastomeric bond system modification was developed, initially characterized for mechanical and thermal properties, evaluated for application methods, and capability as a strain arrestor bond system demonstrated as a part of this contract.

#### **1.2 SUMMARY AND CONCLUSIONS**

The following is a summary of the major conclusions reached on this program.

1. Silicone polymers are required to meet the high and low temperature extremes of the Shuttle mission.
2. Open-cell low modulus foams are necessary to provide attachment dimensional stability during Shuttle mission pressure fluctuations.
3. GE-RESD PD200-16 has been demonstrated as an effective strain isolation system at 116°K (-250°F), a level lower than the contract requirement of 200°K (-100°F).



## SECTION 2

### ADHESIVE SYSTEM REQUIREMENTS (TASK 1)

#### 2.1 GENERAL

It must be noted that as a result of the time period for inception of this contract, the primary ceramic insulation under consideration was based upon Mullite ( $3\text{Al}_2\text{O}_3 \cdot 2\text{SiO}_2$ ), and the design requirements were established for that material. However, with the recent shift in emphasis from Mullite to Silica, the ceramic adherend tests were conducted utilizing GE-RESD Silica RSI.

The work performed under this contract was based upon the point design conditions specified by NASA/Manned Spacecraft Center (MSC) and defined in detail in the General Electric report "Requirements", 26 August 1971. The summarized requirements are shown below.

The thermal protection system shall be capable of meeting the performance requirements during and following exposure to environments of ground handling, storage, lift-off and orbital insertion, on-orbit, entry and landing. This will include conditions of pressure, humidity, rain, salt spray, thermal gradient, acoustics and vibration (Figure 2-1).

#### 2.2 DESIGN

Typical shuttle vehicle areas that may be covered with a reusable ceramic insulation include leading edges, nose caps, windward body sections, wings, fins, and control surfaces. The maximum surface temperature requirements for each of these areas defines the applicable insulative material system to be used, and allowable primary structure or mounting panel temperatures will establish the required insulation thickness.

The primary structure arrangements for these various regions of the vehicle can include monocoque and semi-monocoque constructions with the RSI integrally attached.

In the integral panel concept (Figure 2-2), the insulation is bonded directly to the primary air frame structure, and all of the air loads are transmitted directly to this structure. Adhesive bonding makes direct attachment to the primary structure the most efficient approach.

During the Space Shuttle mission lifetime the bond system will be subjected to a variety of structural and thermostructural loading conditions ranging from orbital cold soak at temperatures near or below the glass transition to post entry cooldown during which the bond soaks out to temperatures near its maximum use temperature. Although the use

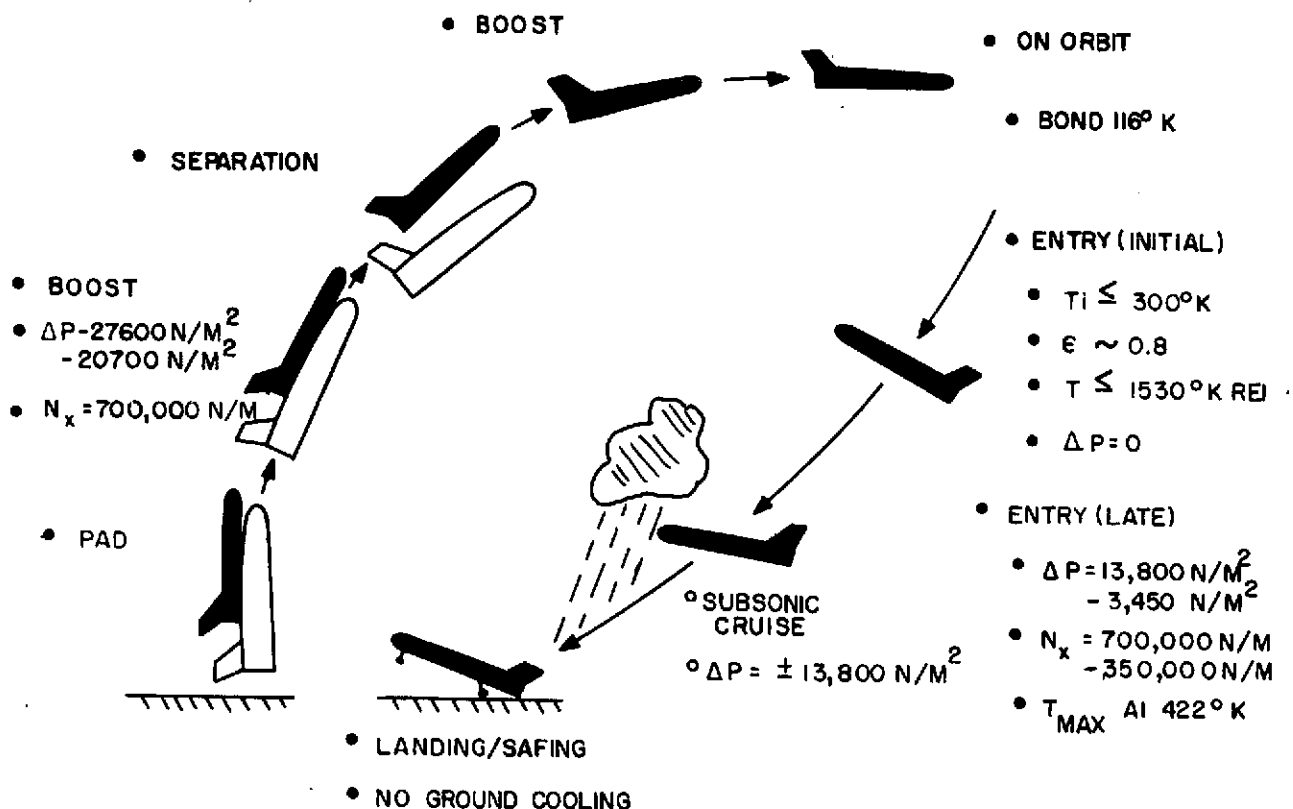


Figure 2-1. TPS Diagram Requirements

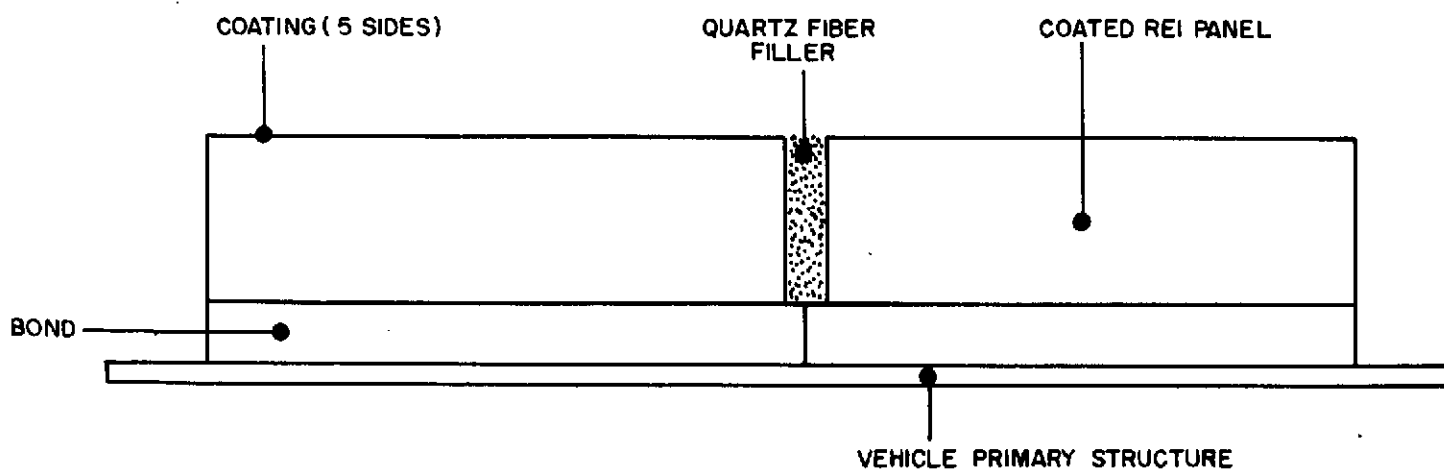


Figure 2-2. TPS Installation

of mechanical attachment systems and partial bond systems offers certain structural advantages, and possible advantages in REI tile venting, continuous bonding is still the most reliable and dependable system for attaching the coated REI tile to the structural substrate.

## 2.3 MECHANICAL

The first potentially critical condition for the bond system is orbital cold soak. If the design temperature is less than 161°K (-170°F), it is likely that glass transition will be encountered in silicone polymer bond systems. This transition is accompanied by a rapid increase in the tensile and shear stresses in both the bond and the REI, stresses which could exceed the strength capability of these materials. After this hardening takes place and the soak temperature further decreases below 161°K (-170°F) the rate of change of bond stress decreases. Analyses indicate that the REI is slightly more critical than the bond in the above situation, although it is the hardening of the bond which induces stresses in the REI.

For a typical 508 mm (20") tile continuously bonded to a primary structure panel, Figure 2-3 shows the change in bond stresses with cold soak temperature. For smaller tiles it is reasonable to expect that the situation would be less severe. This figure demonstrates the need for (a) making the glass transition temperature as low as possible or (b) making the low temperature bond strength high enough to accommodate the increase in strength.

As was previously indicated, use of essentially continuous attachment is deemed necessary for RSI due to the limited strength and strain capability of these high temperature ceramic materials. This precludes the use of individual mechanical attachments and requires the use of a soft foam pad material for strain isolation as part of the attachment system.

Typical tensile stresses that will develop in the foam bond material system, due to the thermal gradients resulting from entry heating, are shown in Figure 2-4 as a function of time for several heating rates representative of a typical cross range orbiter. It may be noted from Figure 2-4, that the required strength is relatively low. However, the maximum stresses occur at a time period in the mission after the temperature has peaked (Figure 2-5).

A number of material properties are important in the design of an RSI thermal insulation system. Several of these properties are critical. They are:

1. Ultimate strength in tension and shear
2. Modulus of elasticity
3. Thermal expansion

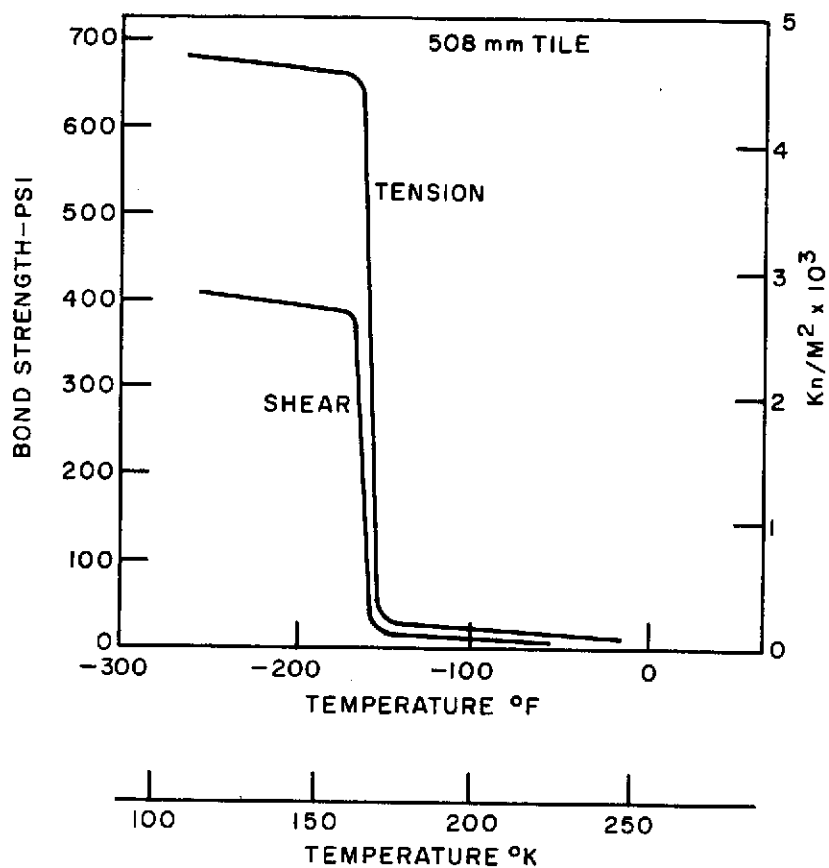


Figure 2-3. Variation of Bond Stress With Soak Temperature

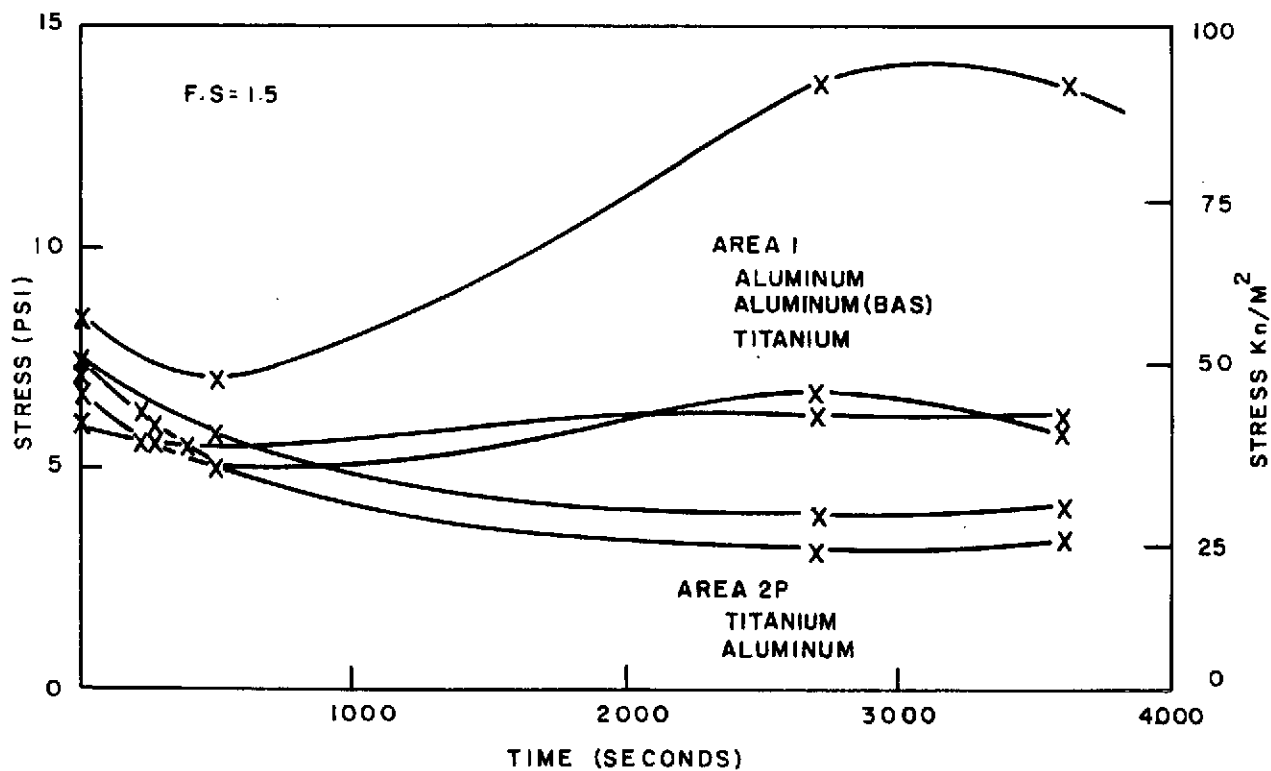


Figure 2-4. Bond Tensile Stress Histories

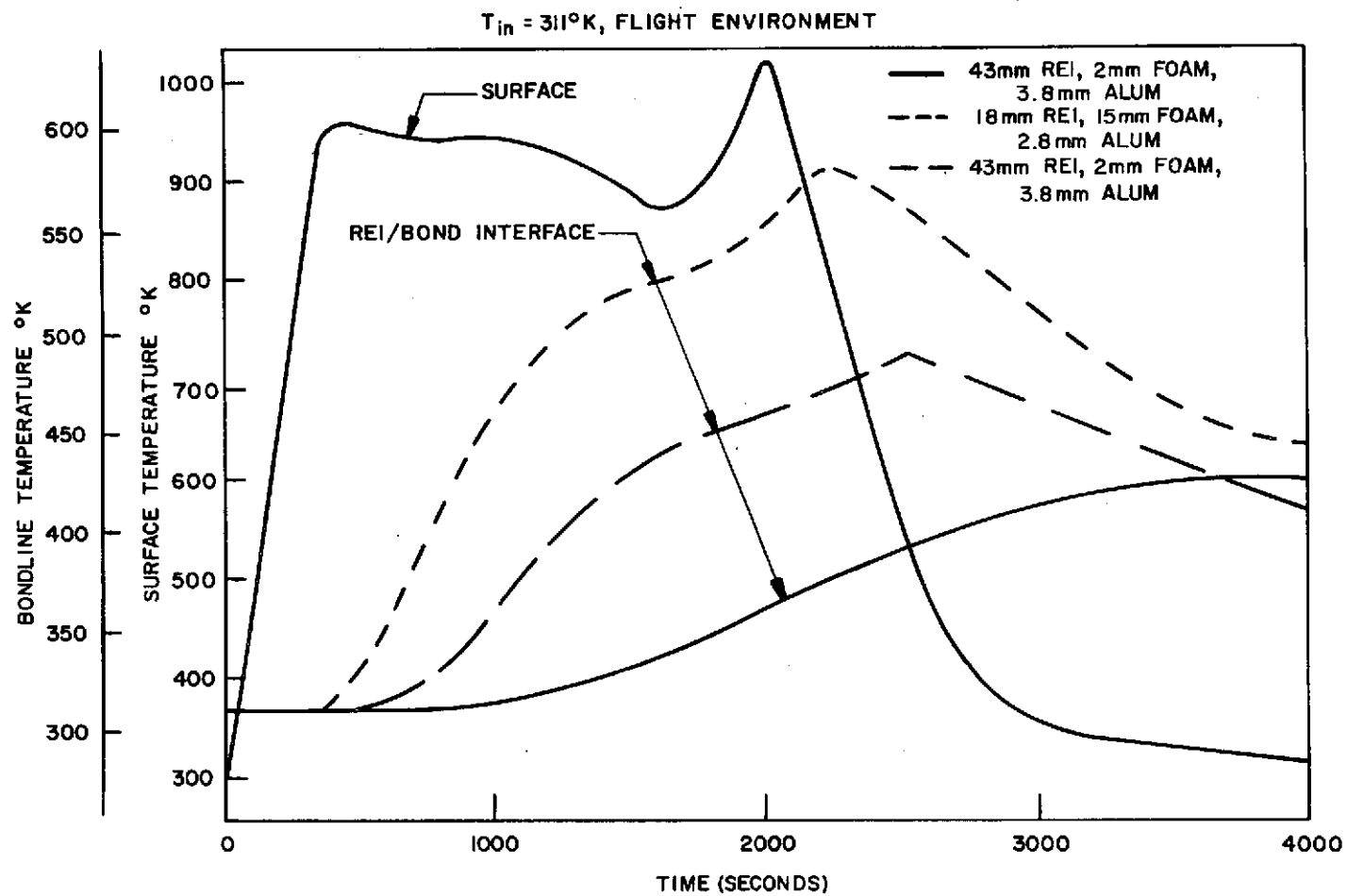


Figure 2-5. Area 1 Prototype Panel Temperature Histories

## 2.4 WEIGHT

The requirements for bond low shear stiffness result in a bondline thickness of at least 1.78 mm (0.070"). The densities of typical candidate adhesive systems range from about 1.06-1.44 gm/cc (66 to 90 lb/ft<sup>3</sup>) which at a bondline thickness of 1.78 mm (0.070") translate into a bond weight of 1.88-2.56 kg/m<sup>2</sup> (0.385 to 0.525 lb/ft<sup>2</sup>). Reduction of the bond weight, since the bondline thickness is relatively fixed, can best be achieved by reducing its density. Fortunately, this is also the direction desired for reducing the shear stiffness of the bond. However, a decrease in density will also decrease the strength of the bond. Accordingly, a trade-off is required between bond strength and bond density for the application.

## 2.5 THERMAL

The adhesive system must be capable of performing its intended function for 100 missions at the maximum normal entry design bondline temperatures without excessive thermal degradation or change in properties. These temperatures are 450°K (350°F) for an aluminum structure and 616°K (650°F) for titanium, with a factor of safety. In addition, the system must be compatible with the 116°K (-250°F) temperature experienced during orbital stay. Figures 2-5 and 2-6 show typical area 1 and 2P temperature histories for various combinations of REI tile and bond thickness.

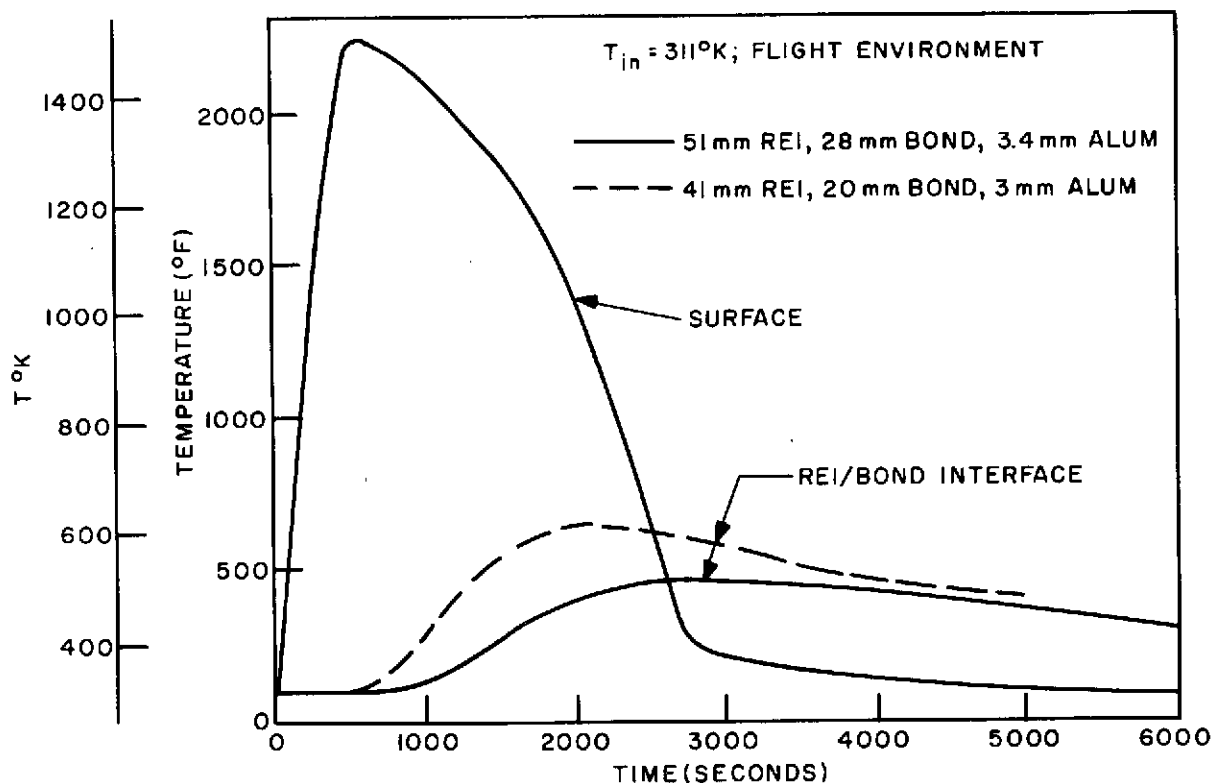


Figure 2-6. Area 2P Prototype Panel Temperature Histories

Area 1 and area 2P are NASA/MSC point design designations representing two extremes of shuttle heating for RSI applications. Area 1 is representative of heating which produces surface temperatures of 1033°K (1400°F) and in area 2P surface temperatures of 1533°K (2300°F) are reached.

A most important factor to consider with regard to the case of orbital soaks below the glass transition temperature of the bond is that due to its flexibility, the bond acts as a strain isolator for the coated REI tile during critical times of entry heat-up. Thermodynamic analysis indicates that at these critical times, which are on the order of 300 to 600 seconds, the bond is still at its orbital soak temperature, not having had time to warm up. If the bond soaks below its glass transition temperature and is still in this hardened state at the critical heat-up times, it will no longer provide strain isolation to the REI tile, and can induce a new set of more severe requirements on the REI and the coating.

During entry, moderately high tensile and shear stresses of approximately equal magnitude are developed due to thermal gradients. A more severe condition for the bond, however, occurs in post entry. Both tensile loads in the structure and cool-down gradients cause high bond stresses at the edge of the tile, as shown in Figure 2-7. The bond soak-out can occur during the later portion of flight or in fact after landing depending on vehicle location and REI thickness. This is shown on Figure 2-8. This means that maximum tensile loading in the substructure can induce maximum bond stress requirements at bond temperatures ranging from 589°K (600°F) down to approximately 200°K (-100°F). In addition, the local pressure at these times is about one atmosphere, as is shown in Figure 2-9. Also shown are typical times above 533°K (500°F) and 589°K (600°F) for a typical Shuttle mission.

## 2.6 REFERENCES

D. J. Tillian, NASA. Houston memo to R. J. Michalak as transmitted by R. J. Michalak, "MSC Point Design Requirements for Orbiter TPS", PIR 9136-EYP-062, July 27, 1971.

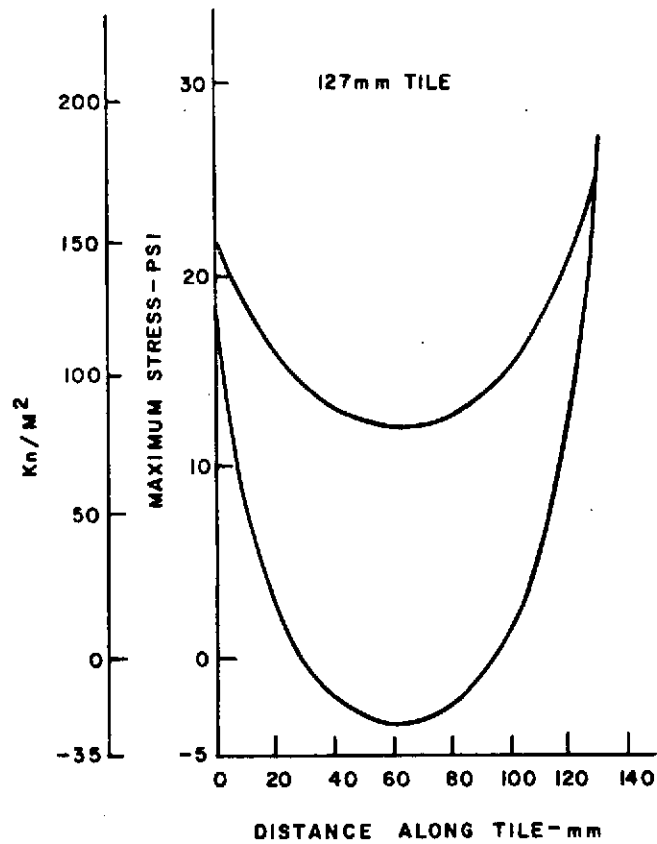


Figure 2-7. Bond Stress Distribution - Post Entry Maneuver/ Cool Down

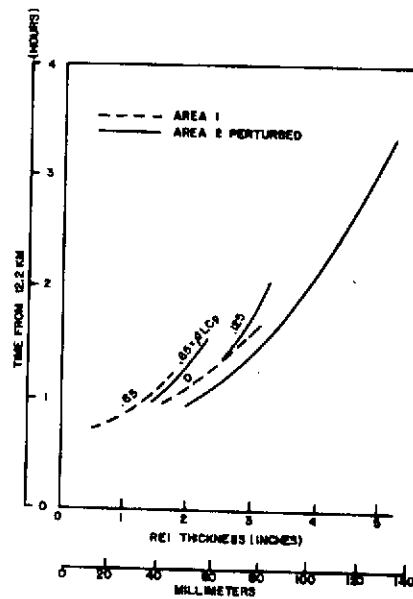


Figure 2-8. Approximate Time Required to Soak to Maximum Substrate Temperature



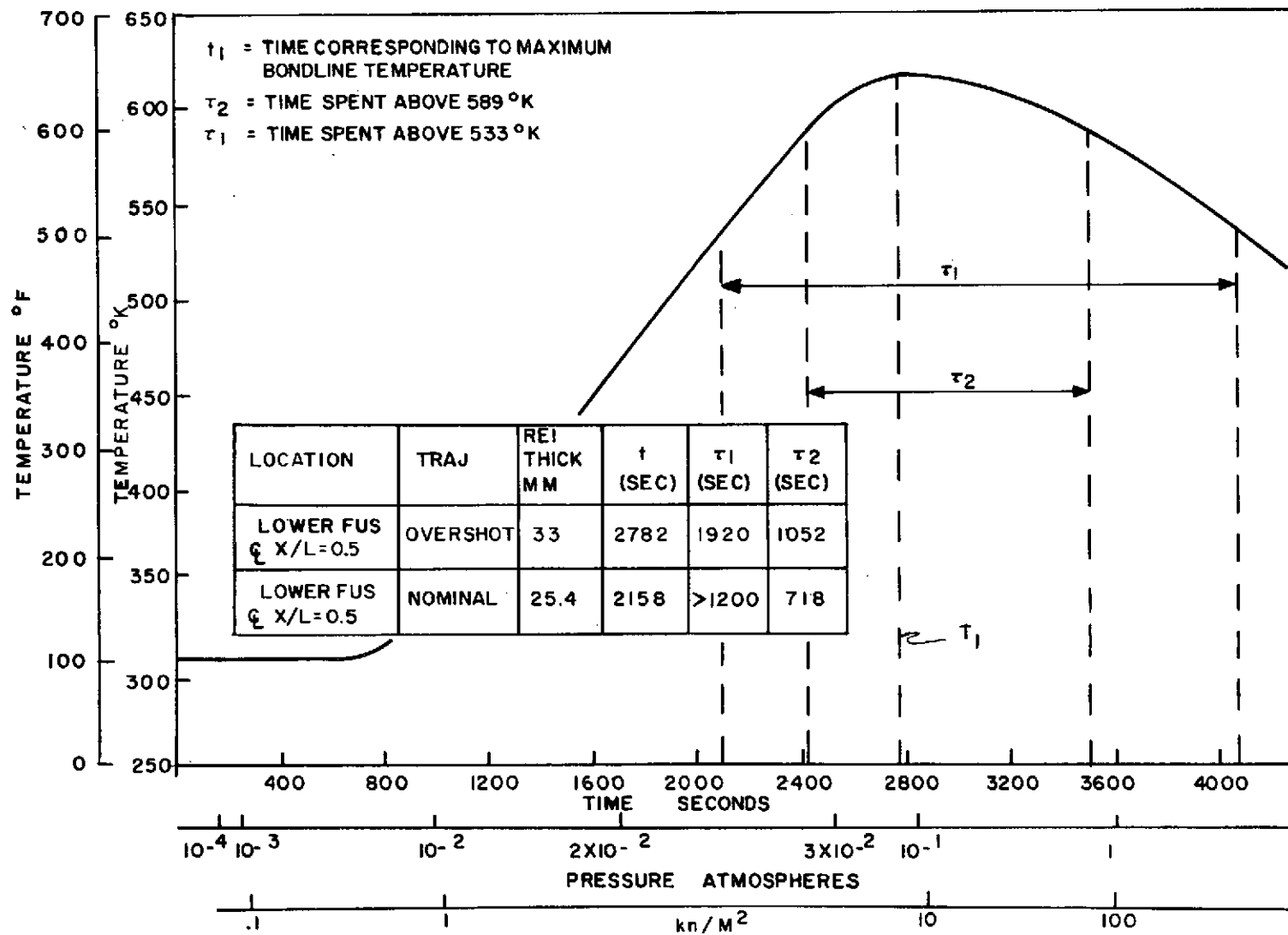


Figure 2-9. REI-Bondline Soak-Out Effects

## SECTION 3

### POLYMER RESEARCH AND DEVELOPMENT (TASK 2)

#### 3.1 CANDIDATE POLYMER/ADHESIVE SELECTION

Analysis of the requirements for the RSI attachment indicate the most probable application method to be by adhesive bonding. As indicated, the use of a high shear stiffness adhesive induces high shear stress concentrations at the interface between the surface insulation and the structure, and, as a result, imposes unnecessarily high strength requirements on the bond and RSI. The use of a finite thickness flexible adhesive, on the other hand, results in the attenuation of stress concentrations and in a reduction of the shear stress requirements for both the adhesive and the insulation.

Careful evaluation of the available commercial flexible materials with capability of meeting all the requirements led to the selection of the room temperature vulcanizing silicone rubbers (RTV). The following were selected for further consideration and evaluation from the prime candidate systems indicated in Table 3-1, in great measure, on low temperature capability, and are based upon GE RTV-560 silicone rubber which was the only material identified to meet both the high and low temperature requirements.

##### 3.1.1 GE PD-200 (BASE)

PD-200 (Base) is a solid methyl-phenyl silicone which can be cured to a strong rubbery state at room temperature with tin soap catalysts such as T-12 or Nuocure 28. It cures by a condensation mechanism with the elimination of volatile by-products. Venting is necessary to achieve cure in the inner portions of large bonded areas of non-porous materials. The properties of PD-200 (Base) are listed in Appendix A-1.

##### 3.1.2 GE PD-200

PD-200 is an open cell, methyl-phenyl silicone foam exhibiting an extremely fine cell structure which is uniformly distributed. It is formulated and chemically blown at ambient temperature and pressure utilizing open pan type molds. Initial foaming and cure requires one hour. At this point the foamed bun is slit to remove the surface skins, then step wise post-cured to 450°K (350°F) over a 26 hour period to stabilize weight and dimensions. Upon completion of post cure, the foam is slit to design thickness using commercial rubber slitting equipment. The properties of PD-200 are listed in Appendix A-2.

TABLE 3-1. RTV SILICONE ADHESIVE CANDIDATES

| Compound  | Chemical Type                | Polymerization Mechanism | Glass Transition Temperature |      | Strength | Decomposition Temperature |
|-----------|------------------------------|--------------------------|------------------------------|------|----------|---------------------------|
|           |                              |                          | °K                           | °F   |          |                           |
| RTV 630   | Methyl Vinyl Silicone        | Addition                 | 211                          | -80  | High     | High                      |
| PD-195    | Methyl Phenyl Vinyl Silicone | Addition                 | 155                          | -180 | High     | High                      |
| RTV 560   | Methyl Phenyl Silicone       | Condensation             | 155                          | -180 | Lower    | Lower                     |
| RTV 511   | Methyl Phenyl Silicone       | Condensation             | 155                          | -180 | Lower    | Lower                     |
| RTV 602   | Methyl Phenyl Silicone       | Condensation             | 211                          | -80  | Lower    | Lower                     |
| DC 93-046 | ---                          | ---                      | 208                          | -85  | Lower    | Lower                     |
| DC 93-072 | Methyl Vinyl Silicone        | Addition                 | 216                          | -70  | High     | High                      |
| SWS 821   | ---                          | ---                      | 200                          | -100 | Medium   | Lower                     |
| SWS 820   | ---                          | ---                      | 200                          | -100 | High     | Lower                     |

### 3.1.3 PD-200 (Modified)

In that low density combined with low modulus and low thermal conductivity are desirable for RSI bonding, a decision was made to explore lower density modifications of the standard PD-200 to produce open cell methyl-phenyl silicone foams. This effort is discussed in greater detail in Section 4. As can be seen from Figure 3-1, a modified PD-200 in a density range less than 0.32 gm/cc (20 pcf) can offer considerable advantage in weight reduction and in strain isolation. For example, 25.4 mm (1.0 inch) of foam at 0.50 gm/cc (28 pcf) results in a required tile thickness of 43.2 mm (1.7 inch) and a weight of 21.5 Kg/m<sup>2</sup> (4.4 lb/ft<sup>2</sup>) (Curve A), while use of a 0.24 gm/cc (15 pcf) foam (Curve B) results in a weight of 19.1 Kg/m<sup>2</sup> (3.9 lb/ft<sup>2</sup>), a weight reduction of 2.4 Kg/m<sup>2</sup> (0.5 lb/ft<sup>2</sup>).

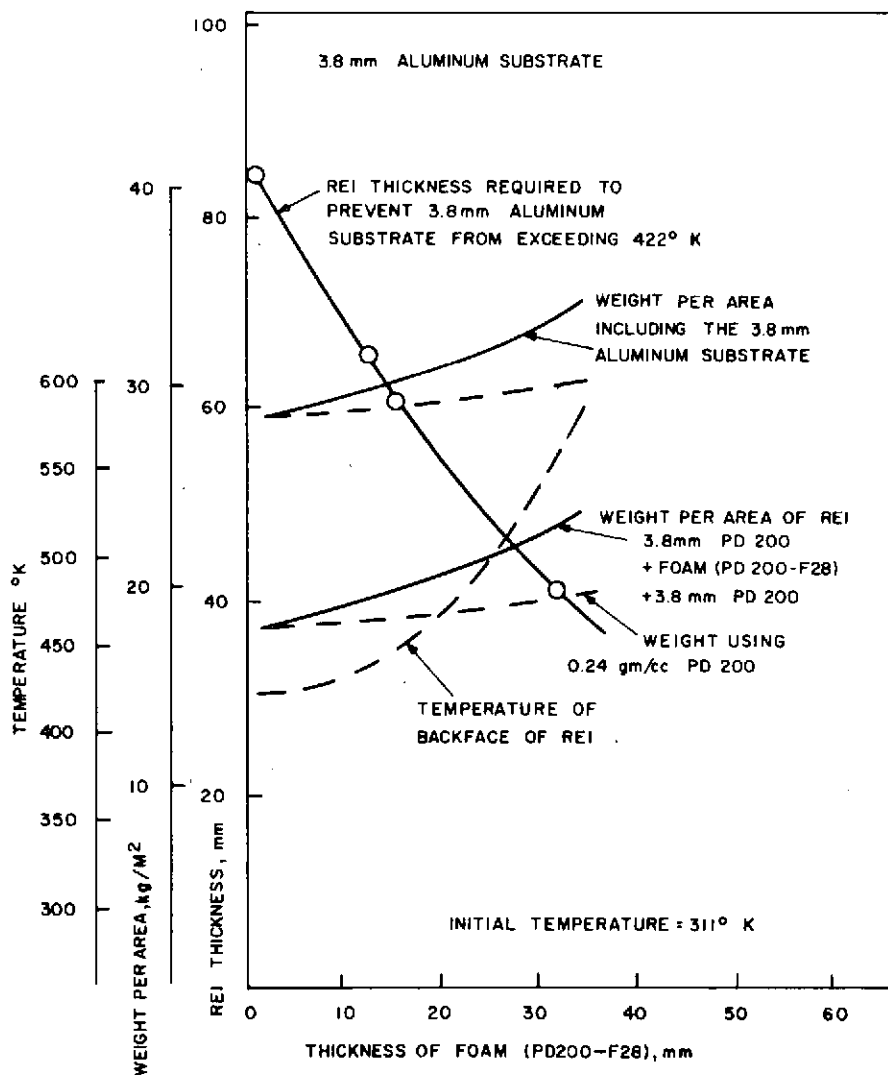


Figure 3-1. Effect of Varying PD 200-F28 Thickness, Area 2 Perturbed

## 3.2 EVALUATION OF CANDIDATE COMMERCIAL MATERIALS

Four commercially available materials were screened during the course of the program, three as candidate foam bonds, and one as a candidate adhesive film. Each is discussed below.

### 3.2.1 PERMACEL ES-5168 RUBBER FILM

The Permacel Division of Johnson and Johnson Corporation, New Brunswick, New Jersey, was contacted to provide information regarding their silicone rubber film ES-5168. The material is a "B-staged" unsupported, unvulcanized silicone rubber film which is calendered onto a carrier film, and is available in a range of thickness from 0.25 to 0.76 mm (0.010 to 0.030 inch).

A mid-range thickness 0.38 mm (0.015 inch) sample was obtained to determine feasibility for use, and also to determine the mechanical properties at room temperature when fused to a GE PD-200 silicone foam. The application of this, or a similar material would greatly aid in establishing bondline weight and thickness control in contrast to the established use of a "wet" bondline which subsequently cures to a solid polymer.

Butt tensile specimens were prepared, per Figure 3-2. Fabrication of the specimens was accomplished in two steps:

1. The PD-200 foam was bonded to the aluminum butt tensile blocks using GE-RTV-560 with 0.5 wt. %T-12 catalyst, and cured at 355° K (180° F) for 6 hours.
2. The assembly was then joined with the ES-5168 film while under slight compression, and cured at 394° K (250° F) for 16 hours.

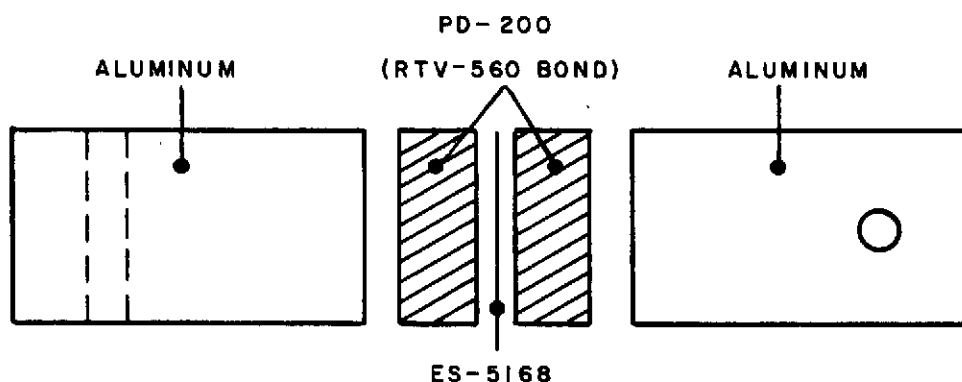


Figure 3-2. Butt Tensile Specimens

When tested, all failures were adhesive at the ES-5168/PD-200 interface with tensile strength of  $103.4$  to  $124.1 \times 10^3 \text{ N/M}^2$  (15 to 18 psi) with no evidence of flow of the silicone rubber film into the foam cellular structures.

#### Conclusions:

1. With this system, greater adhesive flow is mandatory to insure mechanical interlock and bond to cellular systems.
2. The cure temperature of ES-5168  $>394^\circ\text{K}$  ( $>250^\circ\text{F}$ ) is not practical for either field or in-house use.
3. This adhesive system may have practical use when bonding non-cellular materials, where high temperature and pressure do not present application problems, and where a soft bond of controlled thickness is required.
4. Further efforts on this material were not conducted under contract.

#### 3.2.2 CHR R-10480

After a review of literature, the Connecticut Hard Rubber Company, New Haven, Connecticut, was contacted regarding a low compression set silicone sponge rubber CHR R-10480. A sufficient quantity of the  $0.32\text{--}0.34 \text{ gm/cc}$  ( $20\text{--}21 \text{ lb/ft}^3$ ) material was obtained to conduct a preliminary screening for feasibility as a strain isolation pad for ceramic TPS. Cross-sectional views of the material as received at  $4.5\times$  and at  $10\times$  magnification are shown in Figures 3-3 and 3-4, where it may be noted that the foam structure is composed of elongated cells of widely varying size at an angle of  $15\text{--}20^\circ$  to the skinned foam face. It is also obvious that the foam structure is primarily closed cell, and, therefore, the rubber was initially screened in a vacuum chamber for permeability and dimensional stability prior to further evaluation. Based upon the results of the screening test, the material was eliminated as a candidate for space use in the current investigation. The screening was conducted as noted below.

A section of the  $12.7 \text{ mm}$  ( $0.5''$ ) thick sheet of Cohrlastic foam was cut to nominal  $76 \times 178 \text{ mm}$  ( $3'' \times 7''$ ). From this section a  $152 \text{ mm}$  ( $6''$ ) "dog bone" was cut using a die cutting tool (Figure 3-5). The "dog bone" was subjected to a vacuum exposure of  $1013.25 \text{ N/M}^2$  ( $10^{-2}$  atmospheres) for 1 hour (3600 sec) and visually examined throughout the exposure. After 5 minutes (300 secs) exposure, the  $152 \text{ mm}$  ( $6''$ ) "dog bone" grew in length to  $178 \text{ mm}$  ( $7''$ ). The gauge width had increased from  $25.4 \text{ mm}$  ( $1''$ ) to approximately  $33 \text{ mm}$  ( $1.3''$ ). After 1 hours (3600 secs) exposure, the "dog bone" sample had reduced in size to  $96.5 \text{ mm}$  ( $3.8''$ ) in length and  $17.8$  ( $0.7''$ ) in gauge width (Figure 3-6). Upon standing at ambient conditions for 16 hours (57,600 sec), the material returned to its original dimensions. It should be noted that dimensional changes of this type are typical for closed cell silicone foams.

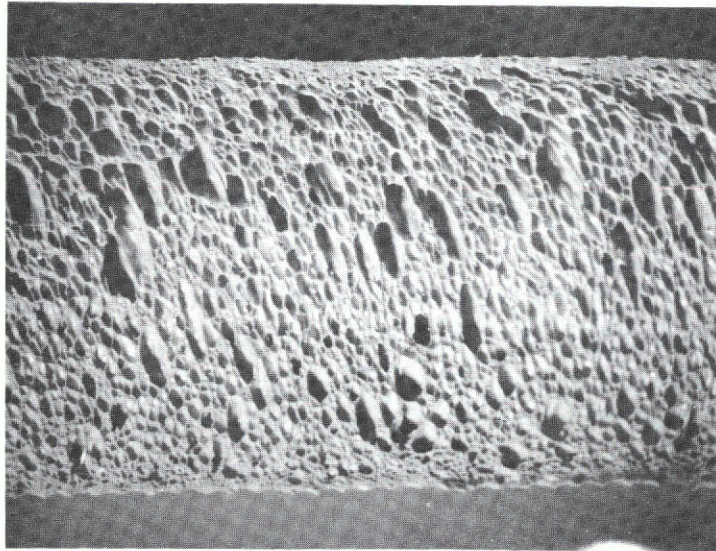


Figure 3-3. Cohrlastic R-10480, Cross-Section, 4.5X  
0.34 gm/cc (21 pcf)

This page is reproduced at the  
back of the report by a different  
reproduction method to provide  
better detail.

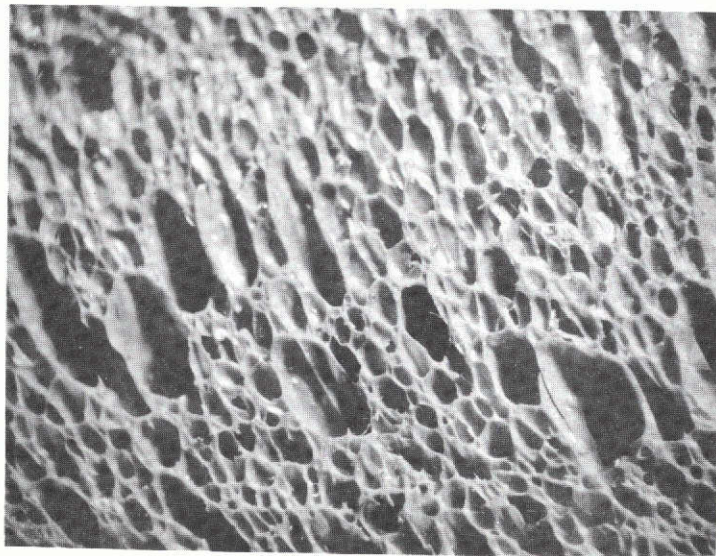


Figure 3-4. Cohrlastic R-10480, Cross-Section 10X  
0.34 gm/cc (21 pcf)



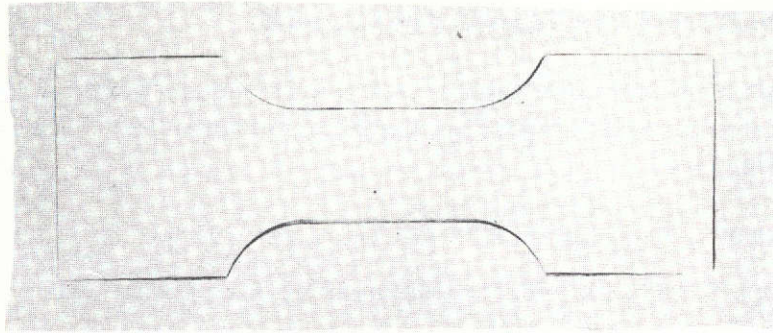


Figure 3-5. Cohrlastic R-10480 .34 gm/cc (21 pcf) Cut From Panel With Dog Bone Cutting Tool.

This page is reproduced at the back of the report by a different reproduction method to provide better detail.

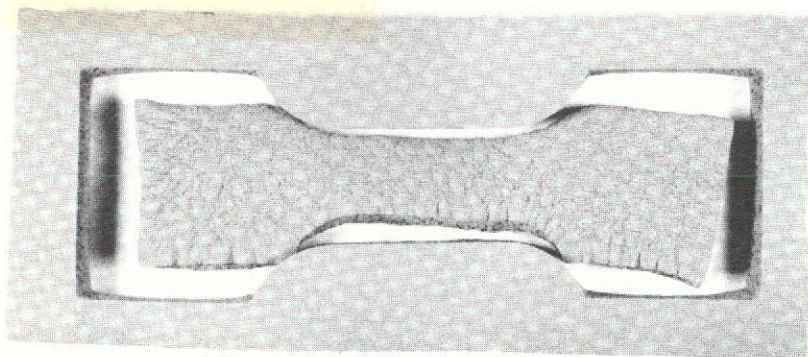


Figure 3-6. Cohrlastic R-10480, After Dog Bone Was Exposed To Reduced Pressure For 60 Minutes.



### 3.2.3 RAYBESTOS-MANHATTAN SILICONE SPONGE

Samples of two types of Raybestos-Manhattan Silicone Sponge were obtained for feasibility screening as strain isolation bonding pads for ceramic TPS. As received, the materials were designated:

1. Green RL-1973, 6.4 mm (0.25") thickness at 0.26 gm/cc (16.2 pcf).
2. Gray RL-2822, 12.7 mm (0.5") thickness at 0.34 gm/cc (21.3 pcf).

Cross sectional photographs of the materials as received were taken at 10X (Figures 3-7 and 3-8) and show the foam structure to be composed of tiny, uniformly distributed cells. It is also obvious that the foam structure is primarily closed cell, therefore the samples were initially screened in a vacuum chamber for permeability and dimensional stability prior to further evaluation.

Based upon the results of the screening test, the material was eliminated as a candidate for space use in the current investigation, as large dimensional changes are not compatible with the fabrication of a strain isolation system using ceramic insulation materials. The screening was conducted as follows:

Sections of the 12.7 mm (0.5") RL-2822, and the 6.4 mm (0.250") RL-1973 foams were cut to a nominal 152 x 152 mm (6" x 6"). From these sections, 152 mm (6")

This page is reproduced at the back of the report by a different reproduction method to provide better detail.



Figure 3-7. Raybestos-Manhattan RL-2822 0.34 gm/cc (21.3 pcf)  
X Section 10X

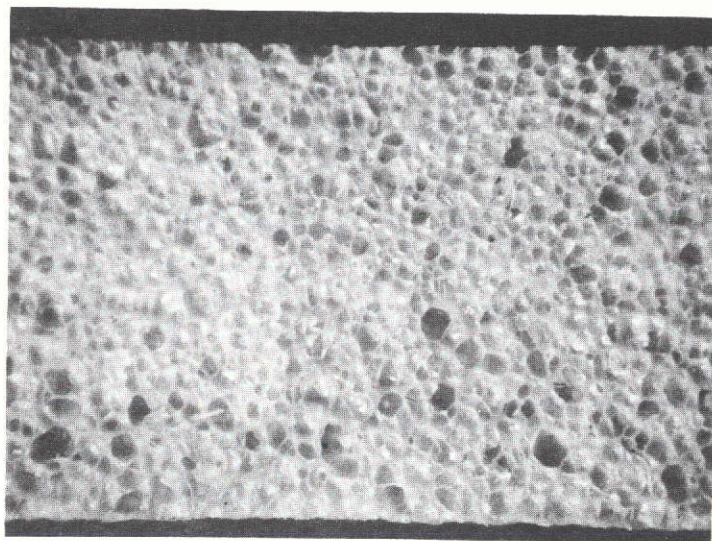


Figure 3-8. Raybestos-Manhattan RL-1973 0.26 gm/cc (16.2 pcf)  
X Section 10X

"dog bones" were cut using a die cutting tool. The "dog bones" were subjected to a vacuum exposure of  $1013.25 \text{ n/m}^2$  ( $10^{-2}$  atm) for two hours (7200 sec.) and visually examined throughout the exposure, while approximate dimensional changes were noted.

During Vacuum Exposure. Upon introduction to vacuum, both materials began to swell as a result of expansion of the gases trapped within the closed cell structure. The dimensional changes were:

RL-1973    +15-16% in the X direction.

RL-2822    +11-12% in the X direction.

No reduction to the original size was observed during the two hour (7200 second) vacuum exposure. Photographs during the vacuum test were not obtained due to the limited port aperture of the vacuum chamber. Dimensional changes were obtained by means of a comparison scale visible through the port.

This page is reproduced at the back of the report by a different reproduction method to provide better detail.

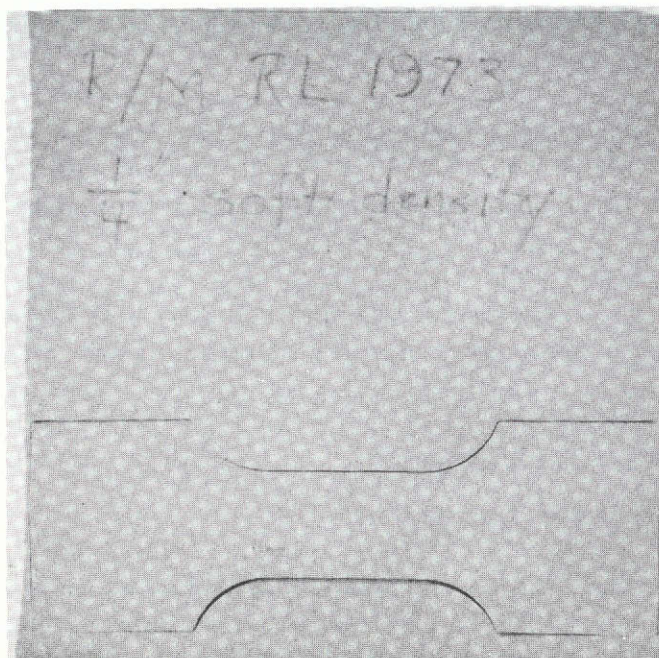


After Vacuum Exposure. Upon removal from vacuum, the materials immediately crushed down to a reduced volume as a result of ambient pressure against the partially evacuated cell system. The dimensional changes upon removal from vacuum were:

|         |  |
|---------|--|
| RL-1973 | -3 to -4% in the X direction<br>-14 to -15% in the Z direction   |
| RL-2822 | -20 to -21% in the X direction<br>-40 to -42% in the Z direction |

Figures 3-9 and 3-10 show the RL-1973 before exposure, and immediately after removal from vacuum, while Figures 3-11 and 3-12 show the same for RL-2822. Upon standing at ambient conditions for sixteen hours (57,600 seconds), the materials returned to their original dimensions. Figure 3-13 shows a comparison photograph of PD200-16.

Subsequent to this investigation, the RL-1973 material was evaluated in a vacuum of  $2 \times 10^{-4}$  mm Hg. This evaluation was conducted as a part of the GE-RESO response to RIC RFP M3-153-JJW-1 and is documented in GE-RESO Proposal N-72915, Volume IV (14 March 1973). Figure 3-14 illustrates the dimensional stability observed in that test evaluation in comparison to the PD200-16.



This page is reproduced at the back of the report by a different reproduction method to provide better detail.

Figure 3-9. Raybestos-Manhattan RL-1973 (.26 gm/cc, 16.2 pcf) cut with die cutting tool from 6.35 mm (0.5") thick sheet.



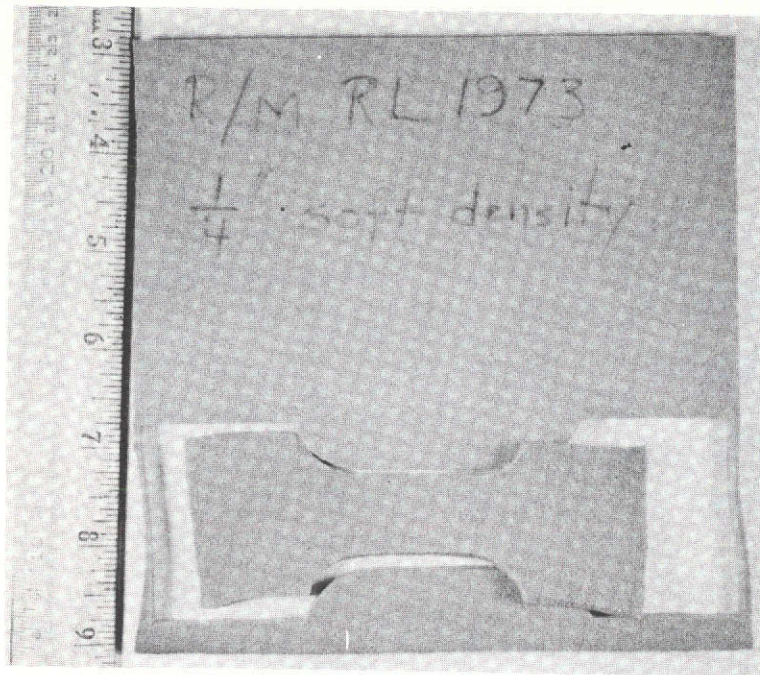


Figure 3-10. Raybestos-Manhattan RL-1973 after exposure to reduced pressure for 2 hours (7200 seconds).

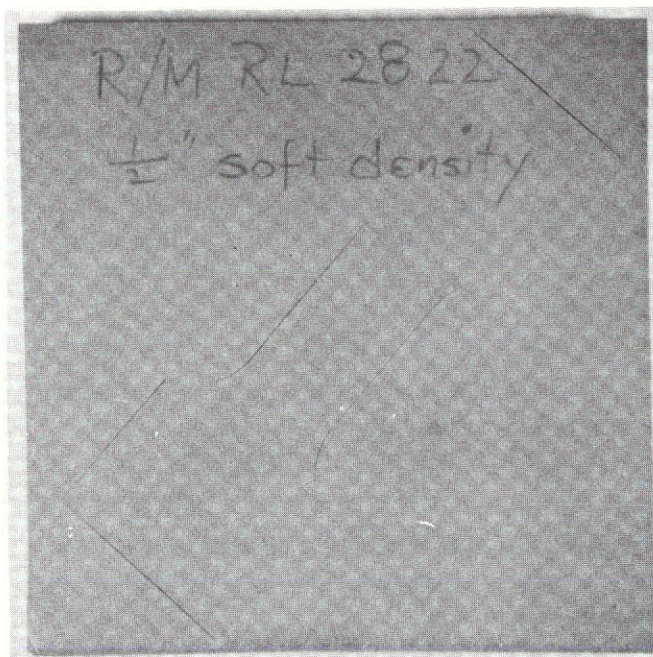


Figure 3-11. Raybestos-Manhattan RL-2822 (.34 gm/cc, 21.3 pcf) cut with die cutting tool from 6.35 mm (0.5") thick sheet.

This page is reproduced at the back of the report by a different reproduction method to provide better detail.





Figure 3-12. Raybestos-Manhattan RL-2822 after exposure to reduced pressure for 2 hours (7200 seconds)

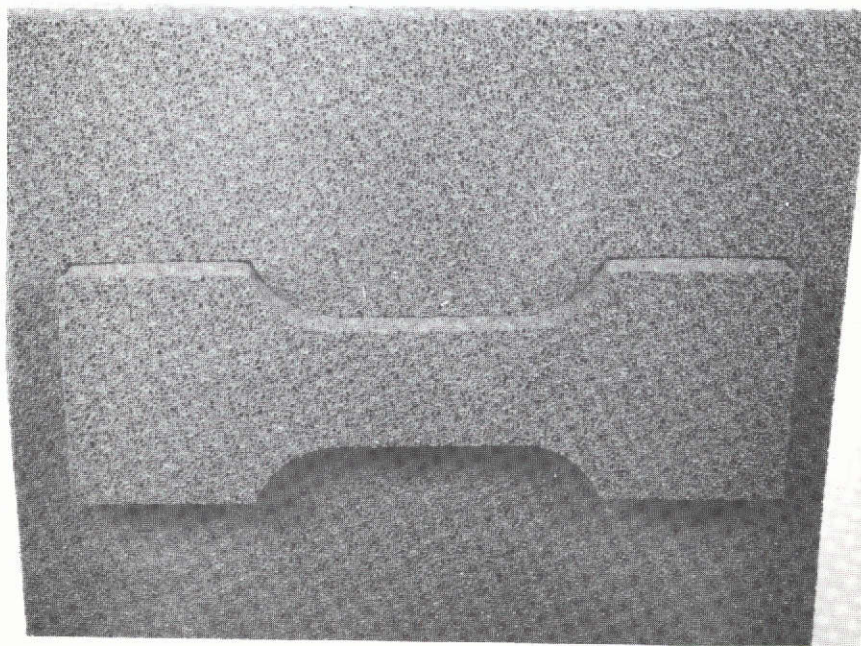
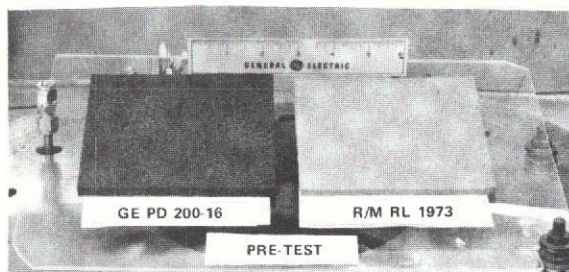
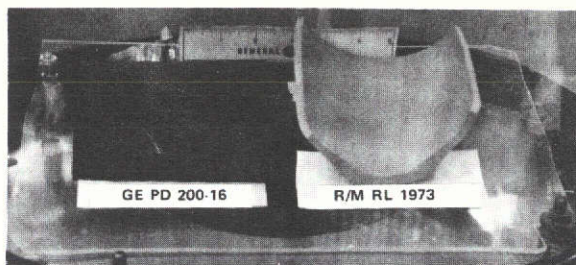


Figure 3-13. PD 200-16 Comparison Specimen

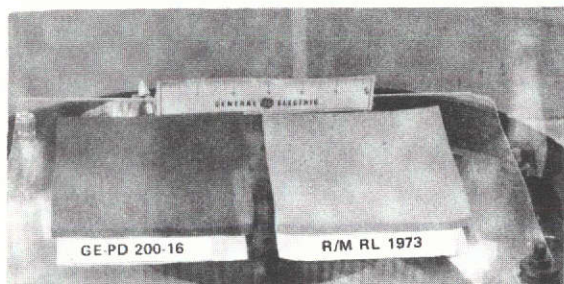




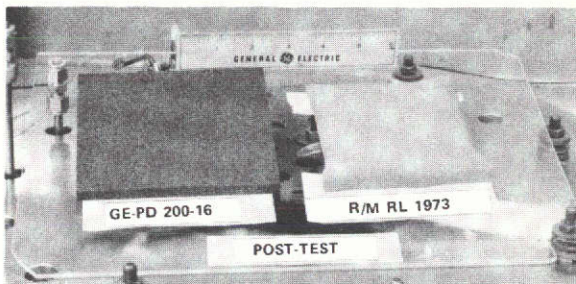
a. Pre-Test



b. Vacuum - 2 mm Mercury



c. 1 Hr. @ .0002 mm Hg



d. Post-Test

Figure 3-14. Dimensional Stability of Strain Isolator Materials

### 3.3 SILICONE BLENDS

Other silicone polymers of considerable interest due to their ability to deep-cure in closed conditions, combined with high mechanical strength at temperature, and low glass transition temperature were the vinyl modified polymers. GE RTV-655 is an example of a vinyl modified methyl phenyl silicone with excellent strength, and a low glass transition temperature. However, RTV-655 suffers a strength reduction at elevated temperatures ( $>450^{\circ}\text{K}$ ,  $>350^{\circ}\text{F}$ ) in air. It was initially postulated in Proposal N-72397 that admixtures of GE RTV-630 ( $T_g\ 211^{\circ}\text{K}$ ,  $-80^{\circ}\text{F}$ ), and 5 wt.% GE RTV-655 ( $T_g\ <200^{\circ}\text{K}$ ,  $<-100^{\circ}\text{F}$ ) would result in a marked lowering of the RTV-630 glass transition temperature. This approach, if successful, would offer the advantage of the slightly greater thermal stability of the RTV-630. Admixtures were prepared, and compression tests conducted to assess any change in glass transition. It was found that a depression of the glass transition did not occur, and indeed, additions up to 15 wt.% resulted in a reduction of the compressive modulus and an elevation of the transition point. The data is shown in Figure 3-15.

This page is reproduced at the back of the report by a different reproduction method to provide better detail.

### 3.4 DEVELOPMENTAL POLYMERS

In addition to the commercially available polymers, modified silicones, namely the silphenylene siloxane polymers developed by Southern Research Institute under a NASA

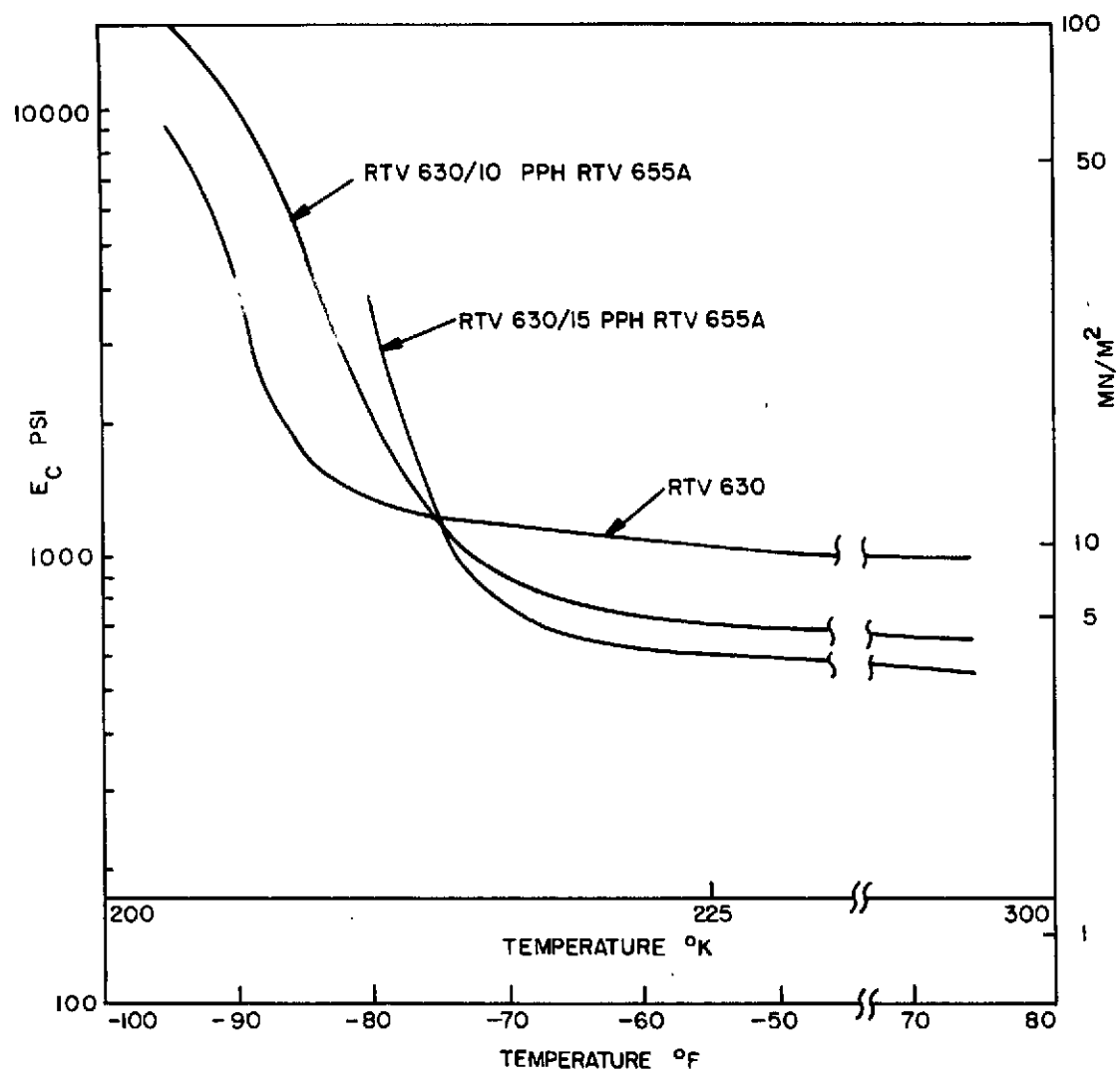


Figure 3-15. Compressive Modulus ( $E_c$ ) of Modified RTV 630

contract (Ref. 3-1) were considered for evaluation. It was mutually agreed at an April 6, 1972, meeting, however, not to pursue those specialty polymers in this contract investigation.

### 3.5 REFERENCES

3-1 "A Study of Polymers Containing Silicone-Nitrogen Bonds", Final Report, MSFC-NASA Contract NAS8-20190.



## SECTION 4

### ADVANCED ADHESIVE DEVELOPMENT (TASK 3)

#### 4.1 GENERAL

Based upon the results of the screening evaluations conducted in Task 2, a decision was made to place the emphasis in Task 4 on adhesive bond systems based upon RTV-560. In particular, since low density combined with low modulus is of importance in the attachment of ceramic RSI, it was decided to emphasize the development of low density modification of the GE-RESID PD-200.

Consequently, various formulation studies were conducted, and a low density 0.26 gm/cc (16 pcf) modification, PD-200-16, was developed. The PD-200-16 was initially characterized for mechanical and thermal properties, successfully thermally cycled to 89°K (-300°F) and to 616°K (650°F), and tested in conjunction with a light weight (0.14 gm/cc, 9 pcf) GE-Silica Ceramic adherend.

#### 4.2 FORMULATION STUDIES

##### 4.2.1 Fybex<sup>®</sup> FIBER ADDITION

Several loadings of DuPont "Fybex" inorganic titanate fibers were prepared to determine if a suitable cell structure with increased strength could be produced at low density.

The first attempt was a maximum fiber loading consistent with ability to foam the RTV-560. To the base resin (RTV 560), was added small amounts of Fybex fiber until the viscosity increase was judged to be within the limits of foam processing. The loading was calculated to be 7.0 wt %. This mixture, designated Base A, was then processed to produce a foam bun 229 x 305 x 38 mm (9" x 12" x 1.5").

During the foaming process it became evident that the 7.0% loading was excessive, and that the viscosity of the final mix was not low enough to allow complete foaming when poured into the open mold. When cured and sectioned, the foam exhibited an irregular cell structure with evidence of many void areas. Microscope examination showed good distribution of the fiber but a highly irregular cell structure.

A second panel of foam, as above, was fabricated containing 3.5 wt % Fybex fiber. The viscosity of the final mix was low enough to allow for complete filling of the open mold and leveling during the foaming process.

The cured panel was sectioned and examined. The cell structure, although greatly improved over Panel A (7%), was still irregular and showed evidence of some small voids.

This panel was processed through a 422°K (300°F) cure, slit to 12.7 mm (0.5") thickness and cut to dog-bone configuration for tensile testing at room temperature. Photomicrographs of the 3.5 wt % material are shown in Figures 4-1 and 4-2 and show the irregular cell size of the titanate loaded RTV-560 in comparison to the fine uniform cell structure of GE PD-200 shown in Figures 4-3 and 4-4. Densities of the two materials are similar, 0.51 gm/cc (32 lb/ft<sup>3</sup>) for the PD-200, and 0.53 gm/cc (33 lb/ft<sup>3</sup>) for the Fybex loaded foam.

Based upon the large, irregular foam structure, and the high modulus (Table 4-1) in comparison to other PD-200 modifications, additional efforts on Fybex loading were not conducted under contract.

#### 4.2.2 NUCLEATION SITE INVESTIGATION

The standard PD-200 silicone foam at .51 gm/cc (32 lbs/ft<sup>3</sup>) exhibits an extremely fine cell structure which is uniformly distributed. However, when reducing its density, by processing at reduced pressure, its cell structure becomes somewhat coarse as expected. Several modifications were made to the formulation in an attempt to minimize this effect. It was theorized that certain types of material additives might establish nucleation sites for finer cellular formation. The two materials selected were (1) Phenolic microballoons and (2) Carbon black. Each material was incorporated into PD-200 at 5 weight percent based on the silicone rubber, and processed at both ambient and reduced pressure.

##### 4.2.2.1 Microballoons

The formulation containing microballoons presented no difficulty in fabrication by either method. The foam processed at ambient pressure had a resultant density of .51 gm/cc (32 lbs/ft<sup>3</sup>), while the foam processed at reduced pressure had a resultant density of .25 gm/cc (16 lbs/ft<sup>3</sup>). Cross section and microscopic examination show no improvement in cell distribution or cell size although the microballoons were uniformly dispersed. Photomicrographs of the 0.51 gm/cc material are shown at 4.5, 10, and 22x magnification in Figures 4-5, 4-6, and 4-7, where it may be noted that although the foam is still an open type, the cell size and uniformity has not been improved in comparison to the PD-200 (Figure 4-3, 4-4). The 0.26 gm/cc variation is shown in Figures 4-8, 4-9, and 4-10. An arrow has been superimposed on each of the 22x photos pointing to a microballoon cluster. Due to the irregular cell structure, no mechanical properties were obtained on these variations.

##### 4.2.2.2 Carbon Black

Finely divided carbon black was also evaluated as a possible fine cell promoter, although it was recognized that the highly absorptive properties of carbon black might be a handicap and possibly override the large surface area available for nucleation.

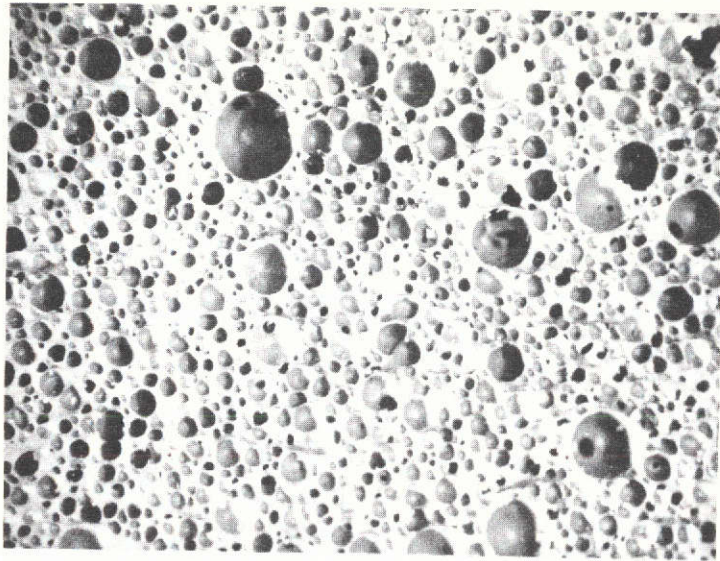


Figure 4-1. PD-200 Modified With 3.5% Titanate Fibers, Cross-Section, 10X  
0.53 gm/cc (33 pcf)

This page is reproduced at the back of the report by a different reproduction method to provide better detail.

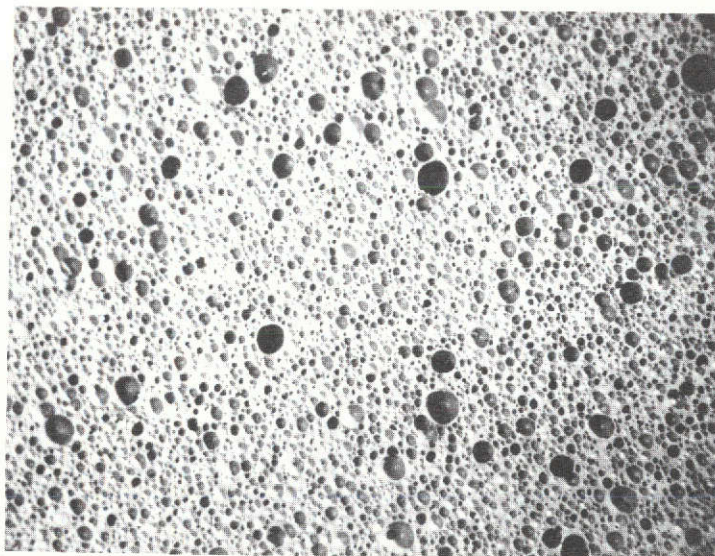


Figure 4-2. PD-200 Modified With 3.5% Titanate Fibers, Cross-Section, 4.5X  
0.53 gm/cc (33 pcf)



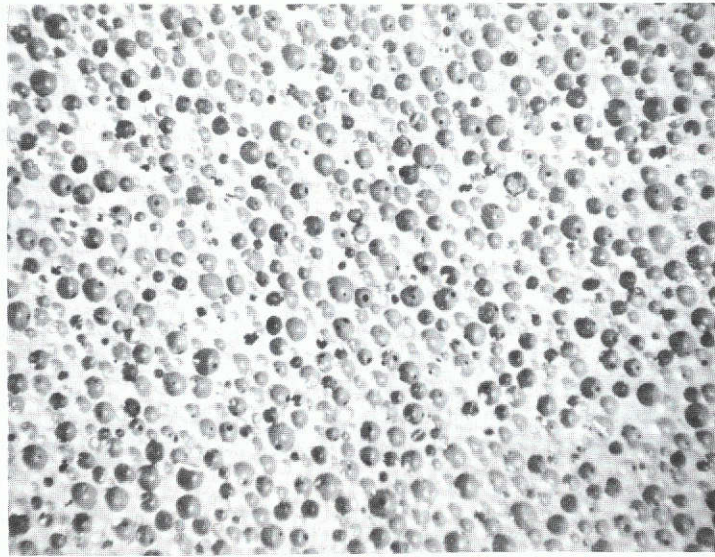


Figure 4-3. PD-200, Cross-Section, 10X  
0.51 gm/cc (32 pcf)

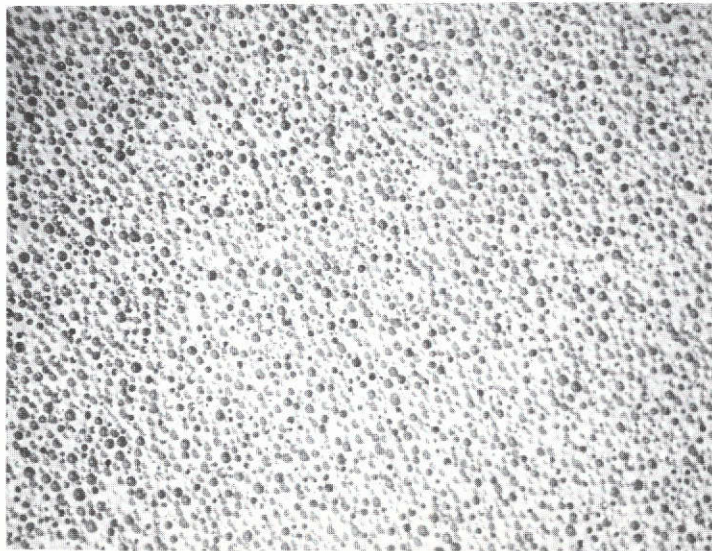


Figure 4-4. PD-200, Cross-Section, 4.5X  
0.51 gm/cc (32 pcf)

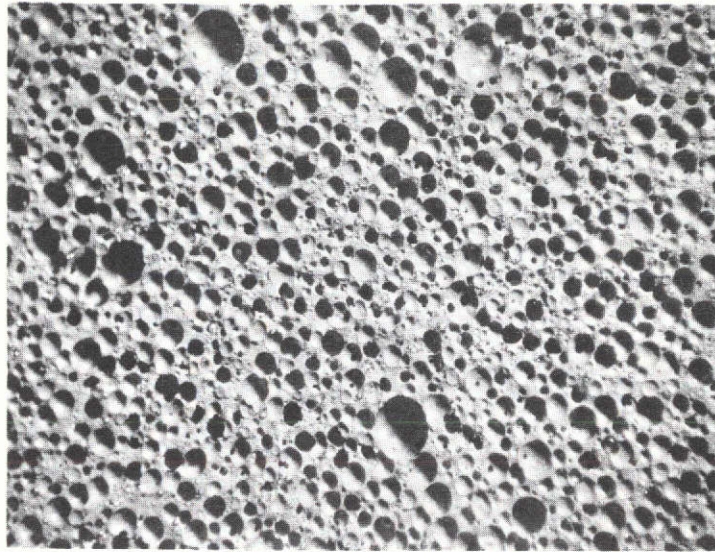


Figure 4-5. PD-200 Modified With 5% Microballoons, Cross-Section, 4.5X 0.51 gm/cc (32 pcf)

This page is reproduced at the back of the report by a different reproduction method to provide better detail.

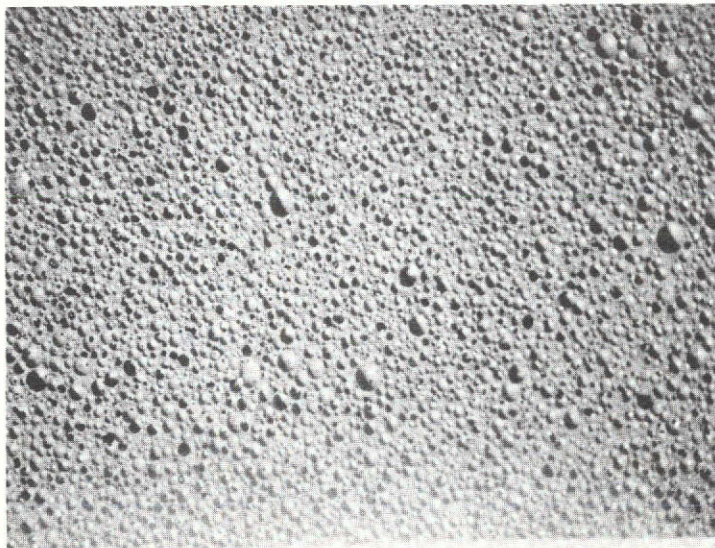


Figure 4-6. PD-200 Modified With 5% Microballoons, Cross-Section, 10X 0.51 gm/cc (32 pcf)



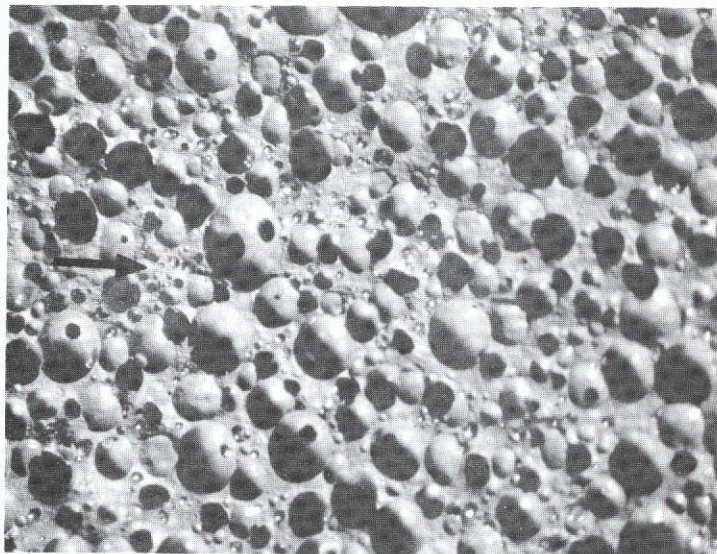


Figure 4-7. PD-200 Modified With 5% Microballoons, Cross-Section, 22X 0.51 gm/cc (32 pcf)

This page is reproduced at the back of the report by a different reproduction method to provide better detail.



Figure 4-8. PD-200 Modified With 5% Microballoons, Cross-Section, 4.5X 0.26 gm. (16 pcf)

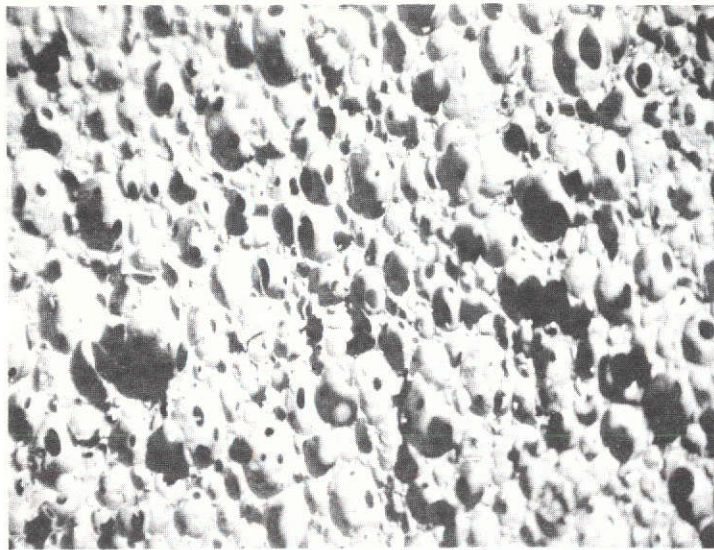


Figure 4-9. PD-200 Modified With 5% Microballoons, Cross-Section, 10X 0.26 gm/cc (16 pcf)

This page is reproduced at the back of the report by a different reproduction method to provide better detail.

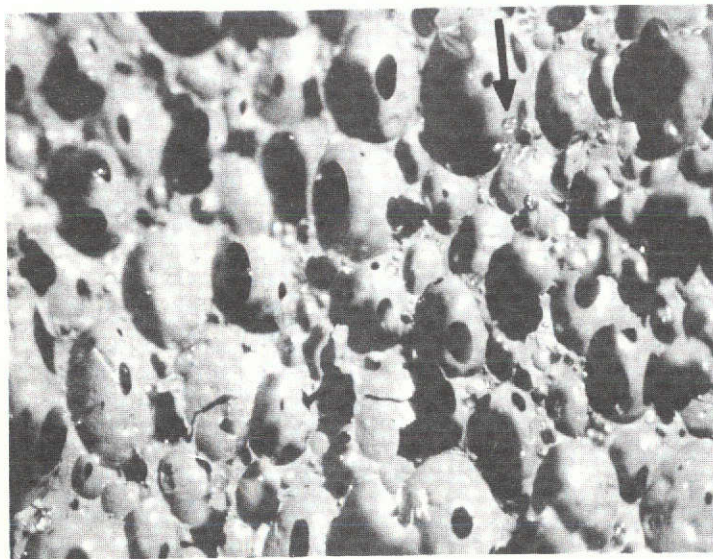


Figure 4-10. PD-200 Modified With 5% Microballoons, Cross-Section, 22X 0.26 gm/cc (16 pcf)



The carbon black was added at 5 wt % based upon the RTV-560, and foam processed at ambient conditions. The carbon black formulation "blew" properly, however, failed to cure and collapsed. The failure to cure is presumed to be a result of absorption of the catalyst by the carbon black. This concept has not been further investigated, as the approach of adding sufficient additional catalyst to satisfy the carbon demand adds numerous unwanted variables to the fabrication process.

#### 4.2.3 DENSITY REDUCTION OF PD-200

Formulation adjustments were made to the GE-RESID proprietary PD-200 to reduce the density from the standard 0.51 gm/cc (32 pcf). In the early trials, by means of catalyst level and pressure-during-foaming adjustments, a silicone foam bun at 0.26 gm/cc (16 pcf) was successfully fabricated and slit using standard rubber slitting equipment. Following that trial series, low pressure processed material having densities of 0.27, 0.33, and 0.41 gm/cc (17, 20.4 and 25.6 pcf) were successfully fabricated, cured, and slit to 12.7 mm (0.5 inch) thickness for tensile testing. Photomicrographs of the 0.27 and a 0.38 (24 pcf) gm/cc foam cross-sections are shown in Figures 4-11, 4-12, 4-13, and 4-14. It may be noted that although the cell structure is considerably larger than that of the standard PD-200, considerable uniformity is exhibited and the foam remains an open type. The room temperature tensile properties of the low pressure foam in comparison to the Fybex loaded are shown in Table 4-1.

During the course of the Program, repetitive trials have been conducted in foaming the low density silicone foam, designated PD 200-16 for 16 pcf (0.26 gm/cc) nominal density. Excellent uniformity of cell structure has been observed, as well as good reproducibility of density within "buns", and on a lot-to-lot basis. Typical density data through-the-thickness for several foam batches is shown in Table 4-2, and density data for a number of foam batches is listed in Table 4-3. Scale-up was also successfully accomplished to increase the standard bun size to 584 x 584 x 101 mm (23 x 23 x 4 inch) from the original size of 305 x 305 x 76 mm (12 x 12 x 3 inch), and all data in Table 4-3 is from the large foam bun.

#### 4.2.4 POST-CURE EVALUATION OF PD 200-16

Process studies were conducted on a nominal 0.24 gm/cc (15 pcf) foam lot to evaluate shrinkage, and density change as a function of several candidate post-cure temperatures; 366, 450, and 616°K (200, 350, and 650°F). Sixteen hours was selected as a representative overnight cure cycle. Figures 4-15 and 4-16 show that shrinkage and density increase are markedly reduced in the region of 450°K (350°F), although it may be noted that additional shrinkage does occur above 450°K, it is minor in relation to that up to 366°K.

In addition, tensile test specimens were post-cured and tested for room temperature tensile strength as a function of cure temperature. That data is shown in Figure 4-17.



TABLE 4-1. ROOM TEMPERATURE TENSILE PROPERTIES OF PD-200  
(MOD) FOAM

| Specimen Number | Density gm/cc | $\sigma_u$ KN/M <sup>2</sup> | E <sup>(1)</sup> KN/M <sup>2</sup> | E <sub>s</sub> <sup>(2)</sup> KN/M <sup>2</sup> | e (Percent) |
|-----------------|---------------|------------------------------|------------------------------------|---|-------------|
| A-1             | .52           | 284.1                        | 509.5                              | 717.0   | 39.4        |
| -2              | .53           | 315.1                        | 626.0                              | 779.1   | 40.6        |
| -3              | .53           | 335.8                        | 583.3                              | 758.4   | 44.4        |
| -4              | .53           | 382.0                        | 615.7                              | 855.0   | 44.7        |
| -5              | .53           | 380.6                        | 617.1                              | 875.6   | 43.4        |
| $\bar{X}$       |               | 339.2                        | 590.2                              | 799.8   | 42.5        |
| B-1             | .27           | 107.6                        | 146.2                              | 223.4   | 48.2        |
| -2              | .27           | 117.2                        | 141.3                              | 214.4   | 54.6        |
| -3              | .27           | 119.3                        | 140.0                              | 219.2   | 54.4        |
| -4              | .28           | 115.8                        | 128.2                              | 205.5   | 56.4        |
| -5              | .27           | 112.4                        | 150.3                              | 219.2   | 51.3        |
| $\bar{X}$       |               | 114.4                        | 141.3                              | 216.5   | 53.0        |
| C-1             | .33           | 142.7                        | 185.5                              | 261.3   | 54.6        |
| -2              | .33           | 138.6                        | 194.4                              | 262.7   | 52.8        |
| -3              | .33           | 146.9                        | 201.3                              | 282.  | 52.1        |
| -4              | .32           | 147.6                        | 212.4                              | 295.1   | 50.0        |
| -5              | .33           | 146.9                        | 206.8                              | 293.3   | 50.2        |
| $\bar{X}$       |               | 144.8                        | 200.0                              | 278.6   | 52.0        |
| D-1             | .41           | 206.8                        | 286.1                              | 399.2   | 51.8        |
| -2              | .41           | 144.8                        | 288.2                              | 350.2   | 41.3        |
| -3              | .42           | 198.6                        | 286.1                              | 386.8   | 51.3        |
| -4              | .39           | 173.7                        | 282.7                              | 375.8   | 46.2        |
| -5              | .40           | 146.2                        | 285.4                              | 348.9   | 41.9        |
| $\bar{X}$       |               | 173.8                        | 286.1                              | 372.3   | 46.5        |

(1) Initial modulus, valid up to 10-20 percent strain

(2) Secant modulus at failure

NOTE: A Series Fybex Loaded

B, C, and D Series Reduced Pressure Blown

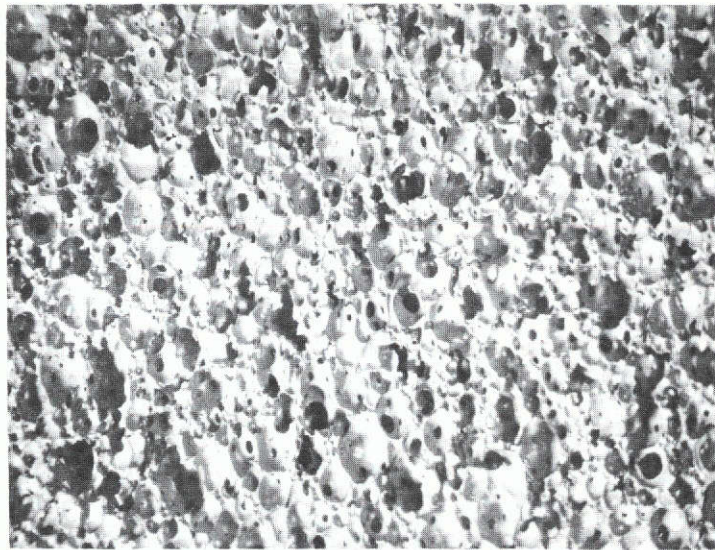


Figure 4-11. PD-200 (Modified), Cross-Section, 4.5X  
.27 gm/cc (17 pcf)

This page is reproduced at the  
back of the report by a different  
reproduction method to provide  
better detail.

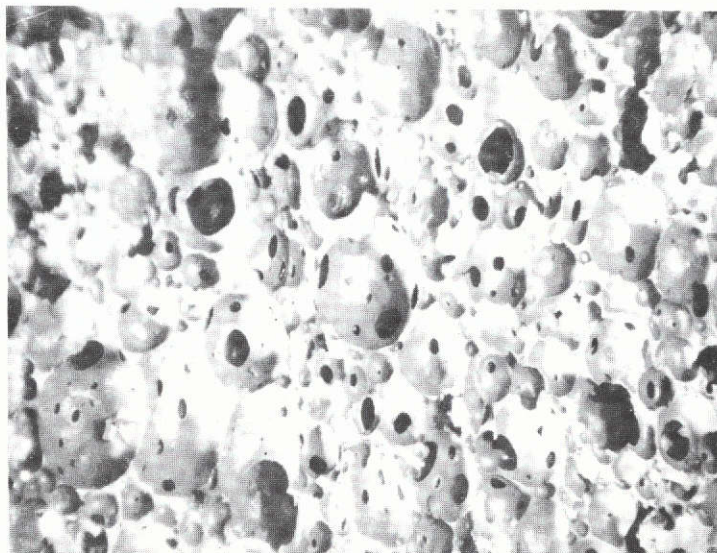


Figure 4-12. PD-200 (Modified), Cross-Section, 10X  
.27 gm/cc (17 pcf)



Figure 4-13. PD-200 (Modified), Cross-Section, 4.5X  
.38 gm/cc (24 pcf)

This page is reproduced at the back of the report by a different reproduction method to provide better detail.

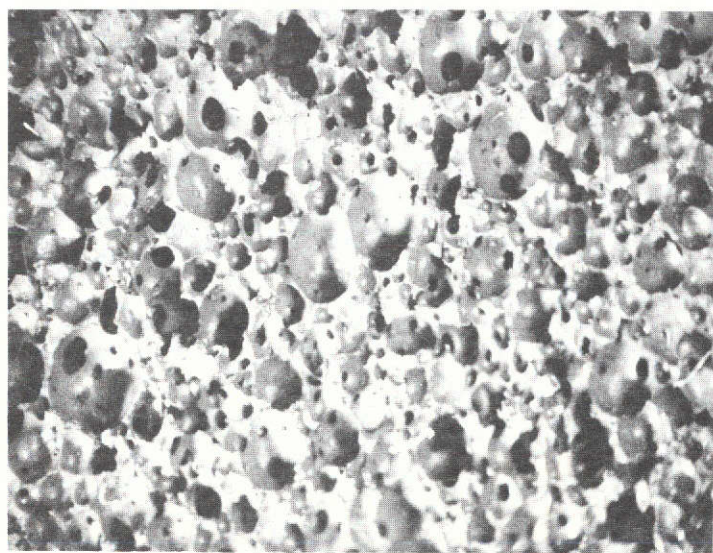


Figure 4-14. PD-200 (Modified), Cross-Section, 10X  
.38 gm/cc (24 pcf)

TABLE 4-2.

## Foam Density Evaluation

| Designation | Density, GM/CC |      |      |      |      |      | $\bar{X}$ |
|-------------|----------------|------|------|------|------|------|-----------|
|             | 1              | 2    | 3    | 4    | 5    | 6    |           |
| B-1         | .271           | .271 | .271 | .274 | .272 | ---- | .272      |
| 17K4        | .279           | .276 | .277 | .279 | .274 | .276 | .277      |
| 17K5        | .285           | .285 | .272 | .276 | .285 | ---- | .281      |
| 17K6        | .274           | .272 | .272 | .272 | .272 | ---- | .272      |
| C-1         | .325           | .328 | .328 | .322 | .330 | ---- | .327      |
| D-1         | .408           | .410 | .413 | .394 | .386 | ---- | .402      |

NOTE: Position #1 is at top of bun, and succeeding positions are at 12.7 mm (0.5 inch) intervals toward the bottom of the bun.

TABLE 4-3  
PD-200 Density Data\*

| LOW DENSITY  |                 |                |
|--------------|-----------------|----------------|
| Panel No.    | RTV-560 Lot No. | Density, GM/CC |
| 15K1         | 618             | 0.224          |
| 15K2         | 619             | 0.224          |
| HIGH DENSITY |                 |                |
| Panel No.    | RTV-560 Lot No. | Density, GM/CC |
| 17K4         | 613             | 0.277          |
| 17K5         | 613             | 0.279          |
| 17K6         | 613             | 0.284          |
| PD 200-16    |                 |                |
| Panel        | RTV-560 Lot No. | Density, GM/CC |
| P-1          | 620             | 0.253          |
| P-2          | 620             | 0.253          |
| SS-1         | 624             | 0.272          |
| SS-2         | 624             | 0.261          |
| SS-3         | 624             | 0.264          |
| SPARE        | 629             | 0.261          |

\* Foamed to 584 x 584 x 101 mm (23" x 4")

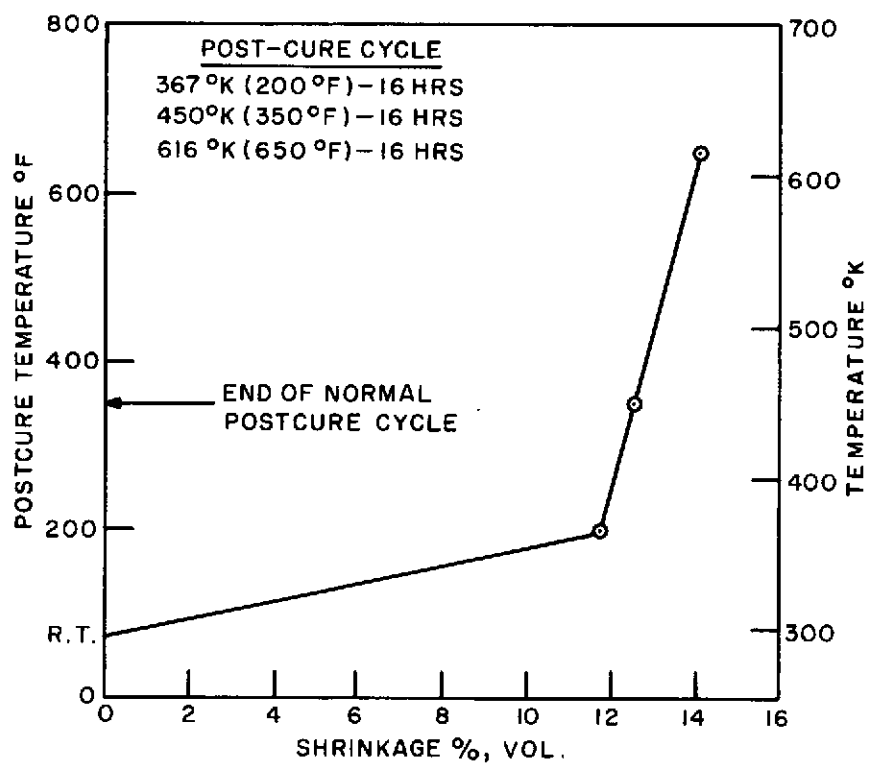


Figure 4-15. PD-200 Mod (Lot 618)  
 Shrinkage vs Post-Cure  
 Temperature

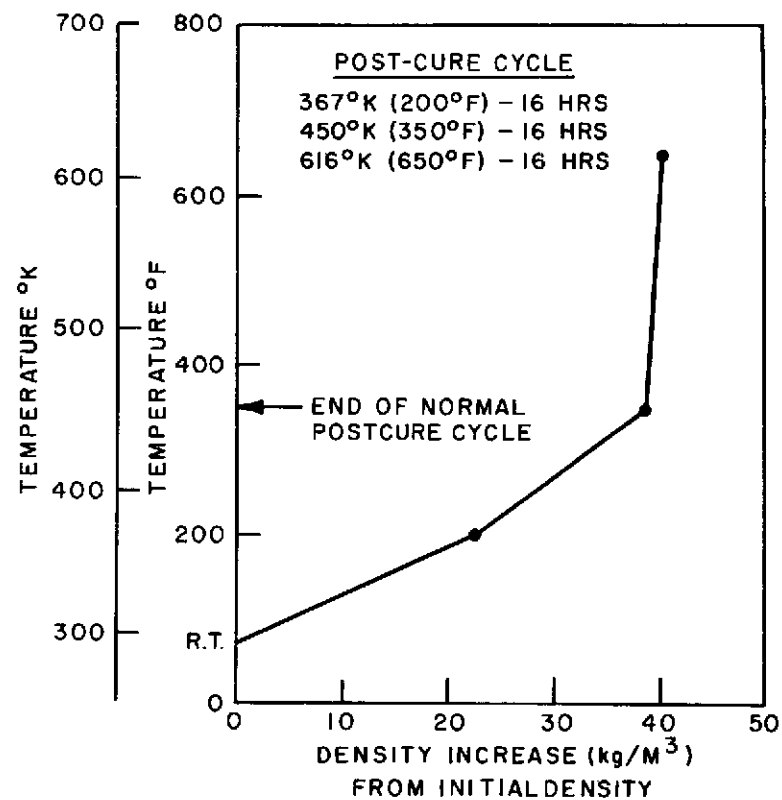


Figure 4-16. PD-200 Mod Post-Cure  
 Temperature vs Density



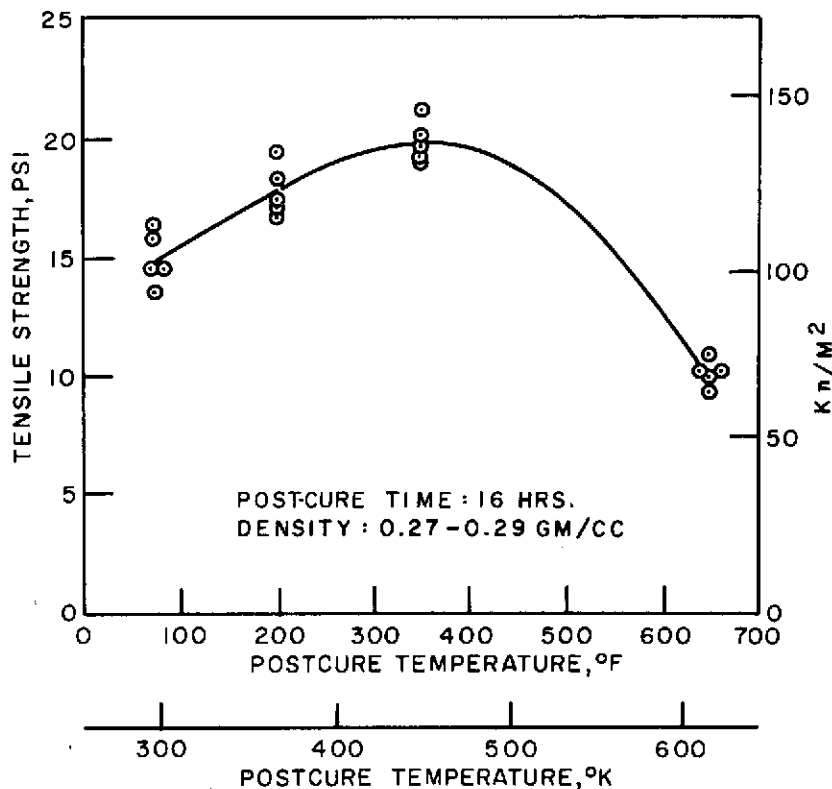


Figure 4-17. Room Temperature Tensile Strength PD-200 (Mod)  
vs Postcure Temperature

Although, in retrospect, an additional data set at, for example, 533°K (500°F) would have been beneficial for a complete data plot, the 450°K post-cure appears to be an acceptable trade-off between foam stabilization, and mechanical property degradation.

#### 4.2.5 CURRENT PROCESS FLOW PLAN

The current flow plan in processing of PD 200-16 is shown in Figure 4-18.

### 4.3 MECHANICAL PROPERTIES

Tests performed include tension, shear and thermal expansion. Tension tests were performed in both the in-plane (XY) and through the thickness (Z) directions. Two lots of material were utilized so that the extent of lot-to-lot property variation could be assessed.

Test results are shown in the following tables and graphs. PD-200-16 exhibits mechanical property trends similar to the higher density version of PD-200 (1,2). Lot-to-lot variation was found to be relatively small, but statistically significant. Tension and shear tests performed in the study described here utilized several new experimental techniques constituting an improvement over techniques used in earlier work (1,2). Extensometers

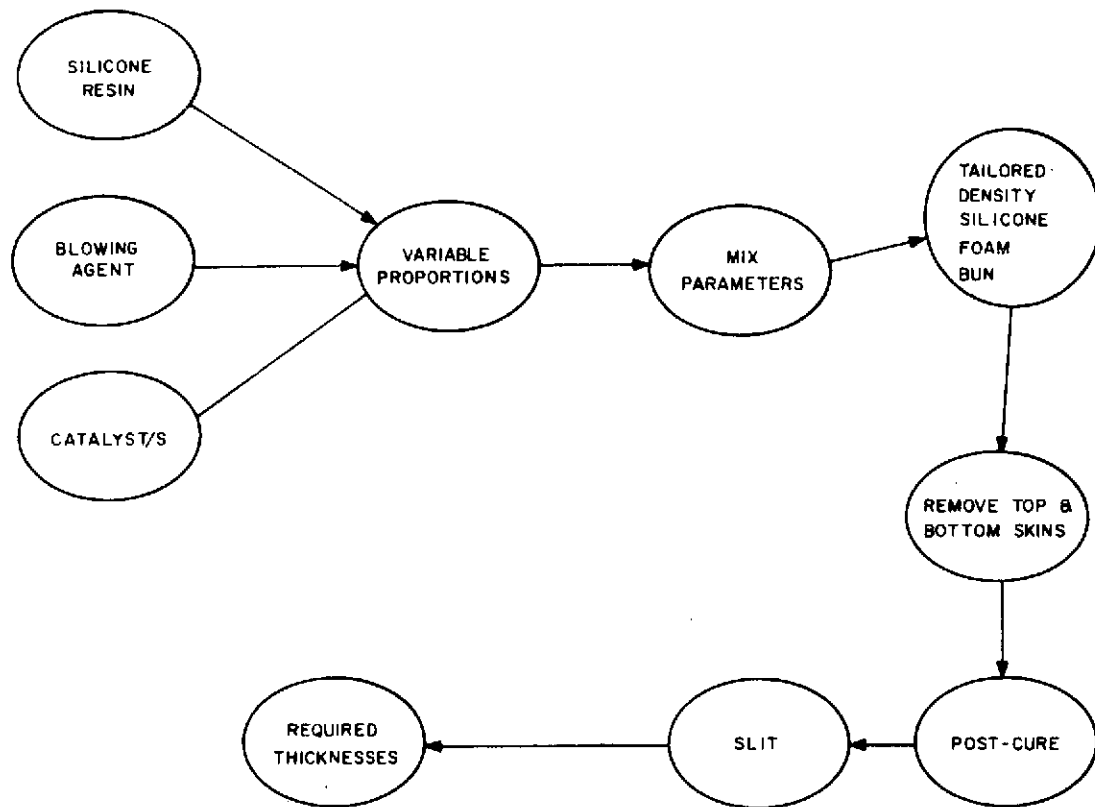


Figure 4-18. PD-200 Manufacture Flow Plan

were used for tensile strain measurements at all temperatures. The shear specimen was increased in thickness so that the effect of deformation in the solid RTV-560 bond-lines would be negligible and, thus, the PD-200 foam modulus of rigidity could be measured directly.

#### 4.3.1 TENSION TESTS

##### 4.3.1.1 Experimental Procedure

The testing procedure made use of two types of tensile specimens: a "dog-bone" specimen for their in-plane tensile tests and a bonded butt tensile specimen was used in through-the-thickness testing. Dimensions and configuration of the "dog-bone" are as shown in Figure 4-19. Butt tensile specimens consisted of a nominal 25.4 x 25.4 x 68.6 mm prism of PD 200-16 bonded to 25.4 x 25.4 mm aluminum loading blocks.

Specimens were tested in a floor model Instron test machine equipped with a Missimers environmental chamber. Liquid nitrogen is introduced into the chamber via a temperature controller valve for low temperature testing.



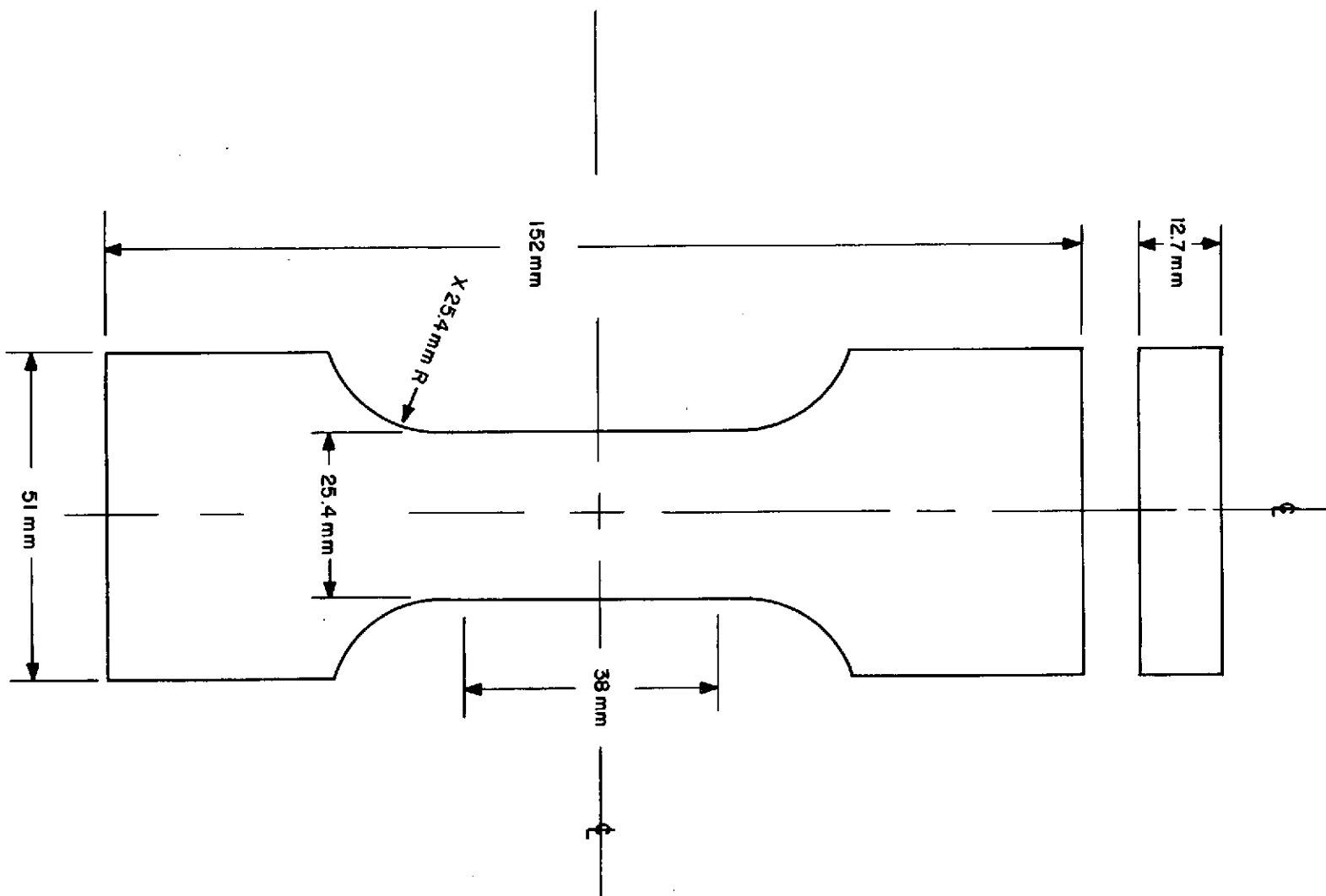


Figure 4-19. Tensile Specimen PD-200-16

In all testing except that done at 116°K (-250°F), strain was measured with a foil strip attached to the specimen gage length and marked in increments of 5% strain. Each 5% strain increment was determined visibly by the test operator and marked directly on the plot of stress vs. time by an Instron marking device which places a pulse on the curve. At 116°K (-250°F), since the specimen is below the glass transition range, and strain to failure is much less than 5%, an extensometer was calibrated at 116°K (-250°F) and applied directly to the specimen, giving a direct plot of stress vs. deformation.

#### 4.3.1.2 Results and Discussion

Plots of stress vs. strain at each temperature range are given for X-Y direction and Z direction testing in Figures 4-20 through 4-29. The curves for both lots of PD 200-16, lot 618 and lot 622, are marked to show any differing aspects of mechanical behavior.

A summary plot of tensile strength of PD 200-16 vs. temperature is given in Figure 4-30. The lot number and direction of testing is marked to distinguish the variables present. A smooth curve is drawn through the lowest strength data points to represent safe design values based on experimental results. Likewise, a plot of initial tensile modulus of PD 200-16 vs. temperature is given in Figure 4-31. The variables are similarly distinguished on the plot. A curve is drawn through an average value of the experimental data to serve as design data.

Since there is no previous data on the behavior of PD-200 with this density, a comparison cannot be made, therefore only the measured characteristics can be discussed.

An obvious observation is that tensile strength in the Z direction of testing is higher than that in the X-Y direction. This may be a consequence of the test method. As described previously, tensile tests in the X-Y direction are performed using a "dog-bone" type specimen. In the Z direction, specimen configuration is a bonded butt tensile specimen. The "dog-bone" specimen gage section does not see any end effects and thus undergoes only a uniaxial tensile stress. However, the gage section in the bonded butt tensile specimen does not undergo a uniaxial tensile stress since the deformation of the material creates a triaxial stress state and thus does not give a true tensile strength reading. Due to the size of the panel, Z direction tests can only be done in this manner.

The existence of end restraints sufficiently near to the region of deformation will alter a uniaxial state of stress to that of a triaxial state of stress. This situation is analagous to that of a necked region in a tensile test of a ductile material. As a result of this imposed triaxial state of stress, the average stress determined by the ratio of load over area is higher than the stress that would be present if simple tension prevailed.

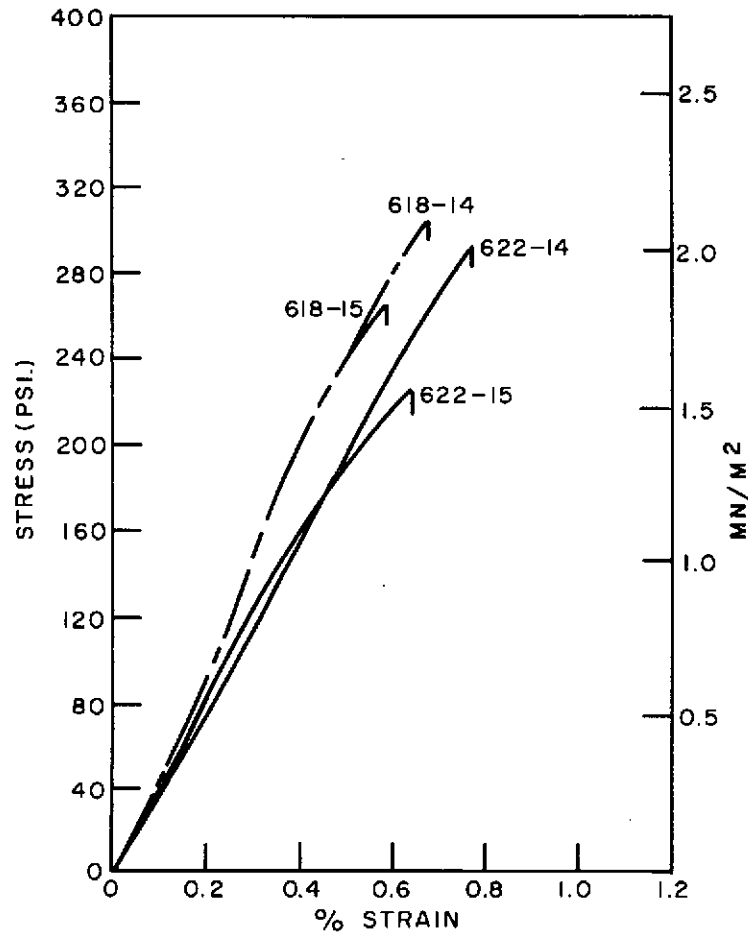


Figure 4-20. Tensile Stress-Strain Behavior For PD 200-16 (XY Direction) at 116°K

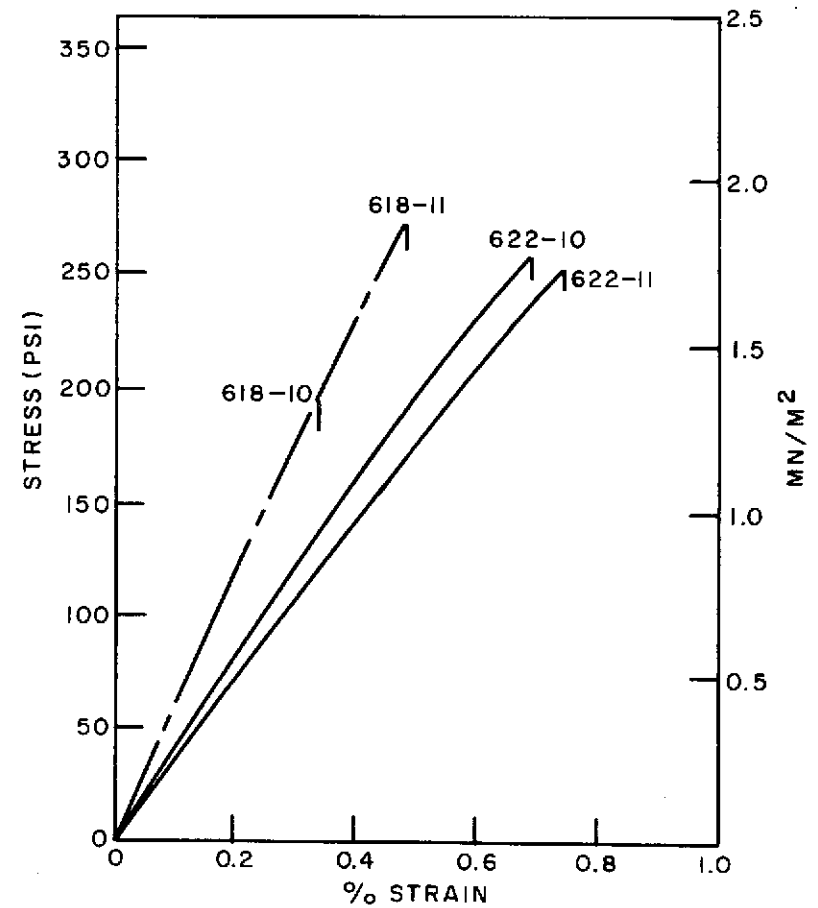


Figure 4-21. Tensile Stress-Strain Behavior For PD 200-16 (Z Direction) at 116°K

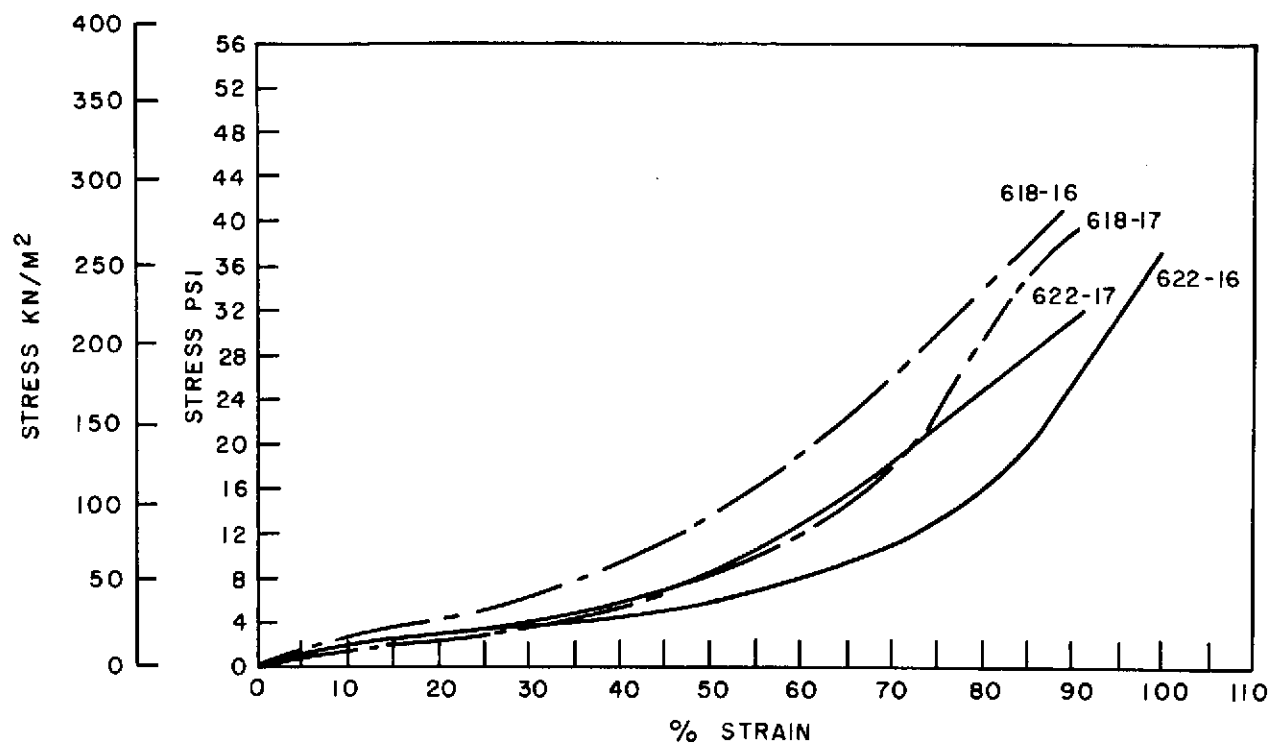


Figure 4-22. Tensile Stress-Strain Behavior For PD 200-16 (XY Direction) at 178°K

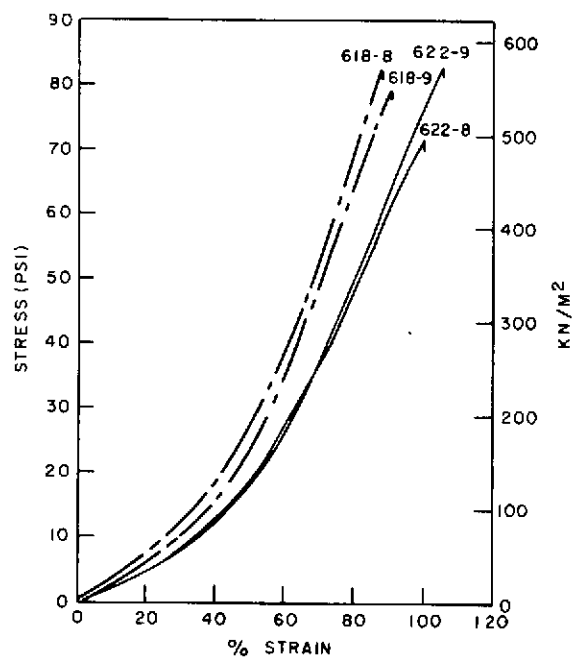


Figure 4-23. Tensile Stress-Strain Behavior For PD 200-16 (Z Direction) at 178°K

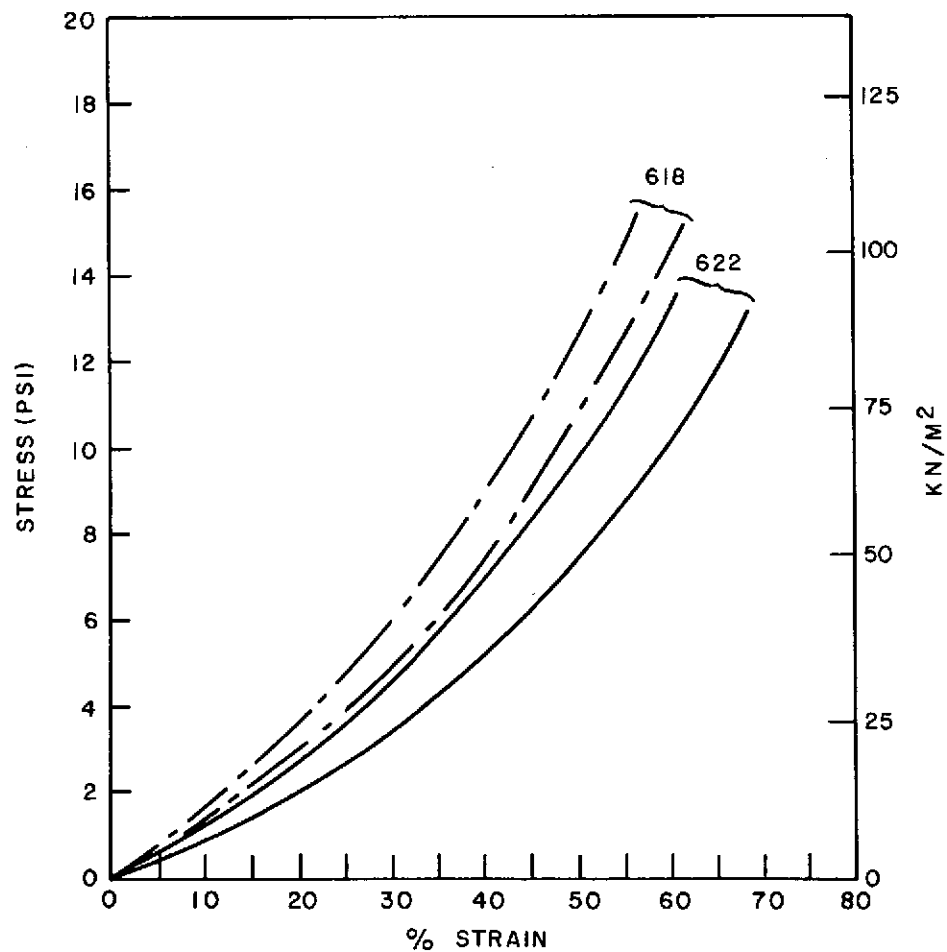


Figure 4-24. Tensile Stress-Strain  
Behavior For PD 200-16  
(XY Direction) at 297°K

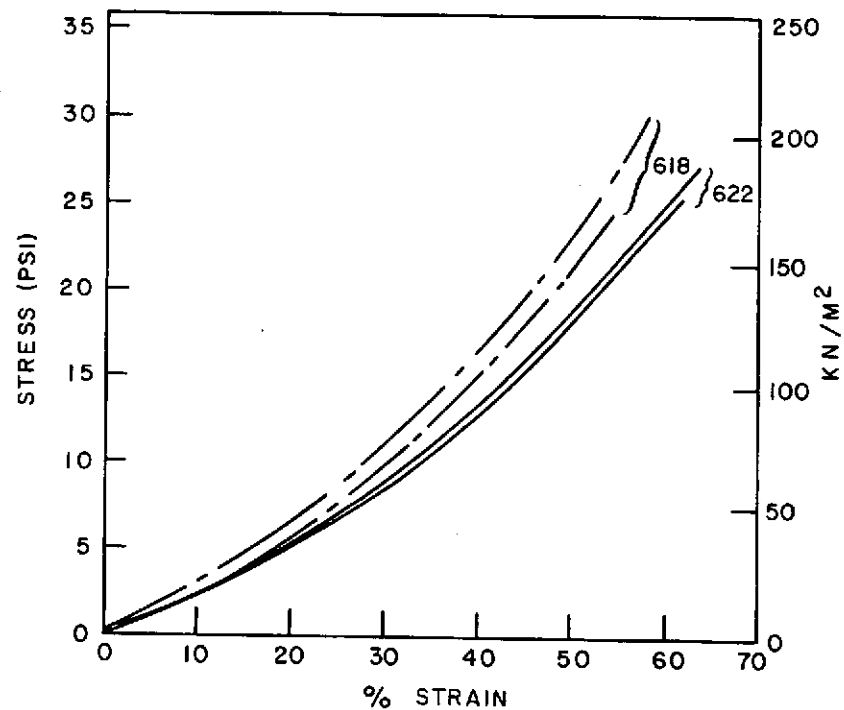


Figure 4-25. Tensile Stress-Strain  
Behavior For PD 200-16  
(Z Direction) at 297°K

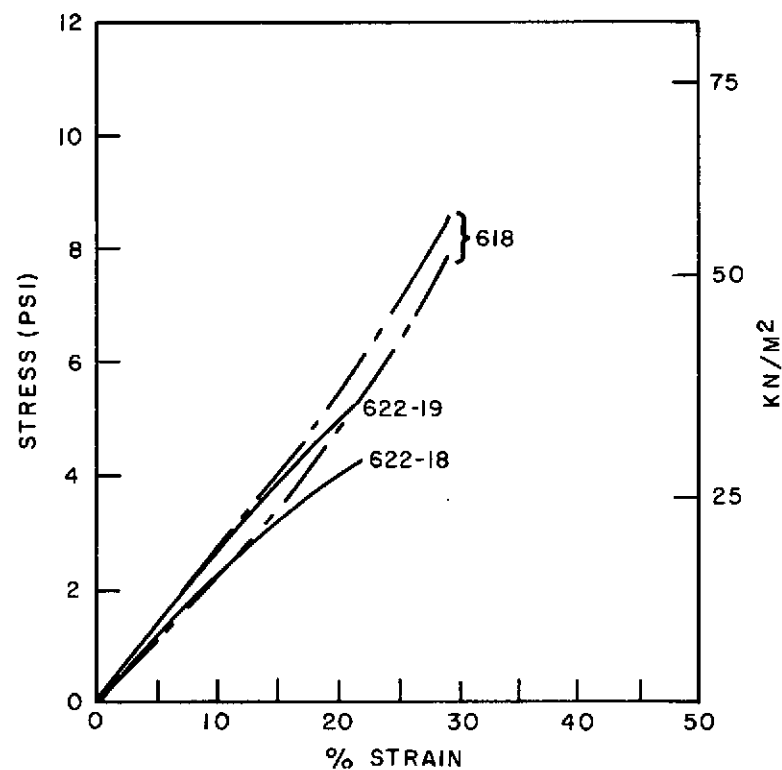


Figure 4-26. Tensile Stress-Strain Behavior For PD 200-16 (XY Direction) at 478°K

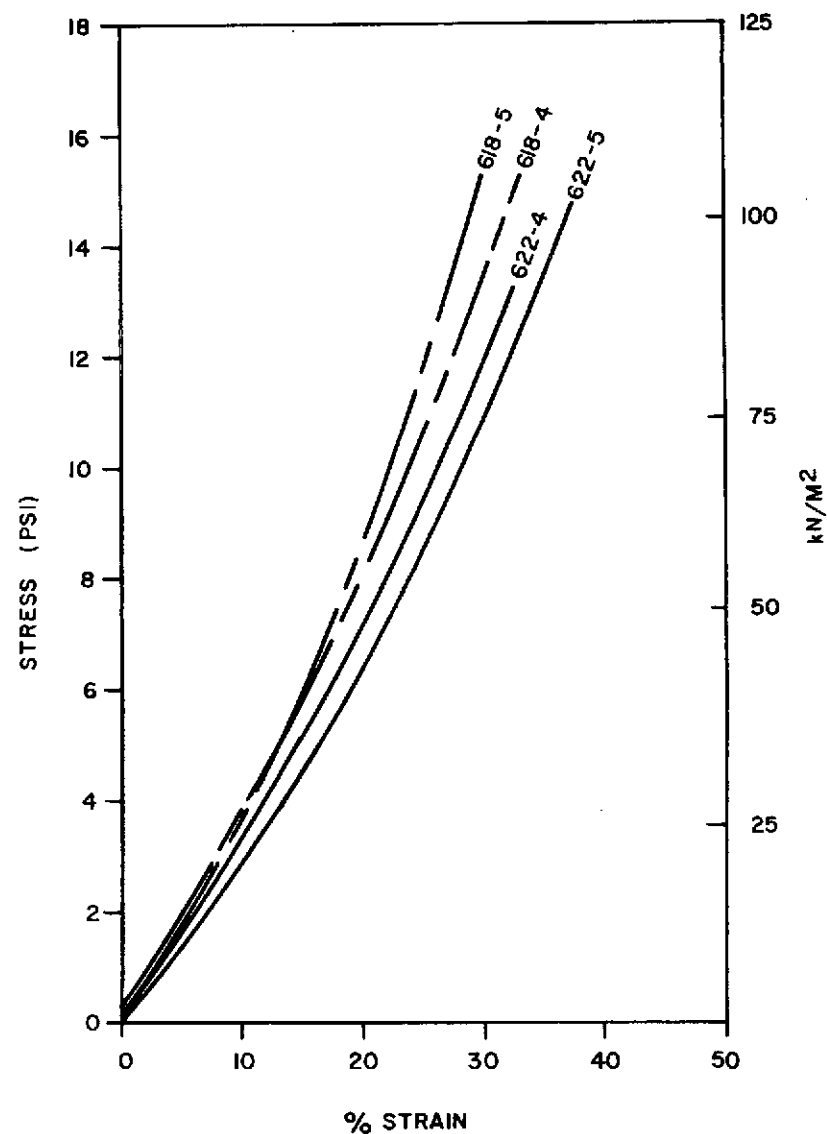


Figure 4-27. Tensile Stress-Strain Behavior For PD 200-16 (Z Direction) at 478°K

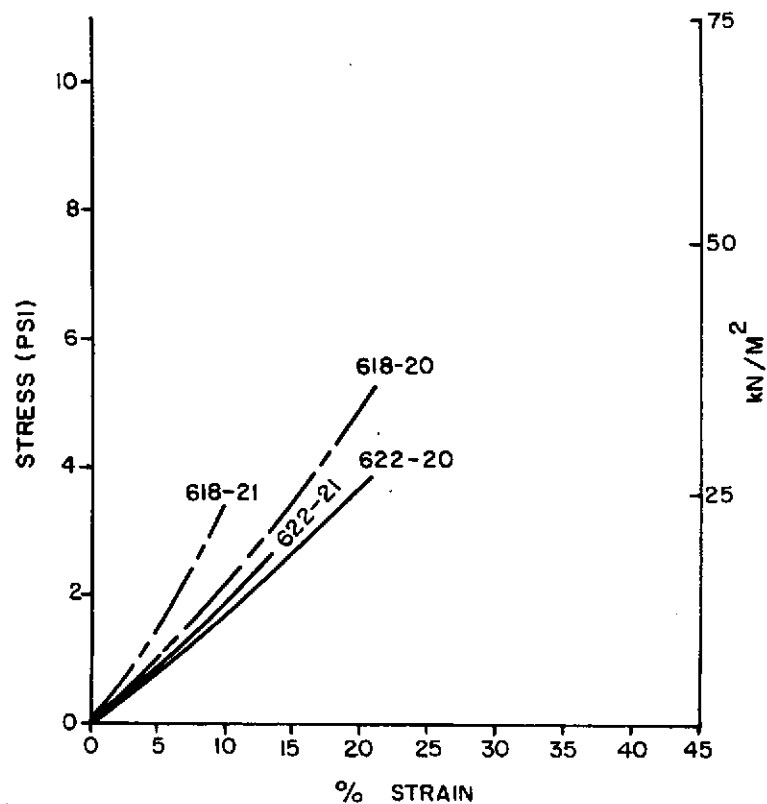


Figure 4-28. Tensile Stress-Strain Behavior  
For PD 200-16 (XY Direction)  
at 589°K

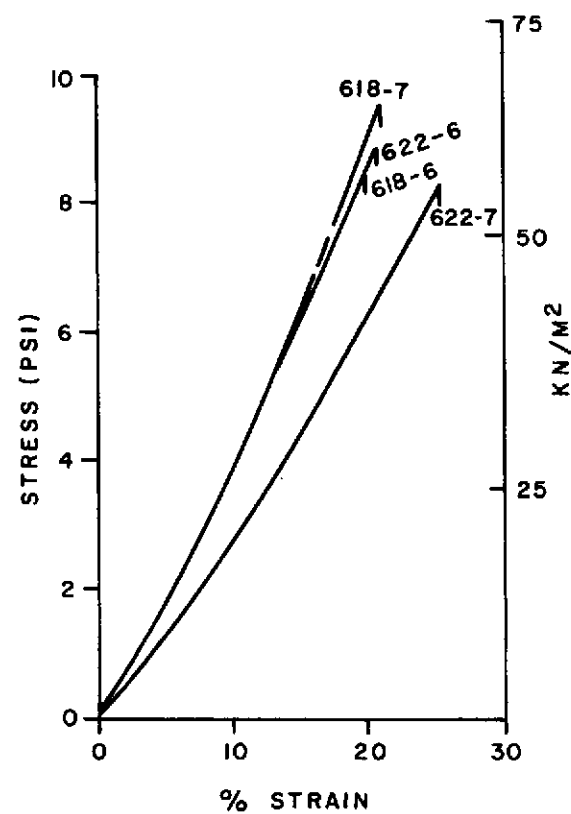


Figure 4-29. Tensile Stress-Strain Behavior  
For PD 200-16 (Z Direction)  
at 589°K

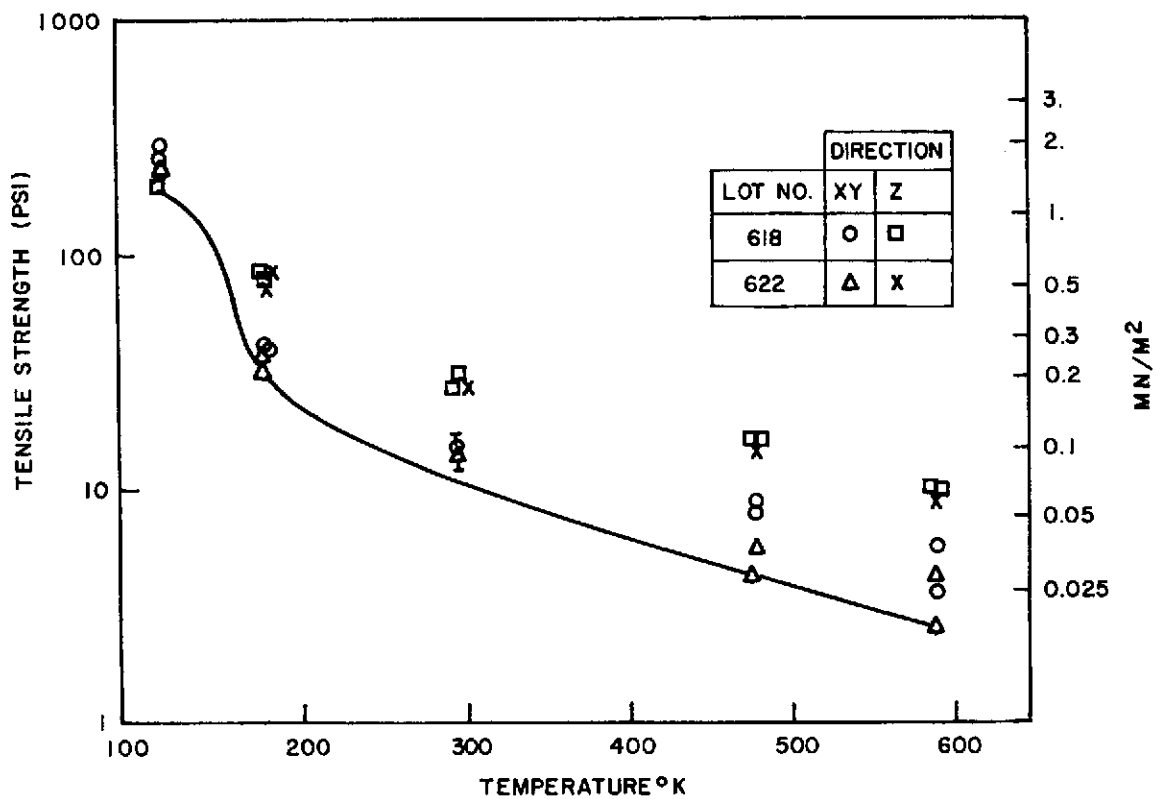


Figure 4-30. Tensile Strength of PD 200-16

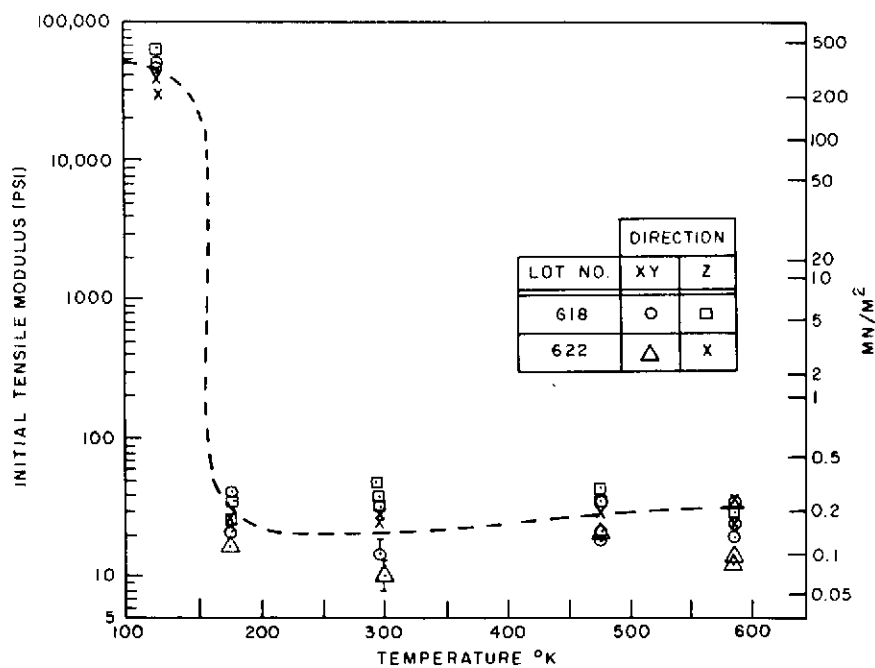


Figure 4-31. Initial Tensile Modulus Of PD 200-16



Another obvious observation is a lot-to-lot variation in mechanical properties. In each type test, specimens from Lot 618 have a higher strength and higher modulus than specimens from Lot 622. This is due, at least in part, to a difference in density between both lots as shown in the tabulated data.

Tensile strength is found to be very dependent upon temperature and will decrease by a factor of approximately 10 in going from the glass transition region up to 589°K (600°F). Decreasing in temperature through the transition region will increase the tensile strength by as much as 10 times.

Initial tensile modulus does not have a very great temperature dependence above the glass transition region. The values lie in the range 68.9-275.8 N/M<sup>2</sup> (10-40 psi). At the glass transition region, the modulus increases about 1000 times with a decrease in temperature through the region.

#### 4.3.2 SHEAR TESTS

##### 4.3.2.1 Experimental Procedure

Shear strength and modulus were obtained by subjecting cylinders of the foam to torsion. Test specimens consisted of 76.2 mm (3.0 inch) O.D., 50.8 mm (2.0 inch) I.D., 12.7 mm (0.50 inch) cylinders bonded between 76.2 mm (3.0 inch) diameter aluminum loading blocks.

Torque was applied by a geared down motor drive and measured by means of a calibrated, strain-gaged torsion load cell. Angle of twist was measured by means of the scheme shown in Figure 4-32. An analysis of load train deformation in the torsion tester showed that strain measurement error for PD 200-16 would be well less than one percent with this system at temperatures above the glass transition ( $T_g$ ). To obtain valid data at 116°K (-250°F) (below  $T_g$ ), the load train deformation was calibrated and subtracted from the observed data. The LVDT output was recorded as a continuous function of torsion load cell output on an XY recorder to provide torque-twist curves from which modulus of rigidity values could be derived.

The various test temperature environments were obtained in a small cylindrical environmental chamber using Calrod<sup>®</sup> heating elements for elevated temperatures and a controlled influx of boiling nitrogen as a coolant for low temperature tests. A typical failed specimen is shown in Figure 4-33.

##### 4.3.2.2 Results and Discussion

Shear test results are given in Table 4-4. Shear strength is shown as a function of temperature in Figure 4-34. Shear stress-strain curves at 116°K (-250°F) are shown in Figure 4-35. The stress-strain behavior at temperatures above the glass transition are presented in Figure 4-36. This curve, along with the tabulated shear modulus data in Table 4-4 reveal that the shape of the shear stress strain curve for PD 200-16 is virtually independent of temperature for  $T_g < T \leq 589^\circ\text{K}$  (600°F).

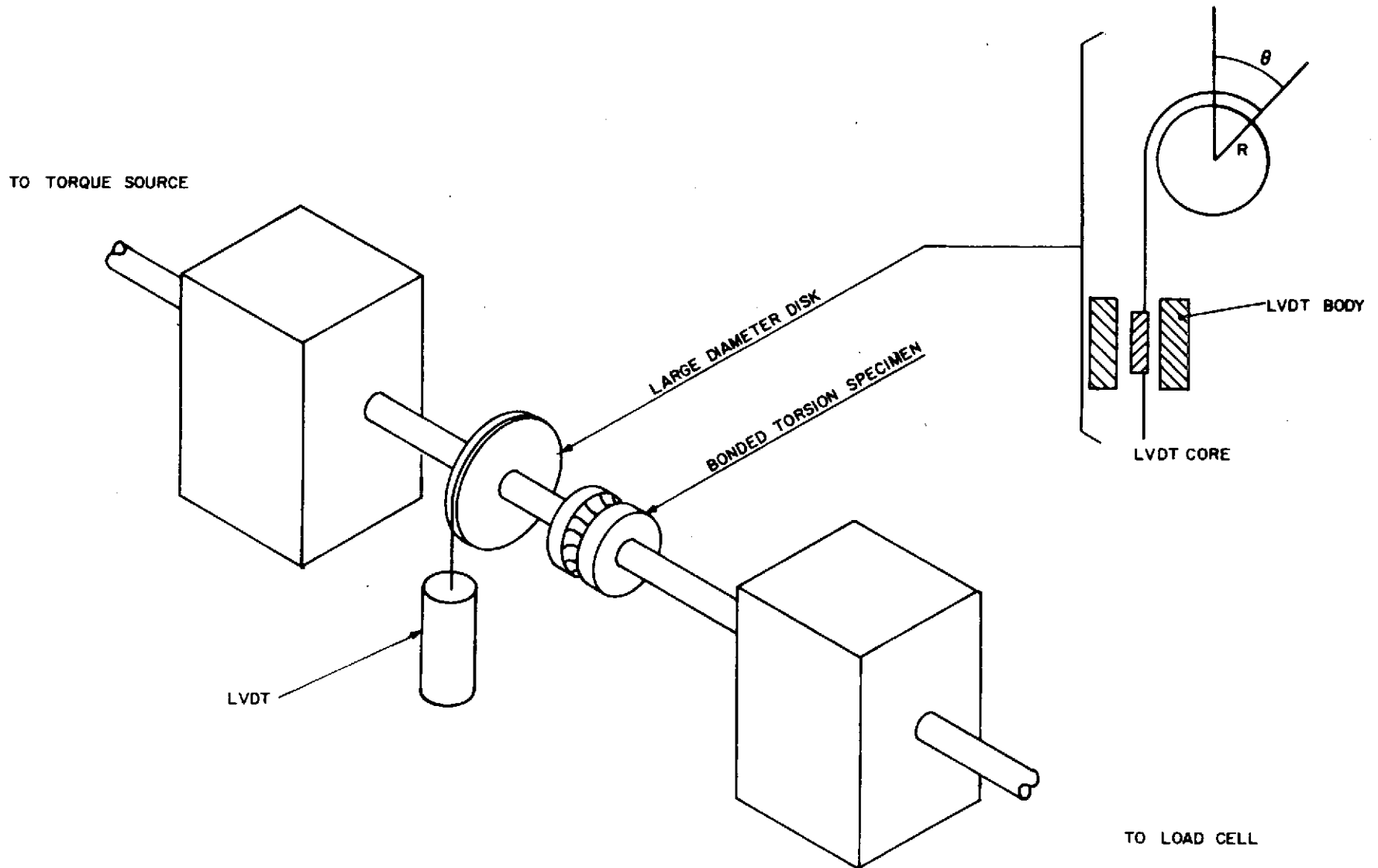


Figure 4-32. Shear Deformation Measurement Scheme

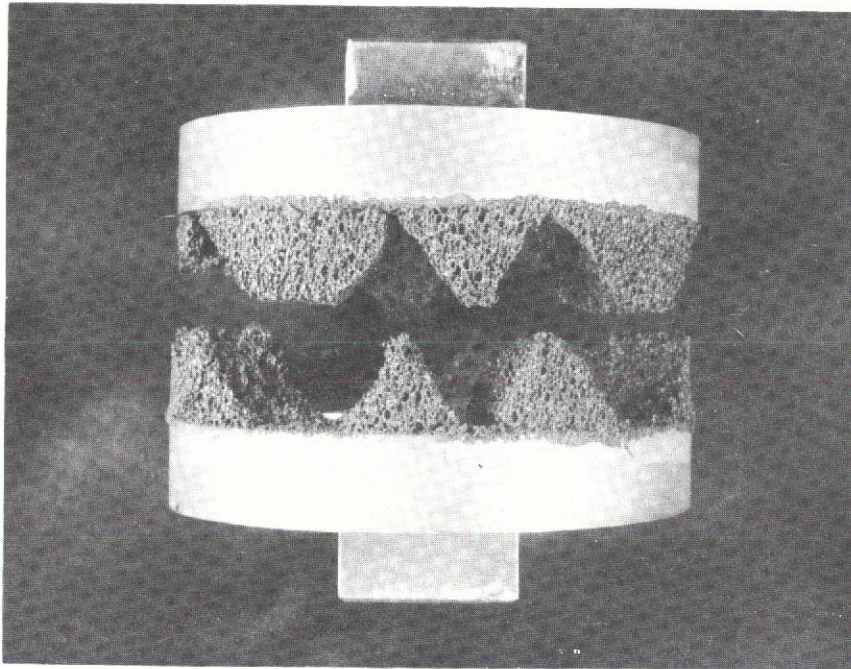


Figure 4-33. Torsional Shear Specimen, Post Test

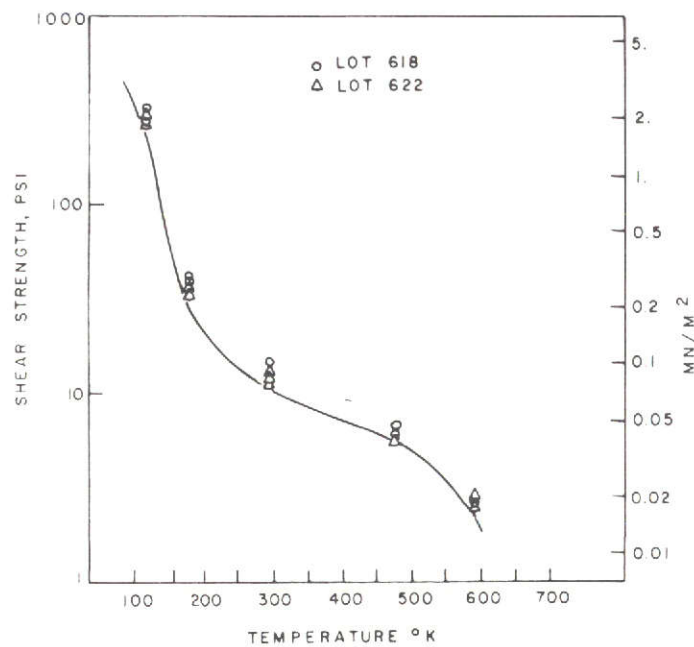


Figure 4-34. Shear Strength of PD 200-16

This page is reproduced at the back of the report by a different reproduction method to provide better detail.

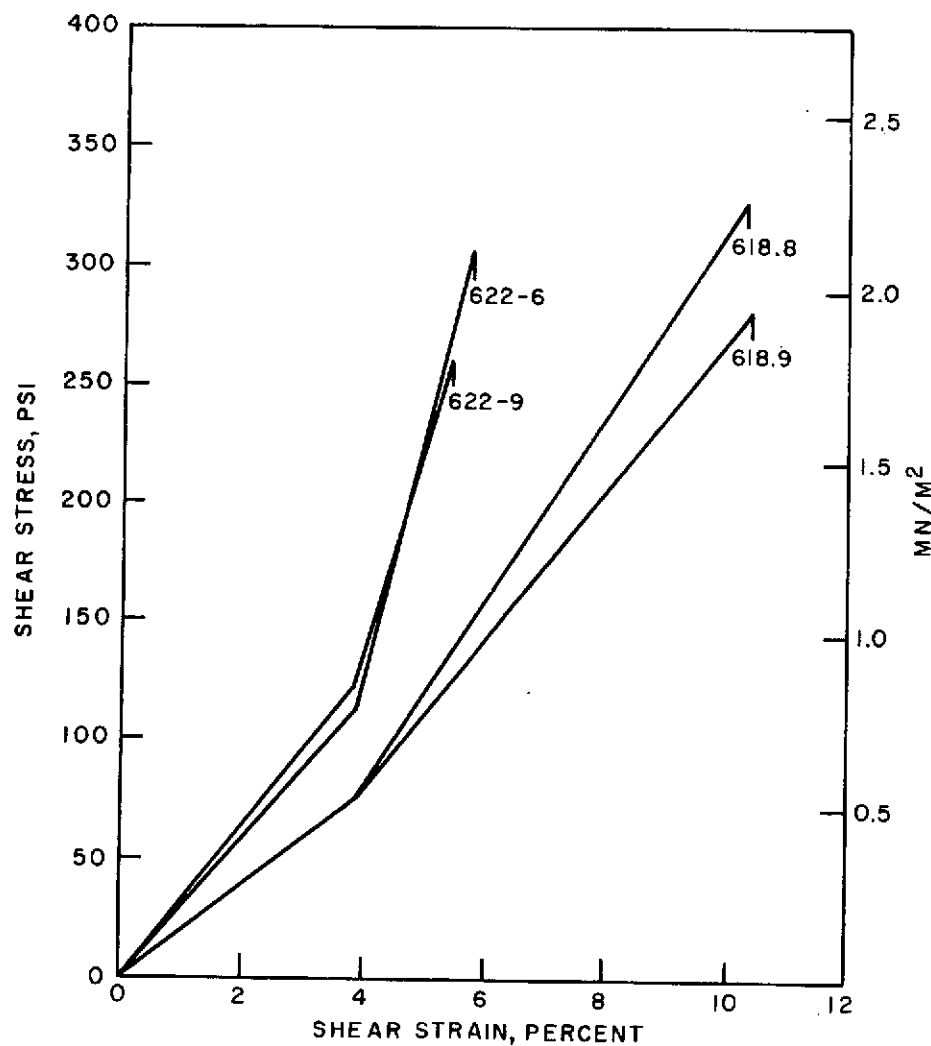


Figure 4-35. Shear Stress Strain Curves  
For PD 200-16 at 116°K

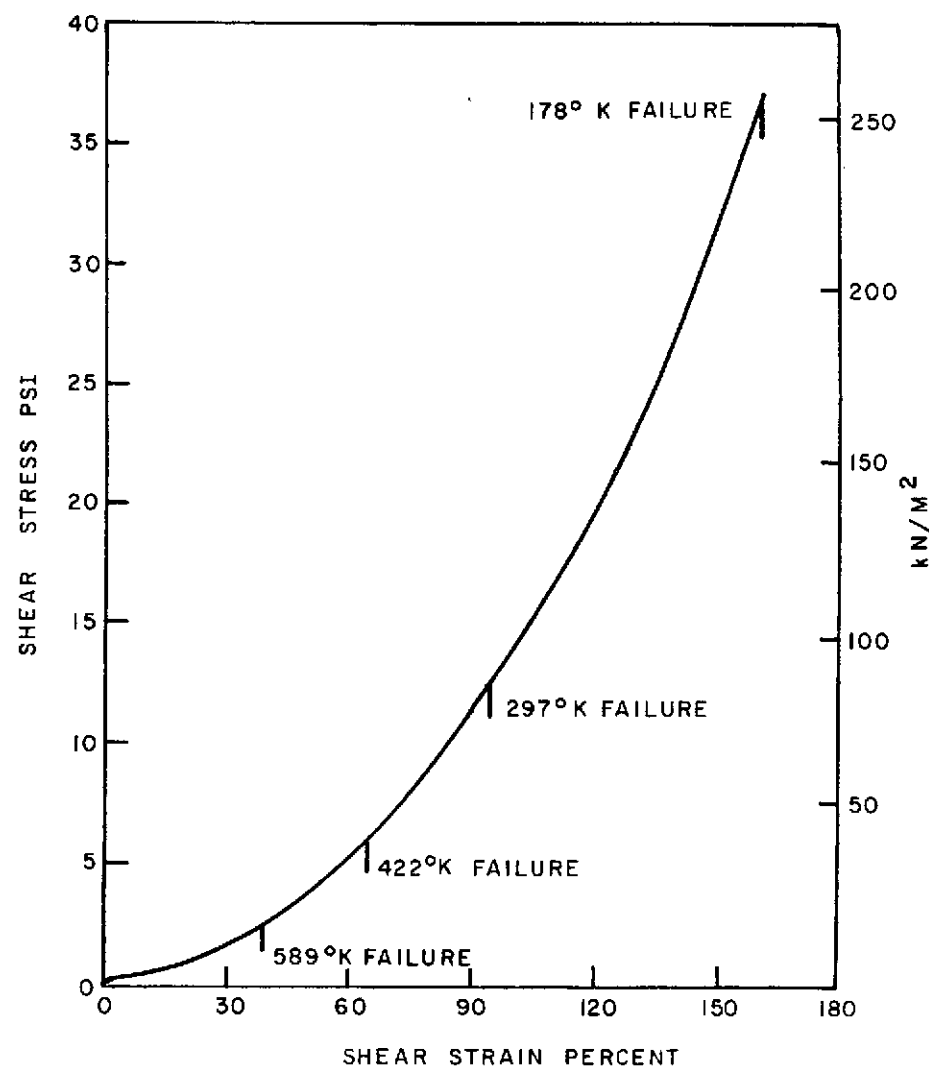


Figure 4-36. Typical Shear Stress-Strain  
Behavior Of PD 200-16 From  
Glass Transition to 589°K

TABLE 4-4. TORSIONAL SHEAR TEST DATA FOR PD 200-16

| Test Temperature<br>(°K) | Lot No. | Specimen No. | (1)<br>$\tau_u$<br>KN/M <sup>2</sup> | (2)<br>$G_1$<br>KN/M <sup>2</sup> | (3)<br>$G_s$<br>KN/M <sup>2</sup> |
|--------------------------|---------|--------------|--------------------------------------|-----------------------------------|-----------------------------------|
| 116                      | 618     | 8            | 2268.4                               | 13720                             | 21994                             |
|                          | 618     | 9            | 1944.3                               | 13652                             | 18685                             |
|                          | 622     | 6            | 2109.8                               | 20546                             | 37025                             |
|                          | 622     | 9            | 1820.2                               | 22132                             | 33715                             |
|                          |         | $\bar{X}$    | 2034.0                               | 17513                             | 27855                             |
| 178                      | 618     | 10           | 288.2                                | 29.0                              | 145.5                             |
|                          | 618     | 11           | 273.7                                | 68.3                              | 192.4                             |
|                          | 622     | 4            | 221.3                                | 35.2                              | 146.2                             |
|                          | 622     | 5            | 242.0                                | 33.8                              | 160.0                             |
|                          |         | $\bar{X}$    | 256.5                                | 41.4                              |                                   |
| 297                      | 618     | 1            | 95.8                                 | 49.0                              | 96.5                              |
|                          | 618     | 2            | 102.7                                | 64.1                              | 103.4                             |
|                          | 618     | 3            | 80.0                                 | 55.8                              | 87.6                              |
|                          | 622     | 1            | 85.5                                 | 80.7                              | 89.6                              |
|                          | 622     | 2            | 82.0                                 | 64.1                              | 84.8                              |
|                          | 622     | 3            | 73.8                                 | 70.3                              | 82.7                              |
|                          |         | $\bar{X}$    | 86.9                                 | 64.1                              | 91.0                              |
| 478                      | 618     | 6            | 42.2                                 | 41.4                              | 82.0                              |
|                          | 618     | 7            | 44.9                                 | 48.3                              | 84.8                              |
|                          | 622     | 7            | 40.5                                 | 33.1                              | 62.0                              |
|                          | 622     | 8            | 42.6                                 | 42.8                              | 74.5                              |
|                          |         | $\bar{X}$    | 42.5                                 | 41.4                              | 75.8                              |
| 589                      | 618     | 4            | 17.9                                 | 60.6                              | 47.6                              |
|                          | 618     | 5            | 16.7                                 | ----                              | 37.2                              |
|                          | 622     | 10           | 17.1                                 | 38.6                              | 36.5                              |
|                          | 622     | 11           | 18.8                                 | 51.0                              | 40.0                              |
|                          |         | $\bar{X}$    | 17.6                                 | 49.6                              | 40.7                              |

NOTES: (1) Ultimate shear strength  
(2) Initial tangent shear modulus  
(3) Secant shear modulus at failure

### 4.3.3 THERMAL EXPANSION

#### 4.3.3.1 Experimental Procedure

Thermal expansion tests were performed in a quartz tube dilatometer using 12.7 mm (0.5 inch) square, 50.8 mm (2.00 inch) long test specimens. Thermal strain was sensed and recorded as a function of the output of a Type T (copper-constantan) thermocouple imbedded in the test specimen. The test chamber is maintained under a slight positive pressure helium environment during a test run. Temperatures are obtained by means of a stainless steel tube coil carrying liquid nitrogen surrounded by a resistance heated clam shell heater. Each test cycle consisted of rapid cooling to about 105°K (-270°F), 20 to 30 minutes soakout followed by heating at a rate of approximately several °K per minute. Each raw data trace was reduced by judiciously selecting approximately 20-30 data points, calculating thermal strain ( $\Delta L/L$ ) and temperature (T), then replotting  $\Delta L/L$  vs. T to yield the curves presented in this report.

#### 4.3.3.2 Results and Discussion

Thermal expansion test results are shown in Figure 4-37 in the form of a plot of  $\Delta L/L$  vs. T data. These results are substantially identical to behavior observed in earlier work. Thus thermal expansion behavior is shown to be independent of density, as would be predicted.

### 4.3.4 TENSILE-STRESS RELAXATION

The stress relaxation behavior of PD 200-16 was examined at room temperature, 180°K (-135°F) and 116°K (-250°F). The 25.4 x 25.4 x 50.8 mm (1" x 1" x 2") specimens were bonded with RTV 560 to 25.4 mm square (1" x 1") aluminum bar stock. This arrangement was used to facilitate attachment to the load source and to provide for a uniform stress distribution on the PD 200-16. The specimens were loaded and held at a constant predetermined value of strain on an Instron test machine. The load drop was indicated on a plot of load vs. time. Tests were continued for a period of 60 minutes before the specimen was unloaded. The data are summarized in the attached Table 4-5.

The data clearly show that the stress-relaxation mechanism is significantly more predominant at 180°K (-135°F) than at either 297 or 116°K (75°F or -250°F). This leads to the conclusion that the degree of viscoelasticity (e.g., stress-relaxation or creep rate) of the RTV 560 system reaches a maximum at a temperature below 297°K (75°F) and possibly somewhere in the range 200 to 172°K (-100°F to -150°F). Since this behavior could be critical to understanding and predicting the low temperature thermostructural response of those structural elements incorporating RTV 560 in their design (including PD 200-16), it is recommended that the viscoelastic parameters of PD 200-16 be thoroughly characterized. (Note: This effort was conducted under NAS9-12855, NASA/MSc).

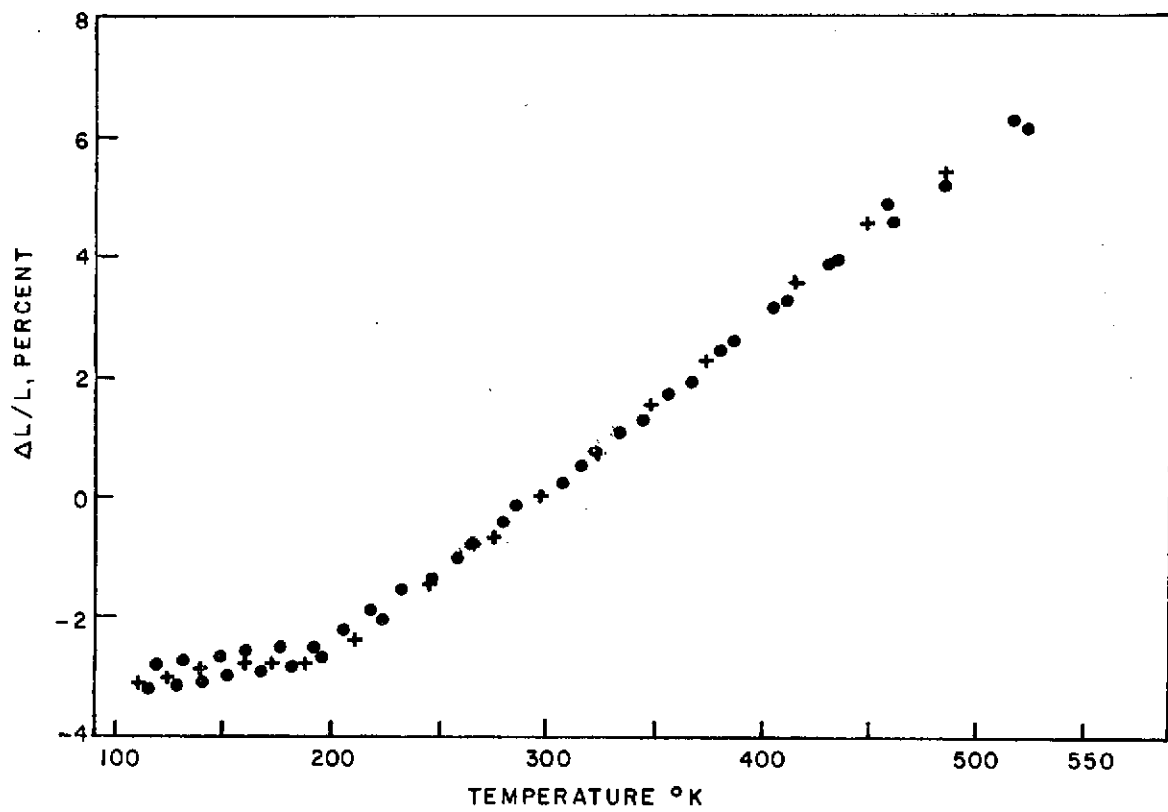


Figure 4-37. Thermal Expansion of PD 200-16

TABLE 4-5. SUMMARY OF STRESS RELAXATION DATA ON PD 200-16

| Temperature<br>(°F)      (°K) |     | Strain Level<br>(Percent) | After 60 Minutes<br>$\sigma/\sigma_0$ (%) |
|-------------------------------|-----|---------------------------|---|
| -250                          | 116 | 0.30                      | 0.912                                     |
|                               |     | 0.40                      | 0.939                                     |
|                               |     | 0.50                      | 0.992                                     |
| -135                          | 180 | 40                        | 0.801                                     |
|                               |     | 50                        | 0.748                                     |
|                               |     | 60                        | 0.767                                     |
|                               |     | 70                        | 0.703                                     |
| 75                            | 297 | 30                        | 0.928                                     |
|                               |     | 40                        | 0.911                                     |

#### 4.4 THERMAL PROPERTIES

##### 4.4.1 THERMAL CONDUCTIVITY

Guarded hot plate thermal conductivity measurements have been performed on low density PD-200, two discs 203 mm (eight inches) diameter, 6.4 mm (1/4 inch) thick with average 0.26 gm/cc (16.4 pcf) from RTV Lot 619. The measurements were made to characterize the material at the 10 N/M<sup>2</sup> (10<sup>-4</sup> atmosphere) orbital condition over the range 116°K to 589°K (-250°F to 600°F) and from 339°K to 589°K (150°F to 600°F) at 101. and 1. x 10<sup>3</sup> N/M<sup>2</sup> (1 and 10<sup>-2</sup> atmospheres).

The data are presented in graphic form in the attached figures. In Figure 4-38 the convention has been followed of placing flags on the symbols at clock positions equal to the exponent of the nominal pressure in atmospheres, e.g., 2 o'clock for 1 x 10<sup>3</sup> N/M<sup>2</sup> (10<sup>-2</sup> atmospheres). The data have also been cross-plotted in Figure 4-39 for conductivity as a function of ambient atmospheric pressure with mean sample temperatures of 144, 228, 339, and 589°K (-200, -50, +150 and 600°F) as a parameter.

The data have been carefully analyzed at the vacuum conditions to allow for slight biases due to guarding errors. The guarded hot plate apparatus was operated at all times within the ASTM C177 specification guarding requirements, using electronic proportional controllers. However, the combination of a low thermal conductivity level and the low internal heat transfer in the heaters and guards in vacuum has been studied in this laboratory and found to give more critical conditions than is generally known for realization of the best accuracy of which the GHP instrument is capable. Data points identified as probably biased high by a low guard condition are identified in the graph by a (+) sign. Again, note that this is a fine tuning modification, at its most extreme for the 500 micron (7 x 10<sup>-4</sup> atm) point at 339°K (150°F), 10% below the 10 N/M<sup>2</sup> (10<sup>-4</sup> atm) curve.



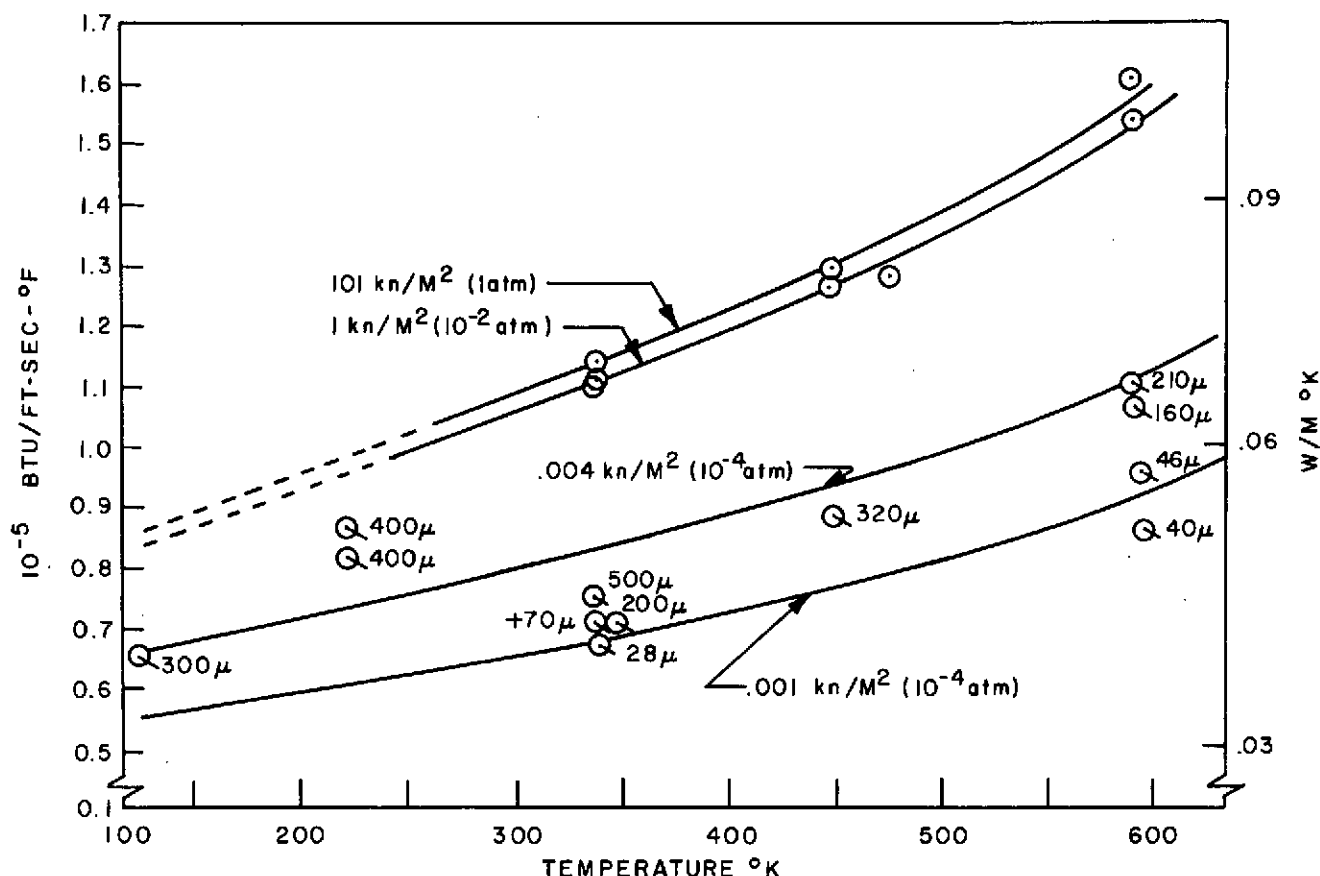


Figure 4-38. Thermal Conductivity of PD 200-16  
(0.26 gm/cc) RTV 560 Lot 619

Accordingly, the  $10 \text{ N/M}^2$  ( $10^{-4} \text{ atm}$ ) curves have been drawn taking account of this bias. The experimental difficulty in exactly specifying  $76 \pm 10$  microns ( $10^{-4} \text{ atm}$ ) was caused by absorbed atmospheric moisture in the vermiculite used to insulate the test stack. This moisture is usually driven off by running the instrument to  $478\text{--}589^\circ\text{K}$  at  $101 \times 10^3 \text{ N/M}^2$  ( $400\text{--}600^\circ\text{F}$  at 1 atmosphere) and then pumping down. (In this case the  $144^\circ\text{K}$  ( $-200^\circ\text{F}$ ) conditions were measured first, the moisture remaining.)

The conductivity data of Figure 4-39 shows that the conduction is not significantly reduced down to pressures of  $1 \times 10^3 \text{ N/M}^2$  ( $10^{-2} \text{ atm}$ ). Below this pressure the conductivity does drop sharply, apparently centered around a pressure of  $101 \text{ N/M}^2$  ( $10^{-3} \text{ atm}$ ). At  $339^\circ\text{K}$  ( $150^\circ\text{F}$ ) the reduction is 40%. This is a significant performance advantage for the new low density PD-200 bond system, which in its  $0.48 \text{ gm/cc}$  (30 pcf) formulation had no measureable ambient pressure thermal conductivity dependence (Ref. 4-1).

For the important  $339^\circ\text{K}$  ( $150^\circ\text{F}$ ) mean sample temperature condition two pressure dependence curves have been plotted in Figure 4-39. The solid line was derived from the smoothed data of Figure 4-38; the dashed line from direct plotting of the  $339^\circ\text{K}$  points themselves. At  $339^\circ\text{K}$  ( $150^\circ\text{F}$ ) the guarded hot plate is capable of at least  $\pm 5\%$  accuracy (note that the 70 micron point is known to be biased somewhat high, but less than 10%). However, the discrepancy between the two possible curves in this transition range is somewhat magnified by the expanded scale on which it has been plotted - the previously mentioned 500 micron  $339^\circ\text{K}$  ( $150^\circ\text{F}$ ) point is about 20% below the smoothed curve.

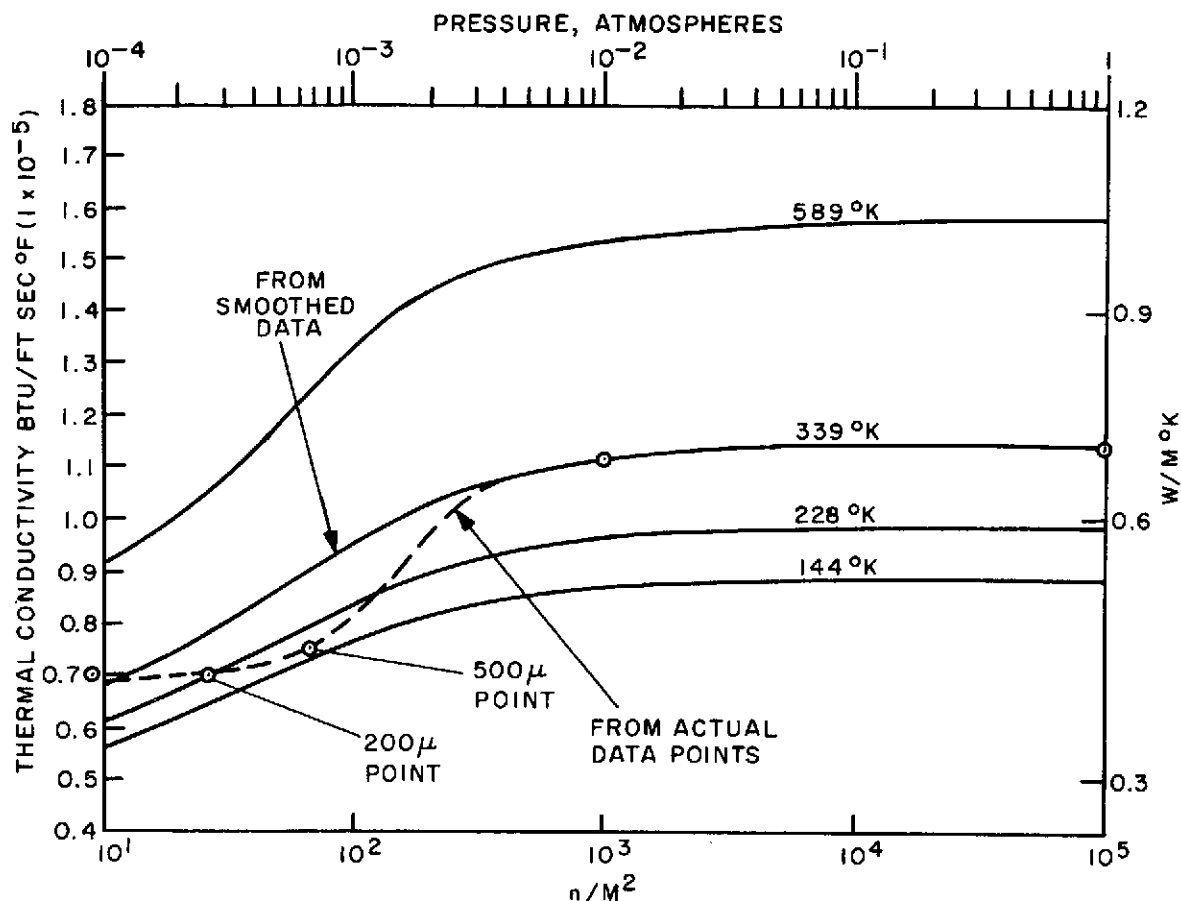


Figure 4-39. Pressure Dependence of the Thermal Conductivity of PD 200-16 (0.26 gm/cc)

#### 4.4.1.1 Mercury Intrusion Porosity Measurements

Three specimens of PD-200 were submitted for Pore Size Determination by Mercury Intrusion.

The specimens were:

1. Lot #622 0.24 gm/cc (14.8 pcf) untested
2. Lot #622 0.24 gm/cc (14.8 pcf) tested (Thermal Conductivity)
3. Lot #602 0.48 gm/cc (30 pcf)

The data obtained from Pore Volume Distribution Measurements by Mercury Intrusion is a normalized graph plot of the test data showing the cumulative liquid mercury intrusion in cc/gm with respect to pore diameter as well as pressure. By mercury penetration under pressure one can determine the size and quantity of void spaces and pores in porous materials. In addition, one can calculate specific surface area and obtain a measure of particle size distribution. The instrument for making the above determination must indicate the quantities of a nonwetting liquid, mercury, that may be forced under various pressures into the pores of the material in question and into the void spaces among particles. The material under examination is first dried and evacuated to remove absorbed gases and vapors. Mercury will

then penetrate the pores or void spaces in proportion to their size and to the pressure applied to the mercury. Macro size samples can also be used for these measurements with a maximum sample size of 9.5 mm (3/8") diameter by 25.4 mm (1") long being utilized, and are recommended for greater accuracy.

The raw data from Figures 4-40, 4-41, and 4-42 was examined in the following manner. Since the indicated pore volume is a function of the cc of mercury intruded in the sample, this volume was used to determine an approximate pore distribution over the entire range of pore size by first normalizing the data to % of maximum intrusion and then computing the incremental % intrusion. A plot of pore size versus % pore distribution is shown in Figure 4-43. Great differences are seen to exist in the Lot #622 specimens. Whereas a relatively Gaussian Distribution of pore sizes exists for the untested material it is quite obvious that the pores in the tested material have a much different distribution. It appears as though the pores, in the range of 320 to 200 microns were enlarged during thermal conductivity testing. During thermal conductivity testing the sample was heated to 616°K (650°F). As can be seen, the pores in the tested material in the above size range have virtually all been enlarged (ruptured) to provide a material with 71% of the pores larger than 340 microns (Table 4-6).

As would be expected, Lot #602 with a density of 0.48 gm/cc (30 pcf) shows the majority of the pores (80%) smaller than 150 microns, thus accounting for the higher density.

#### 4.4.2 SPECIFIC HEAT

The data in Figure 4-44 are for specific heat measurements made in nitrogen on PD-200 as normally post cured 450°K (350°F) for 16 hours as well as for material that had been heated continuously at 616°K (650°F) for 16 hours in air, after the normal post cure. In addition, data are presented for PD-200 which, after the normal post cure was subjected to an exposure of 100 cycles at 616°K (650°F) for 20 minutes/cycle. It is seen that aging at the higher temperatures reduces the specific heat by approximately 5% at 366°K (200°F). There was no evidence of degradation up to 756°K (900°F).

An exothermic transformation is evident for the normally post cured material at around 616°K (650°F). This is not seen for the heat aged samples.

Measurements were made down to 150°K (-190°F) without evidence of a glass transition temperature which would have been revealed as a sharp increase in the specific heat value.

#### 4.4.3 TGA

A thermogravimetric analysis (TGA) curve for PD-200 is shown in Figure 4-45. The test was run in vacuum. It is seen that the onset of rapid degradation as evidenced by a rapid increase in weight loss does not occur until approximately 756°K (900°F).

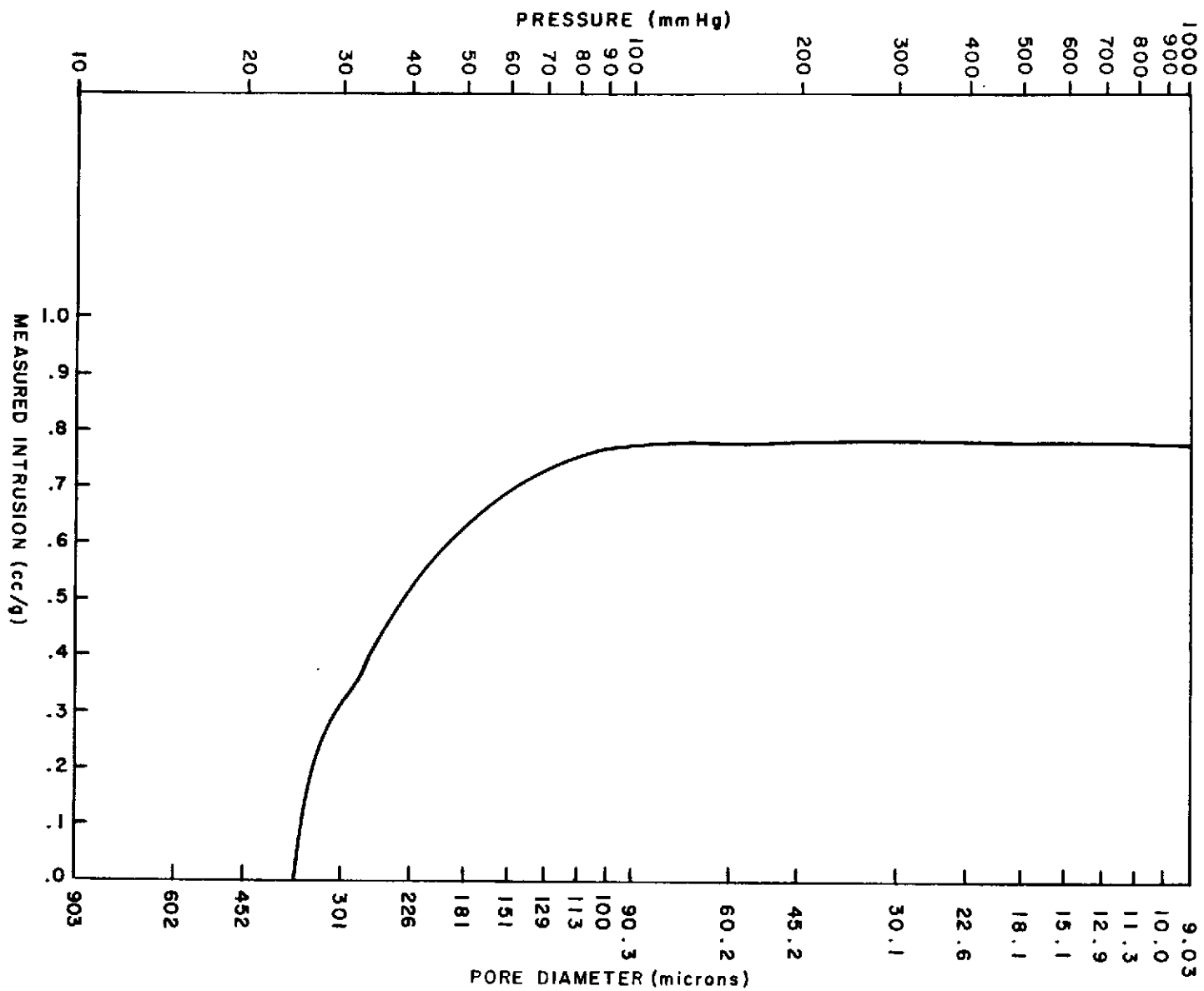


Figure 4-40. Macro-Pososimeter Test, Lot #622 Untested

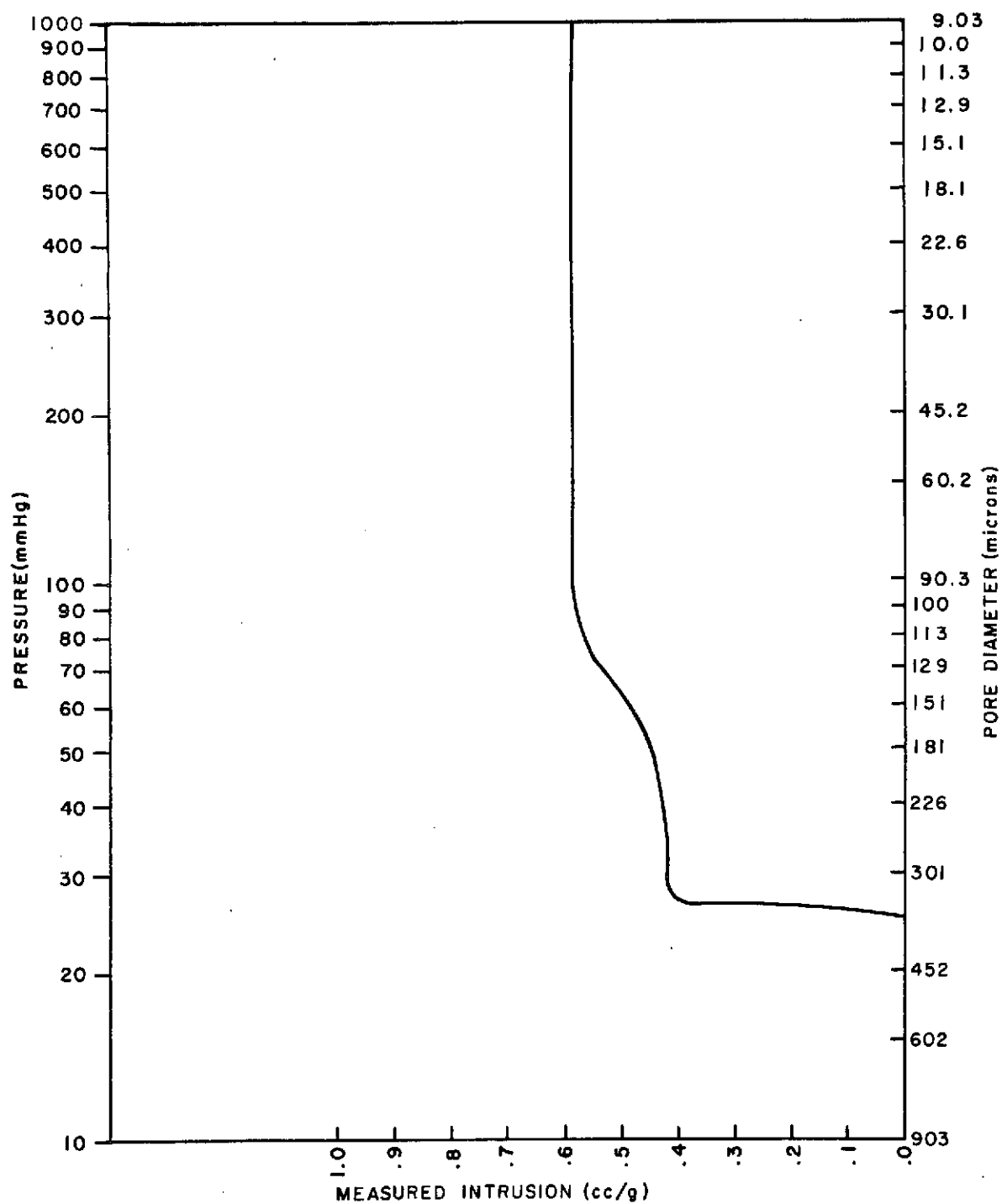


Figure 4-41. Macro-Porosimeter Test, Lot #622 Tested

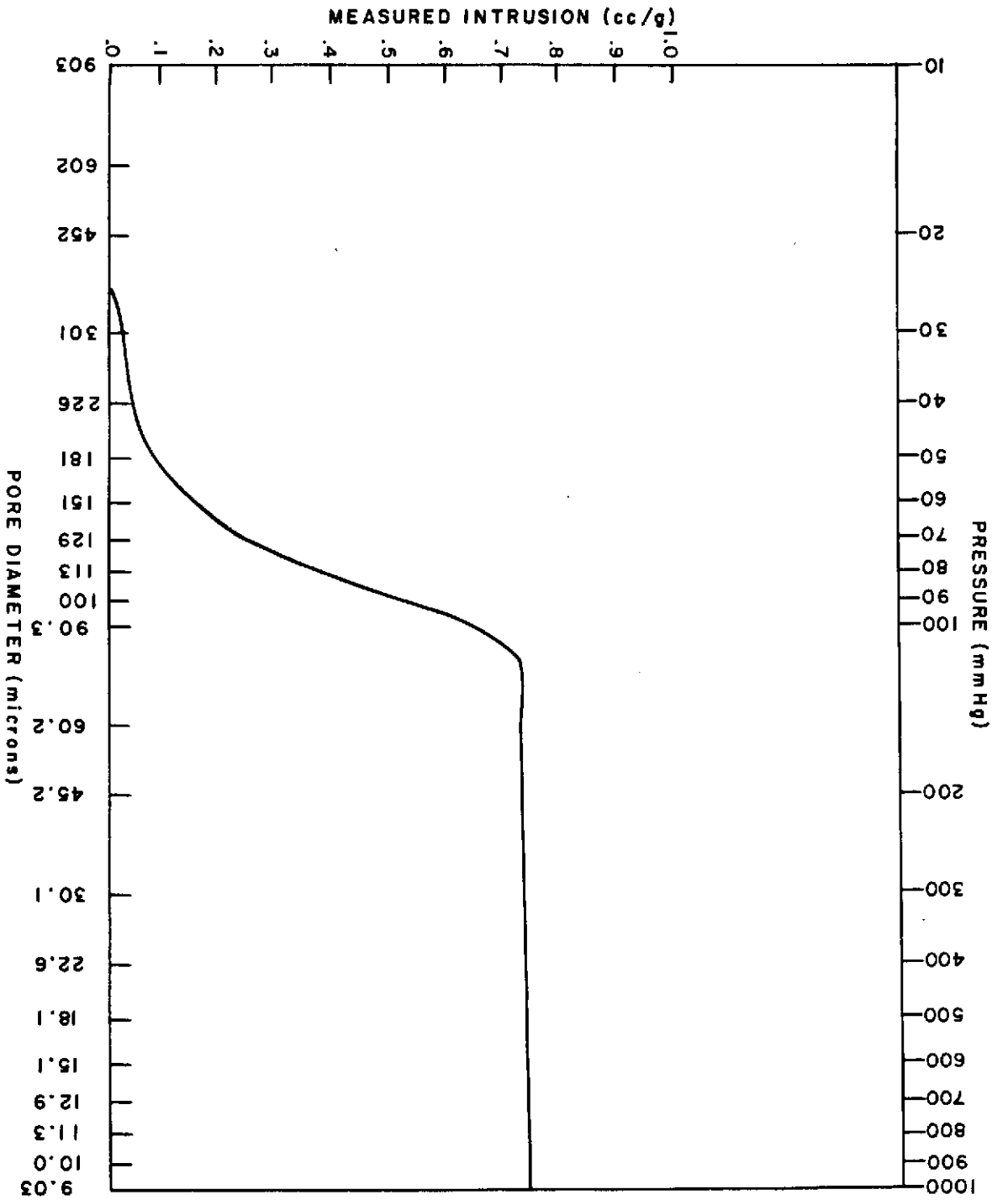


Figure 4-42. Macro-Porosimeter Test, Lot #602

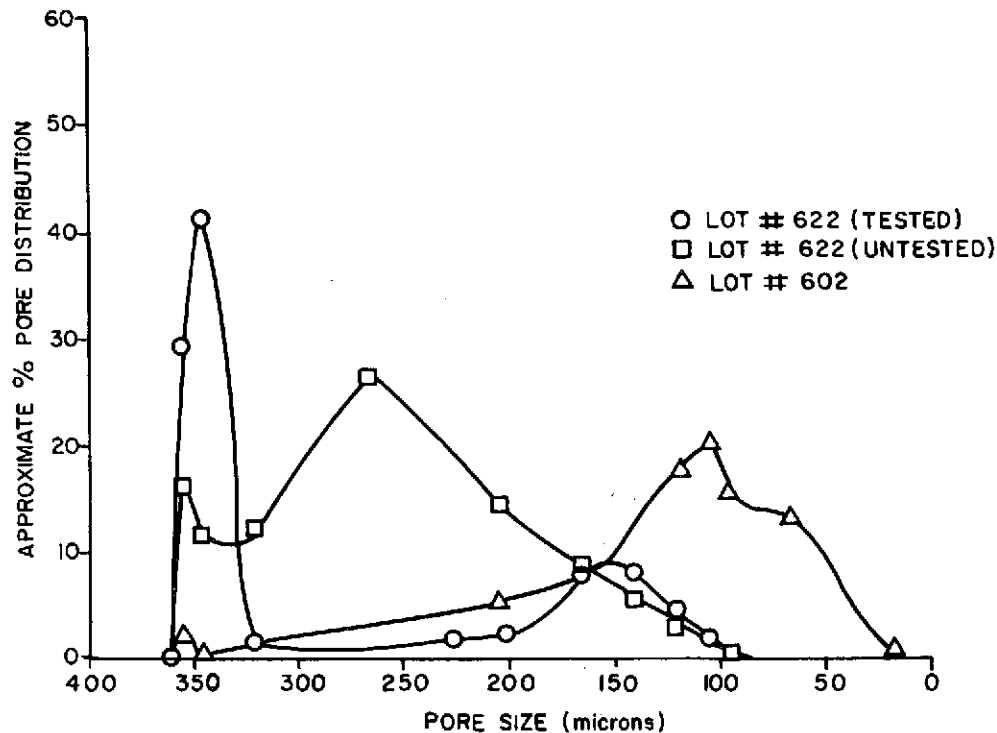


Figure 4-43. Pore Size vs Percent Pore Distribution

Since PD-200 is based on RTV-560, this is also the decomposition temperature of the adhesive system used for PD-200. Since the design temperature for the bond between the ceramic and PD-200 is  $\sim 616^{\circ}\text{K}$  ( $650^{\circ}\text{F}$ ), it is seen that a significant overshoot capability is built into this attachment system. This is a significant factor, especially for a man-rated system.

#### 4.4.4 Thermal Cycling (Low Temperature)

Thermal cycle tests have been conducted on PD-200-16 bonded with RTV-560 to aluminum. The assembly consisted of a  $203 \times 203 \times 38$  mm ( $8'' \times 8'' \times 1.5''$ ) panel of mul-lite bonded to an aluminum panel with RTV-560 and a 6.4 mm (0.25") thick pad of PD-200-16. The assembly was cycled to  $116^{\circ}\text{K}$  ( $-250^{\circ}\text{F}$ ) over a period of 4 hours, cold soaked for 75 minutes and warmed to room temperature over a 4 hour period.

The same assembly was then cycled to  $89^{\circ}\text{K}$  ( $-300^{\circ}\text{F}$ ) over a 6 hour period, cold soaked for 75 minutes and warmed to room temperature over a 6 hour period. No evidence of ceramic cracking, PD-200-16 tear, or adhesive delamination was observed in any of the tests despite the fact that the exposure temperatures were considerably lower than the glass transition temperature of the RTV-560 utilized both in the PD-200-16 foam bond and as the adhesive.

Figure 4-44. Specific Heat of PD-200 (Lot 602)



TABLE 4-6. CALCULATED PORE DISTRIBUTION FOR SAMPLES OF PD-200

| Indicated Cumulative Pore<br>Volume cc/gm |                        |                      |          | Cumulative % of Pores Having Volumes Larger<br>than Indicated Diameter (and increments (%) ) |                      |                |
|---|------------------------|----------------------|----------|--|----------------------|----------------|
| Pore<br>Diameter<br>Microns               | Lot #622<br>(untested) | Lot #622<br>(tested) | Lot #602 | Lot #622<br>(untested)   | Lot #622<br>(tested) | Lot #602       |
| 360                                       | 0                      | 0                    | 0        | 0<br>(16)  | 0<br>(29.4)          | 0<br>(2.4)     |
| 350                                       | 0.125                  | 0.170                | 0.018    | 16<br>(11.5)   | 29.4<br>(41.5)       | 2.4<br>(0.3)   |
| 340                                       | 0.215                  | 0.410                | 0.020    | 27.5<br>(12)   | 70.9<br>(1.4)        | 2.7<br>(1.3)   |
| 300                                       | 0.309                  | 0.418                | 0.030    | 39.5<br>(26.3)   | 72.3<br>(1.9)        | 4.0<br>(2.7)   |
| 225                                       | 0.515                  | 0.429                | 0.050    | 65.8<br>(14)   | 74.2<br>(2.4)        | 6.7<br>(5.1)   |
| 180                                       | 0.625                  | 0.443                | 0.088    | 79.8<br>(8.6)  | 76.6<br>(7.8)        | 11.8<br>(7.3)  |
| 150                                       | 0.692                  | 0.488                | 0.142    | 88.4<br>(5.2)  | 84.4<br>(7.8)        | 19.1<br>(12.9) |
| 130                                       | 0.733                  | 0.533                | 0.238    | 93.6<br>(2.8)  | 92.2<br>(4.7)        | 32.0<br>(17.8) |
| 110                                       | 0.755                  | 0.560                | 0.370    | 96.4<br>(1.8)  | 96.9<br>(2.1)        | 49.8<br>(20.2) |
| 100                                       | 0.769                  | 0.572                | 0.520    | 98.2<br>(0.8)  | 99.0<br>(1.0)        | 70.0<br>(15.4) |
| 90  | 0.775                  | 0.579                | 0.634    | 99.0<br>(1.0)  | 100.0                | 85.4<br>(12.9) |
| 40  | 0.783                  |                      | 0.730    | 100.0  |                      | 98.3<br>(2.7)  |
| 10  |                        |                      | 0.742    |  |                      | 100.0          |

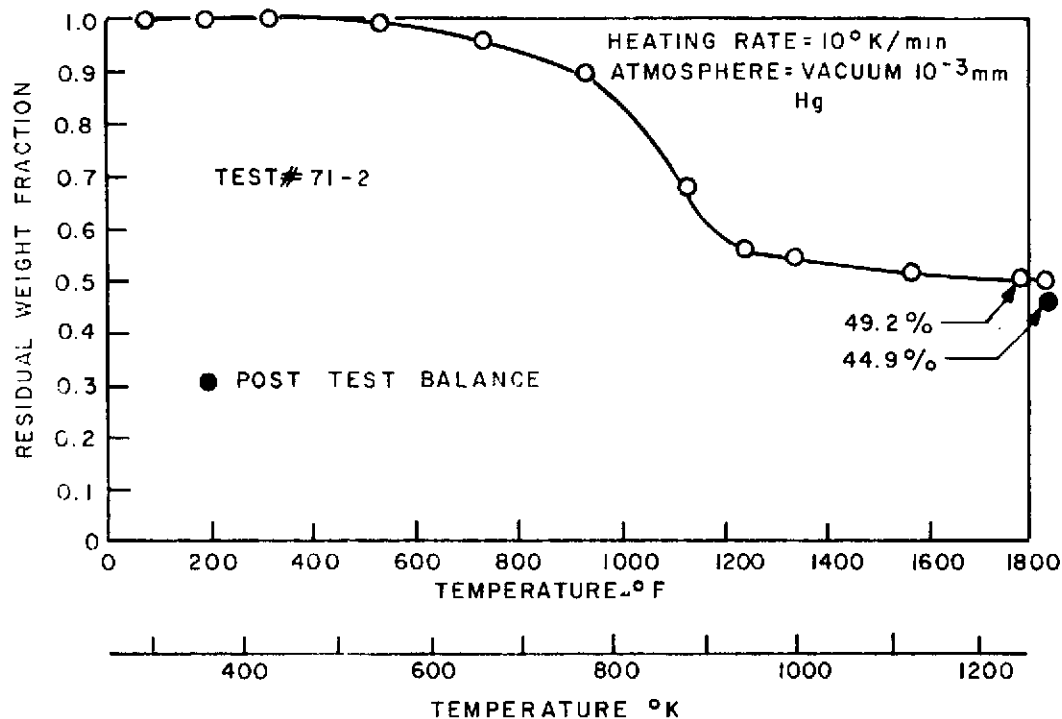


Figure 4-45. Thermogravimetric Analysis of PD 200 Cured At 450°K for 15 Hours

#### 4.4.5 EFFECT OF LONG TERM COLD SOAK ON TENSILE PROPERTIES OF PD-200-16

In prior mechanical test measurements the specimens were placed in the desired temperature environment and held there long enough to achieve thermal equilibrium before testing (20-40 minutes). Consequently, time-temperature effects were not considered.

The future uses of PD-200 may require a long term soak at low temperatures. The mechanical behavior, particularly initial elastic modulus, had not previously been determined as a function of time at a low temperature.

To preliminary characterize the time-temperature behavior 20 "dogbone" specimens were cut from a panel of PD-200-16. These were randomly selected for testing as follows:

1. Five specimens tested at room temperature
2. Five specimens tested at 116°K (-250°F) after attaining thermal equilibrium
3. Five specimens tested at 116°K (-250°F) after soaking at that temperature for 192 hours.

Results of the three sets of tests are given in Table 4-7 which lists: specimen, density, initial modulus, ultimate strength, ultimate strain and mode of failure.

At 116°K (-250°F) the properties measured in this study showed a greater variability in mechanical properties than previous data. However, the properties are in the same range.

Testing at 116°K (-250°F) after 192 hours soak revealed modulus values within the range found for the specimens tested after attaining thermal equilibrium at 116°K (-250°F). More problems are experienced in testing these soaked specimens since it is imperative that the specimen be inserted in the grips and the extensometer attached in the minimum of time to prevent any appreciable temperature increase in the specimen. These problems are reflected in the results of the tests.

Average values of the results on the specimens tested after equilibrium and after 192 hours are similar, and thus it appears as though there is no time-temperature effect. However, because of the large variation in properties no final conclusion on the time-temperature effect can be made from these tests.

It is recommended that to investigate time-temperature dependence, one specimen be used for each temperature and that test be performed at predetermined time intervals (geometric progress of time). Replicate specimens should be run to investigate the variability of time-temperature dependence between specimens. A dynamic technique such as a torsional pendulum would be appropriate for such testing, since the material is not strained to an irreversible level and the tests can be run many times on the same specimen.

#### 4.4.6 ARC TEST

In conjunction with an in-house testing program, space was found available in a series of arc tests conducted in the GE Hyperthermal arc facility. The tests were conducted in the tunnel mode of the facility. Air is heated to a high enthalpy in the Tandem Ger-dien heater and expanded into a 152 cm (five foot) diameter test tank holding the model. The tank pressure was held at 12 mm Hg.

The model tested was 152.4 mm (6.0 inch) wide x 139.7 mm (0.460 inch) thick, bonded to a 1.52 mm (0.060 inch) thick aluminum back plate using GE RTV-560. The specimen was mounted at 30° to the flow which would simulate flow against an exposed bonding edge surface.

The enthalpy was such that during the run time of 250 seconds (with 200 seconds of soak-out) a surface temperature of 1505°K (2250°F) was realized with a bond temperature of 700°K (800°F) maximum.

TABLE 4-7. TENSION TEST RESULTS ON PD 200-16 SPECIMENS  
TESTED AT VARIOUS TEMPERATURES AND CONDITIONS

(A) - Room Temperature Tests

| Specimen  | $\rho$<br>gm/cc | E<br>KN/M <sup>2</sup> | $\sigma_u$<br>KN/M <sup>2</sup> | $\epsilon_u$<br>(%) | Failure<br>Mode* |
|-----------|-----------------|------------------------|---------------------------------|---------------------|------------------|
| 6         | .25             | 105.5                  | 111.7                           | 64.0                | R                |
| 4         | .26             | 99.3                   | 117.2                           | 68.0                | R                |
| 12        | .26             | 88.9                   | 114.4                           | 63.2                | R                |
| 2         | .26             | 100.0                  | 99.3                            | 63.2                | R                |
| 11        | .26             | 99.3                   | 106.2                           | 62.6                | R                |
| $\bar{X}$ |                 | 98.6                   | 109.6                           | 64.8                | -                |

(B) - 116°K Tests

| Specimen | $\rho$<br>gm/cc | E<br>MN/M <sup>2</sup> | $\sigma_u$<br>KN/M <sup>2</sup> | $\epsilon_u$<br>(%) | Failure<br>Mode* |
|----------|-----------------|------------------------|---------------------------------|---------------------|------------------|
| 10       | .26             | 276.8                  | 1834.0                          | .721                | E. R.            |
| 15       | .26             | 562.4                  | 1572.0                          | .274                | G. L.            |
| 14       | .26             | 315.7                  | 1447.9                          | .490                | G. L.            |
| 3        | .26             | 253.8                  | 2096.0                          | .880                | E. R.            |
| 18       | .26             | 531.2                  | 1530.6                          | .288                | G. L.            |
| X        |                 | 388.0                  | 1696.1                          | .531                | -                |

(C) - 116°K After 192 Hours

| Specimen  | $\rho$<br>gm/cc | E<br>MN/M <sup>2</sup> | $\sigma_u$<br>KN/M <sup>2</sup> | $\epsilon_u$<br>(%) | Failure<br>Mode*                         |
|-----------|-----------------|------------------------|---------------------------------|---------------------|--|
| 8         | .26             | 390.7                  | 1599.6                          | .451                | G. L.                                    |
| 9         | .26             | (1)                    | 1323.8                          | (1)                 | R  |
| 7         | .26             | 343.1                  | >1600.                          | >.466               | Grip                                     |
| 17        | .26             | 363.1                  | >1531.                          | >.418               | Could<br>not<br>grip<br>kept<br>slipping |
| 5         | .25             | 449.5                  | 1461.7                          | .306                | R  |
| $\bar{X}$ |                 | 386.6                  | > 1503.                         | >.410               |  |

\* R = Radius G. L. = Gage Length E. R. = Edge of Radius

(1) Modulus and strain could not be resolved.

Post-test, the surface was covered with a fragile char layer with no extensive crack pattern evident. The time-temperature profile at various time intervals is shown in Figure 4-46.

#### 4.5 CERAMIC ADHERENDS

The ceramic adherend of the experimental test matrix (Table 4-8) was reviewed during the 1/18/73 program review meeting, and a mutual agreement was reached to utilize silica as the light weight ceramic rather than mullite. The decision to utilize silica was as a result of the Shuttle program shift in emphasis to silica. The selected material was GE-RESID REI-Silica-9. A description of the material is found in Appendix A-3.

The test specimens consisted of 25.4 x 25.4 x 31.8 mm (1" x 1" x 1.25") prisms of 0.14 gm/cc (9 pcf) silica bonded to aluminum and steel (for high temperature tests) tensile blocks with 6.4 mm (0.25 inch) thick pads of PD 200-16, RTV-560, primer SS-4004 on the silica, and primer SS-4155 on the metals.

All tests were performed in an Instron test machine on specimens in three different material conditions:

- As fabricated
- Thermally aged for 33 hours at 616°K (650°F) in air
- Thermal cycled from room temperature to 200°K, to 616°K, to room temperature

The results of this series of experiments are shown in Table 4-9, and show a degradation in strength from thermal conditioning in air. All test specimens failed as shown in Figure 4-47, cohesive in the silica at the silica/RTV-560 interface.

The as-fabricated tensile strength at room temperature is lower than the tensile strength of either adherend ( $\bar{X} = 85.5 \times 10^3 \text{ N/M}^2$  for the silica lot,  $\bar{X} = 179.2 \times 10^3 \text{ N/M}^2$  for the PD 200-16 lot utilized), and suggests further study of the REI Silica bond interface.

#### 4.6 REFERENCES

- 4-1. Lowe, D. L., "Mechanical Properties of PD 200 Foam Bond (Lot No. 602)", PIR 9134-778A, 9/9/71.
- 4-2. Lowe, D. L., "Mechanical Properties of PD 200 Foam Bond (Lot No. 604)", PIR 9134-794, 9/30/71.

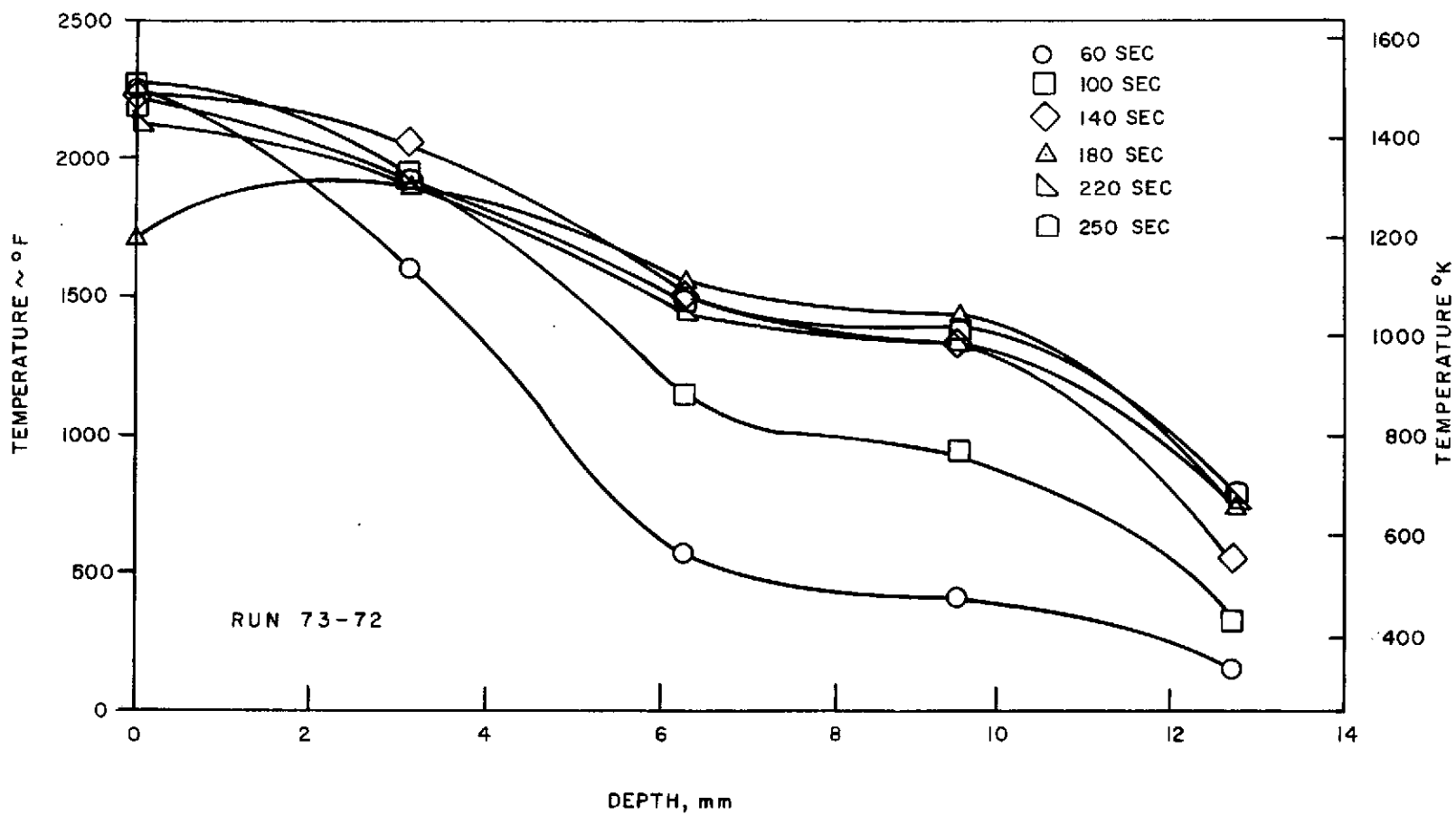


Figure 4-46. PD 200-16 Arc Test

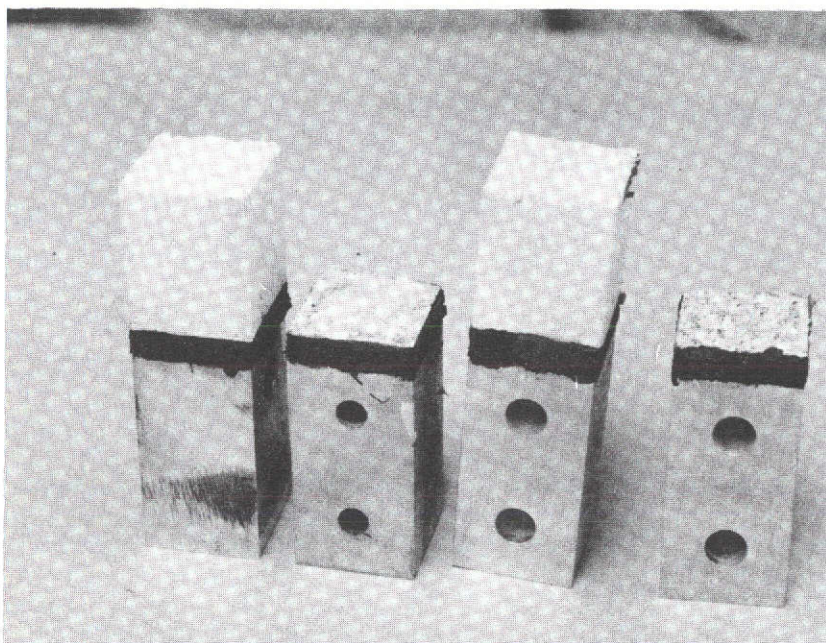


Figure 4-47. Typical Failed Specimens

TABLE 4-8. EXPERIMENTAL MATRIX FOR EVALUATION OF SELECTED ADHESIVE SYSTEM

| Test Type                       | Material Condition | Number Of Tests |       |       |
|---------------------------------|--------------------|-----------------|-------|-------|
|                                 |                    | 200°K           | 279°K | 616°K |
| 1. Thermal Conductivity         | As Received        | Two Specimens   |       |       |
| 2. Specific Heat                | As Received        | One Specimen    |       |       |
| 3. Thermal Expansion            | As Received        | One Specimen    |       |       |
| 4. Shear Strength and Modulus   | As Received        | 5               | 5     | 5     |
| 5. Tensile Strength and Modulus | As Received        | 5               | 5     | 5     |
| 6. BC Tensile (1)               | Aged (2)           | 5               | 5     | 5     |
| 7. BC Tensile (1)               | Cycled (3)         | 5               | 5     | 5     |

(1) "BC" indicates bonded to ceramic insulation. The ceramic recommended is GE REI-Silica-9.

(2) Aged 33 hours at 589°K.

(3) Cycled from 200°K to 616°K.

This page is reproduced at the back of the report by a different reproduction method to provide better detail.

TABLE 4-9.  
CERAMIC ADHEREND BUTT TENSILE TEST RESULTS

| Specimen Condition  | Nominal Failure <sup>(1)</sup> Stress (N/M <sup>2</sup> X 10 <sup>3</sup> )<br>Indicated Temperature |                                |                                |
|---|--|--------------------------------|--------------------------------|
|   | 200°K  | 297°K                          | 616°K                          |
| As-Fabricated   | 25.3<br>56.5<br>21.1<br>(34.3)   | 47.0<br>64.9<br>54.1<br>(55.4) | 44.3<br>31.4<br>(2)<br>(37.9)  |
| Exposed 33 Hours<br>at 616°K                                | 25.7<br>(2)<br>(2)<br>(25.7)   | 27.6<br>26.7<br>15.0<br>(23.1) | 25.0<br>(2)<br>(2)<br>(25.0)   |
| Thermally Cycled:<br>RT to 200°K<br>to RT to 616°K<br>to RT | 24.7<br>28.4<br>28.4<br>(27.2)   | 32.9<br>28.9<br>36.5<br>(32.8) | 40.0<br>32.1<br>24.7<br>(32.3) |

NOTE: 1. Mode of failure was identical for all tests ... See Figure 4-46.

2. Specimen failed in handling

3. Values in ( ) are average values



## SECTION 5

### APPLICATIONS DEVELOPMENT (TASK 4)

#### 5.1 GENERAL

A number of areas were explored in the development of application techniques for the PD 200-16 silicone foam. Among them were:

1. Primer selection and application
2. Substrate preparation
3. Adhesive application methods
4. Contact pressures during bonding and cure
5. Effective system density
6. Application to simulated airframe surfaces

In addition, several simulated service cycle tests at elevated temperature in vacuum were successfully conducted.

#### 5.2 PRIMER STUDY

In early bonding trials of PD 200-16 utilizing RTV-560 and SS-4004 silicone primer, some difficulties were met in the use of an air-cured system with SS-4004 primer. No adhesion problems, however, were encountered when the adhesive system was cured at 344°K (160°F) or greater.

Since successful application of PD 200-16 must also involve field retrofit applications where an air-cure is required, an investigation was begun to evaluate use of GE SS-4155 silicone primer in conjunction with RTV-560 bonding of the silicone foam. The primer, blue in color, is also somewhat less sensitive to primer thickness, than the SS-4004. However, for optimum results, the primer film should be less than 0.025 mm (0.001 inch).

In initial trials, 2.54 mm (0.1 inch) thick x 50.8 mm (2 inch) diameter specimens of PD-200 foam were bonded to 6061-T6 aluminum with SS-4155 primer and RTV-560. The primer was air-dried for 2 hours (7200 seconds) at a minimum relative humidity of 40% prior to RTV-560 application. Attempts were made to peel the system from the aluminum after air-cure, and after oven-cure. In all cases, cohesive failures in the PD-200 were observed. The qualitative data is shown in Table 5-1.

Aluminum and titanium single lap shear specimens with PD-200 were prepared with SS-4155 primer. The PD-200 in the bond area was 3.8 mm (0.15 inch) in thickness at a density of 0.45 gm/cc (29 pcf). The bond configuration was as shown in Figure 5-1. The specimens, room-temperature cured for seven days, and aged for 100 hours in air at 450°K, were tested at 116, 297, and at 450°K. Cohesive failures in the PD-200 foam were observed in all cases. The experimental data is listed in Tables 5-2 and 5-3. Based upon the results of this data, showing that the bond strength of the adhesive exceeds that of the foam at all test temperatures, GE SS-4155 primer is recommended for use in the room-temperature or oven-cure bonding of PD-200 silicone foams to non-porous adherends.

SS-4155 primer was subsequently utilized for all bonding applications on the contract.

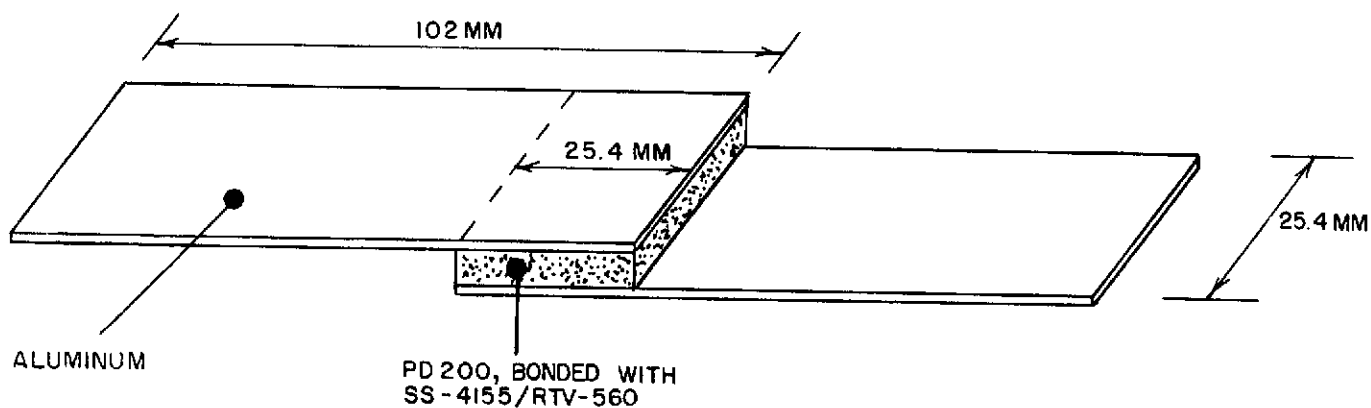


Figure 5-1. Lap Shear Configuration

The current laboratory method for applying the primer to metallic substrates has been limited to brush application per current SPBD\* recommendations. The primer is applied to the substrate using a soft camel-hair brush, following the same process as brush application of the previously used SS-4004. The drying time is determined by the appearance of a white, finely divided precipitate (haze) appearing on the metallic surface - usually 2-3 hours minimum at a minimum of 35% RH. The appearance of the white precipitate is related to the RH level, and at 45-50% RH, the dry time is approximately 2 hours (7200 seconds). The recommended maximum dry time is 48 hours. This haze should not be removed from the surface prior to adhesive application. The primer is applied in as thin a coating as possible, in no case thicker than 0.025 mm (0.001 inch).

\*General Electric Silicone Products Business Department

TABLE 5-1. QUALITATIVE BOND RESULTS, SS-4155 PRIMER

| Primer  | Primer<br>Lot No. | RTV-560<br>Lot No. | 3 Day, R. T. | 7 Day R. T. | Oven<br>Cure* |
|---------|-------------------|--------------------|--------------|-------------|---------------|
| SS-4155 | 94218             | 618                | COH          | COH         | COH           |
|         |                   | 621                |              |             |               |
|         |                   | 622                |              |             |               |
| SS-4155 | 109               | 618                |              |             |               |
|         |                   | 621                |              |             |               |
|         |                   | 622                |              |             |               |

\*344°K (160°F), 6 Hr. (21,600 seconds)

TABLE 5-2. ALUMINUM/PD-200/ALUMINUM LAP SHEAR DATA

| Test Temperature    | 7 Day, RT                      |                     | 100 Hr., 350°F (360,000 sec, 449.7°K) |                     |
|---------------------|--------------------------------|---------------------|---------------------------------------|---------------------|
|                     | Strength, $10^5 \text{ N/M}^2$ | Cohesive Failure, % | Strength, $10^5 \text{ N/M}^2$        | Cohesive Failure, % |
| -250°F<br>(116.3°K) | 27.16                          | 100                 | 28.13                                 | 100                 |
|                     | 27.99                          | 100                 | 31.44                                 | 100                 |
|                     | 27.44                          | 100                 | 30.13                                 | 100                 |
|                     | 29.85                          | 100                 | 28.41                                 | 100                 |
|                     | 28.96                          | 100                 | 29.78                                 | 100                 |
|                     | 28.27                          |                     | 29.58                                 |                     |
|                     |                                | $\bar{X}$           |                                       |                     |
| 75°F<br>(297°K)     | 3.53                           | 100                 | 3.21                                  | 100                 |
|                     | 3.91                           | 100                 | 3.14                                  | 95                  |
|                     | 3.88                           | 100                 | 3.22                                  | 100                 |
|                     | 3.58                           | 100                 | 3.07                                  | 80                  |
|                     | 3.30                           | 100                 | 3.04                                  | 98                  |
|                     | 3.64                           |                     | 3.10                                  |                     |
|                     |                                | $\bar{X}$           |                                       |                     |
| 350°F<br>(449.7°F)  | 2.13                           | 100                 | 1.76                                  | 100                 |
|                     | 2.12                           | 100                 | 1.96                                  | 100                 |
|                     | 2.03                           | 100                 | 1.77                                  | 100                 |
|                     | 1.61                           | 100                 | 2.33                                  | 100                 |
|                     | 2.17                           | 100                 | 2.25                                  | 100                 |
|                     | 2.01                           |                     | 2.01                                  |                     |
|                     |                                | $\bar{X}$           |                                       |                     |

Sand-blast, alkaline clean

RTV-560, Lot 618

SS-4155, Lot 109

TABLE 5-3. TITANIUM/PD-200/TITANIUM LAP SHEAR DATA

| Test Temperature   | 7 Days, R. T.                     |   | 33 Hrs., 650°F (118,800 sec, 616.3°K) |                     |
|--|-----------------------------------|---|---------------------------------------|---------------------|
|  | Strength, $10^5$ N/M <sup>2</sup> | Cohesive Failure, %                           | Strength, $10^5$ N/M <sup>2</sup>     | Cohesive Failure, % |
| -250°F<br>(116.3°K)<br><div style="text-align: right;">—<br/>X</div> | 45.85                             | 80  | 8.41                                  | 100 *               |
|  | 37.85                             | 100   | 9.79                                  | 100 *               |
|  | 38.20                             | 98  | 8.69                                  | 100 *               |
|  | 40.61                             | <div style="text-align: right;">—<br/>X</div> | 8.96                                  |                     |
| 75°F<br>(297°K)<br><div style="text-align: right;">—<br/>X</div>     | 5.85                              | 100   | 1.63                                  | 100                 |
|  | 4.94                              | 100   | 1.95                                  | 100                 |
|  | 5.73                              | 100   | 2.06                                  | 100                 |
|  | 5.50                              | <div style="text-align: right;">—<br/>X</div> | 2.01                                  | 100                 |
|  |                                   |   | 1.92                                  |                     |
| 600°F<br>(588.7°K)<br><div style="text-align: right;">—<br/>X</div>  | 1.14                              | 100   | 1.63                                  | 100                 |
|  | 1.17                              | 100   | 1.77                                  | 100                 |
|  | 1.15                              | 100   | 1.70                                  |                     |
|  | 1.15                              | <div style="text-align: right;">—<br/>X</div> |                                       |                     |

Sand-blast, alkaline clean

RTV-560, lot 618

SS-4155, lot 109

\*Cohesive on one face.

## 5.3 APPLICATION STUDIES

### 5.3.1 PLANE SURFACES

Studies were conducted to determine PD-200 application methods, adhesive weight pick-up, and the density change resulting from the adhesive weight.

The initially most promising of several approaches to applying RTV-560 (adhesive) to the sub-structure (aluminum) was by means of a semi-firm rubber roller. Although application of the adhesive to the sub-structure visually appeared uniform, further examination after cure showed the film thickness to be too thin, 0.08-0.12 mm, (0.003-0.005") for adequate bonding. For normal adhesive bonding (two solid, flat surfaces) that film thickness would be ideal, but for cellular structures (i.e., PD-200) the total thickness of 0.12 mm (.005") did not allow mechanical interlocking, or filleting, as well as chemical bonding of the foam surface.

The alternate approach to the rubber roller application was the utilization of a commercial paint roller (short nap mohair) generally used for "Latex" paints.

Using this application method on a 610 x 662 mm (24" x 30") unprimed (for easy removal of the cured film to allow bond inspection) aluminum sheet resulted in a uniform bond film which averaged  $0.18 \pm 0.02$  mm (0.007"  $\pm$  .001"). Since this method appeared more practical for TPS application, it was further investigated in combination with PD-200 foam sheets.

The initial method of determining bondline thickness was to measure the PD-200 thickness at multiple points, establish the structure thickness, at the same points, bond the composite by roller application methods, then re-measure (by dial indicator) at the previously indicated points. It became apparent from the weight pick up and calculated theoretical bondline thickness that attempting to measure thickness mechanically was not useful due to wide variations in thickness measurements on the easily compressible foam.

Following this, a series of pre-weighed 152 x 152 x 6.4 mm (6" x 6" x .250") PD-200 foam sheets 0.48 gm/cc (30 pcf) were bonded to unprimed aluminum panels utilizing the "paint roller" method. These were cured, stripped from the aluminum, trimmed to remove flash and reweighed. Based upon an RTV-560 density of 1.43 gm/cc



(89 pcf), it was calculated that 8.4 grams of adhesive on the PD-200 sheets was equivalent to 0.25 mm (.010") bond. The results:

| <u>Sheet<br/>Number</u> | <u>Original<br/>Wt. Grams</u> | <u>Bonded<br/>Wt. Grams</u> | <u>Wt.<br/>Grams</u> | <u>Calculated Average Thickness</u> |           |
|-------------------------|-------------------------------|-----------------------------|----------------------|-------------------------------------|-----------|
|                         |                               |                             |                      | <u>Inch</u>                         | <u>MM</u> |
| 1                       | 32.6                          | 40.7                        | 8.1                  | 0.0096"                             | 0.244     |
| 2                       | 29.5                          | 37.8                        | 8.3                  | 0.0098"                             | 0.249     |
| 3                       | 33.1                          | 40.3                        | 7.2                  | 0.0085"                             | 0.215     |
| 4                       | 31.9                          | 40.0                        | 8.1                  | 0.0096"                             | 0.244     |
| 5                       | 31.8                          | 40.7                        | 8.9                  | 0.0105"                             | 0.267     |
| 6                       | 30.2                          | 37.3                        | 7.1                  | 0.0084"                             | 0.213     |
|                         |                               |                             | $\bar{X}$            | 0.0094"                             | 0.239     |

The bondline films were exceptionally uniform, voidless, and with complete coverage. The process was then repeated using PD-200 material having an average initial density of 0.37 gm/cc (23 pcf). The sample size was 102 x 102 x 13 mm (4" x 4" x .50"). The calculated theoretical weight pick-up for a 0.25 mm (0.010") bondline was 3.73 grams. The results were as shown in Table 5-4.

### 5.3.2 SIMULATED AIR FRAME

In this study, the application of PD-200 at 0.27 gm/cc to typical structural surfaces was investigated.

A simulated structure was fabricated (Figure 5-2) and initial application try-outs made. The curvatures on this mock-up are extreme and result in worse-case orbiter application conditions with a conventional protruding head rivet pattern. Photo-documentation was made throughout the study and is included.

The areas addressed during this try-out, included the following:

1. The most practical and reliable application method for in-house and field application.
2. How adequate is the adhesive coverage of the rivet head, and what are the problem areas around the rivets.
3. What vacuum pressure is required to insure positive contact without excessive penetration of the adhesive into the low density foam.
4. What bondline thickness can be achieved utilizing vacuum bag and roller application techniques.

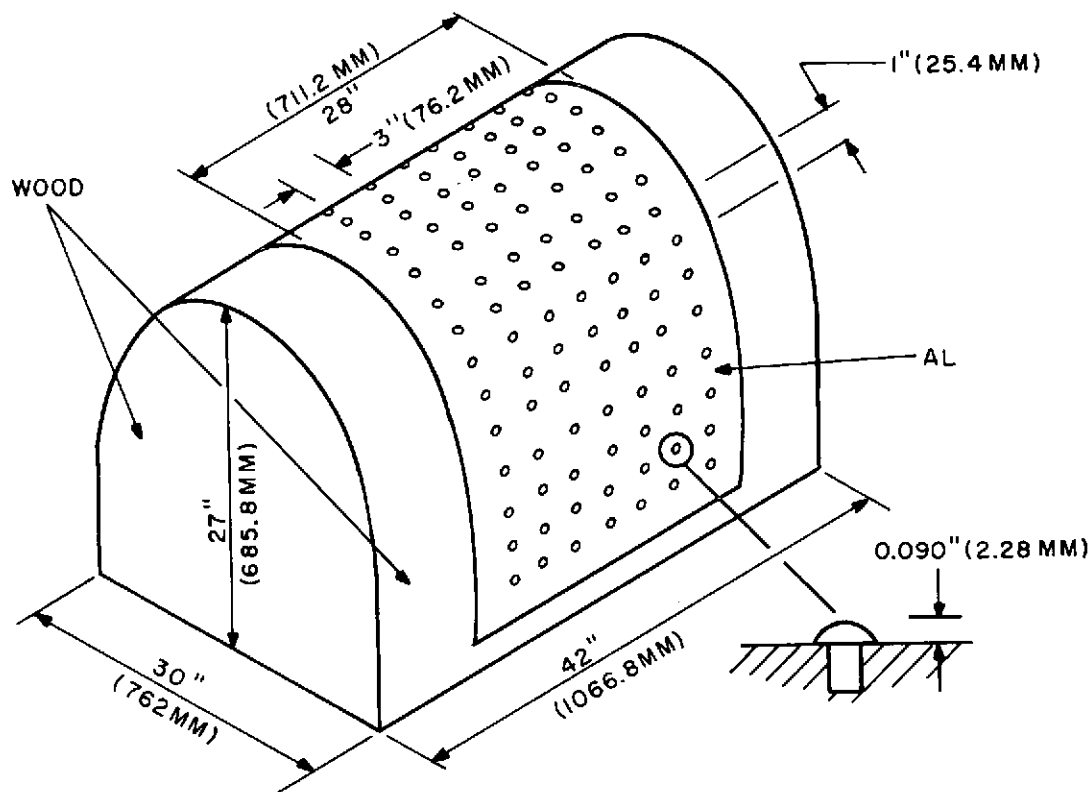


Figure 5-2. Simulated Airframe

#### 5.3.2.1 First Trial Series

In the first trial series, the adhesive was applied directly onto the structure with a metal spatula, then roller to a uniform thickness, staying within the confines of the previously mapped-out area. The vacuum-bag was set in place and a vacuum equivalent to  $34.4 \times 10^3 \text{ N/M}^2$  (5 psi) applied. After an initial cure of 21,600 seconds (6 hours) at room temperature, (catalyst concentration = 1.0%), the assembly was removed and examined.

Results: The bond appeared thin and penetration of the adhesive into the foam was observed. Based on the weight pick-up, the bondline was calculated to be 0.102-0.125 mm (.004"-.005"). The area over the head of each rivet contained numerous air bubbles and/or voids (Figure 5-3).

Conclusions: The positive pressure ( $34.4 \times 10^3 \text{ N/M}^2$ , 5 psi) was too high for this density material (0.27 gm/cc, 17 pcf). The rivet heads appear to be adhesive starved using this approach.

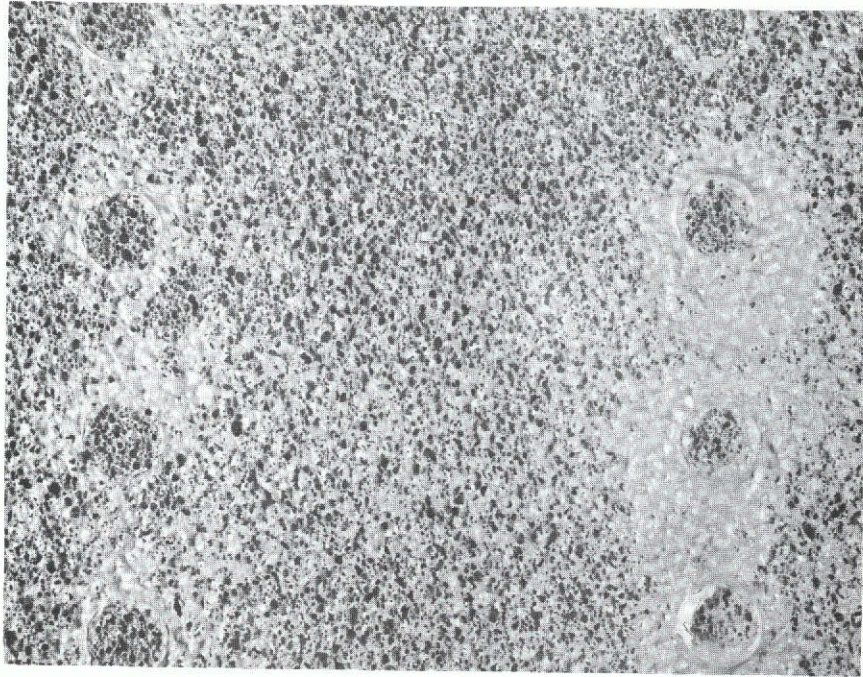
#### Note

The structure was not primed to allow for easy removal of the cured film and to permit bond inspection after cure.

0.2

TABLE 5-4. WEIGHT PICK-UP, PD200 (0.37 GM/CC, 23 PCF)

| Sample Size, MM      | Wt. Grams | Initial Density GM/CC | Bond + PD200 Wt, Grams | $\Delta$ Wt. Gram | $\Delta \rho$ GM/CC | Effective System Density GM/CC | Calc. Film Thickness, MM |
|----------------------|-----------|-----------------------|------------------------|-------------------|---------------------|--------------------------------|--------------------------|
| 101.6 x 101.6 x 12.7 | 48.4      | 0.368                 | 51.7                   | 3.4               | 0.021               | 0.389                          | 0.229                    |
| 101.6 x 101.6 x 12.4 | 47.8      | 0.373                 | 51.2                   | 3.4               | 0.021               | 0.394                          | 0.229                    |
| 101.6 x 101.6 x 13.3 | 50.0      | 0.364                 | 54.5                   | 4.5               | 0.028               | 0.392                          | 0.305                    |
| 101.6 x 101.6 x 13.4 | 50.1      | 0.360                 | 53.5                   | 3.4               | 0.037               | 0.397                          | 0.229                    |



This page is reproduced at the back of the report by a different reproduction method to provide better detail.

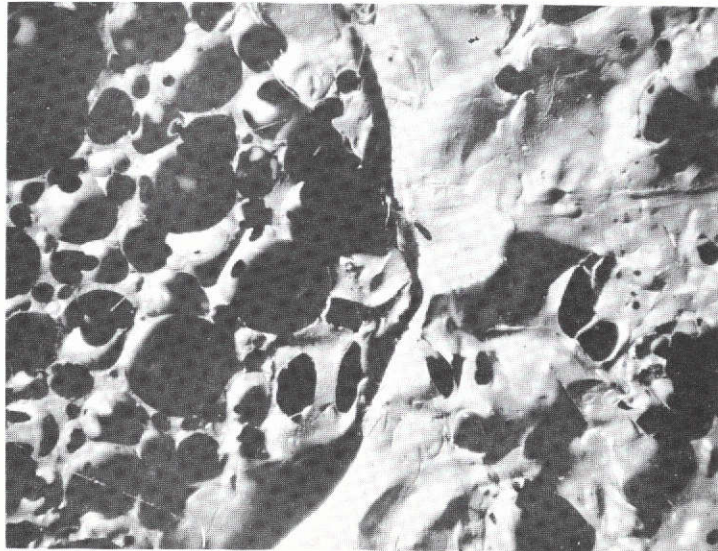


Figure 5-3. Series 1 Rivet Head Bonding

#### 5.3.2.2 Second Trial Bonding Series

Reduced vacuum bag pressures were utilized in the second series. The adhesive was applied as before. The vacuum pressure applied was equivalent to  $20.7 \times 10^3 \text{ N/M}^2$  (3 psi). The cure was 21,600 seconds (6 hours) at R. T. with a catalyst concentration of 1.0%.

Results: The adhesive layer appeared uniform. Based upon the weight pickup calculations, the bondline was calculated to be 0.18 mm (.007"). Again, the rivet heads showed evidence of air bubbles and/or voids (Figure 5-4).

Conclusions: The positive pressure of  $20.7 \times 10^3 \text{ N/M}^2$  (3 psi) appears adequate for this application using 0.27 gm/cc (17 pcf) foam material, however, the rivet heads continue to remain adhesive starved.

#### 5.3.2.3 Third Trial Bonding Series

Experiment series two was repeated with one addition. Additional adhesive was brush coated onto each rivet head prior to the roller application. Vacuum pressure was identical to trial series 2.

Results: Similar, except the evidence of air bubbles and/or voids at the rivets was greatly reduced, and the bondline thickness was calculated to be 0.25 mm (.010") thickness (Figure 5-5).

Repeated trials also exhibited the advantage of additional adhesive application to each rivet head prior to the roller adhesive application to prevent adhesive starvation in the rivet head area.

A positive pressure of  $20.7 \times 10^3 \text{ N/M}^2$  (3 psi) applied by means of a vacuum bag technique has resulted in a bondline thickness of approximately 0.25 mm (0.010 inch) with minimum voids in the rivet area. A positive pressure of  $34.4 \times 10^3 \text{ N/M}^2$  (5 psi) appears to be too high for the low density foam bond (0.27 gm/cc, 17 pcf) and results in excessive penetration of the adhesive into the foam.

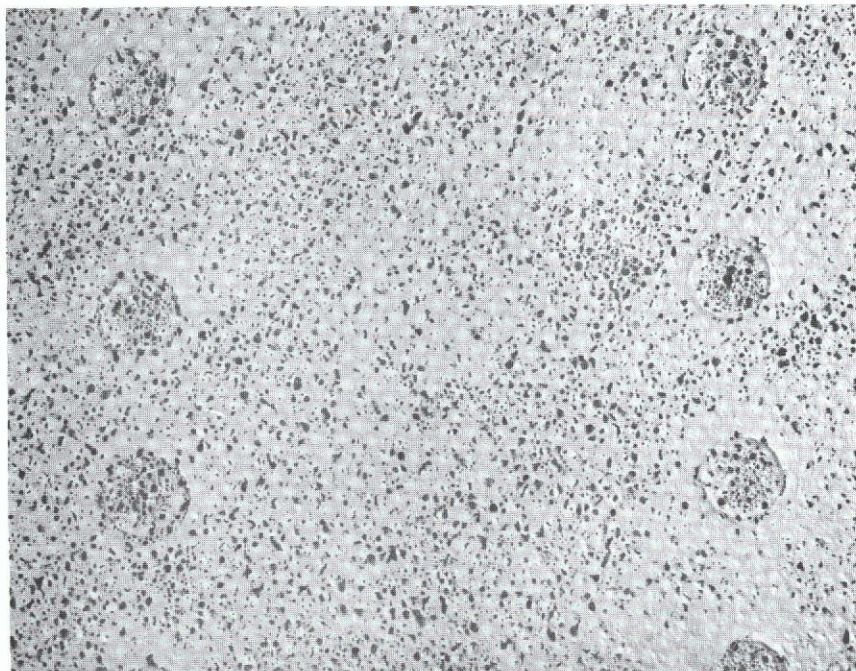
#### 5.3.2.4 Adhesive Application - General Procedure

The catalized RTV-560 (adhesive) is first applied to a clean metal plate with a spatula, and then further spread to uniform thickness (approximately 1.58 mm, 1/16") by means of a paint roller as the adhesive carrier. Once applied to the structure, the adhesive is further spread uniformly until a "texture"\* pattern is observed. At this point the low density PD-200 is draped into position and vacuum bag bonding techniques employed. The vacuum pressure is controlled to permit a positive pressure on the part of  $13.8\text{--}20.7 \times 10^3 \text{ N/M}^2$  (2-3 psi), and the assembly allowed to cure at pressure for 14,400-21,600 seconds (4-6 hours) depending upon the catalyst concentration.

---

\*Experience has shown that the "texture" pattern observed with this adhesive results in a film .18-0.25 mm (.007"- .010") in thickness.





This page is reproduced at the back of the report by a different reproduction method to provide better detail.

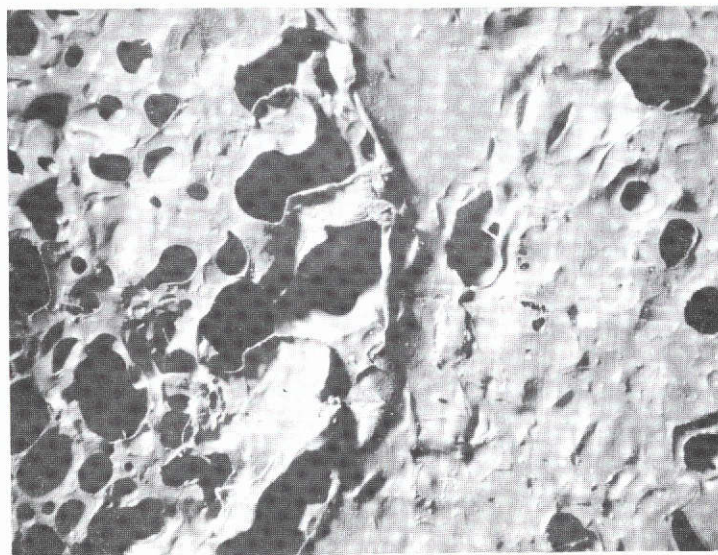


Figure 5-4. Series 2 Rivet Head Bonding





This page is reproduced at the back of the report by a different reproduction method to provide better detail.

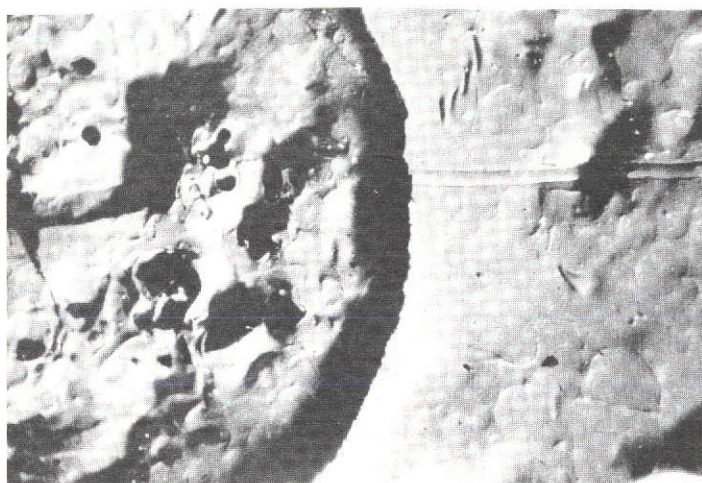


Figure 5-5. Series 3 Rivet Head Bonding



Figures 5-6 through 5-12 show the adhesive application and vacuum bag procedure. A typical REI/PD-200 bonding flow plan is outlined in Figure 5-13.

#### **5.4 SIMULATED SERVICE TESTS**

Several simulated service cycle tests were conducted on REI-Mullite tiles bonded directly to an aluminum structure using PD-200-16 as shown in Figure 5-14. Each RSI tile was 203 x 203 mm (8" x 8") in size, 40.6 mm (1.6 inch) thick for an Area 1 test, and 53.3 mm (2.1 inch) thick for Area 2P testing.

The Area 1 test structure received one thermal cycle to 978°K (1300°F), and a cold soak to 116°K (-250°F) with the imposition of a tensile load in the structure up to limit load of 14,515 Kg (32,000 lb) while the assembly was at 116°K. No failure of the PD 200-16 strain isolator system was evident post-test. The PD 200-16 thickness in this test was 6.4 mm (0.25 inch).

The Area 2P test structure was similar except for the thickness of the tile (53.3 mm as noted above), and 31.8 mm (1.25 inch) of PD 200-16. The test consisted of 1 cycle to 978°K (1300°F) and 10 cycles to 1533°K (2300°F) followed by cold soak and tensile loading. As was the case for Area 1, testing was conducted at 7.6 mm ( $10^{-2}$  atm). No failure of the PD-200-16 was observed in this test.

Additional comprehensive testing has been conducted on NASA contract NAS9-12855 and is fully reported in Reference 5-1.

#### **5.5 REFERENCES**

- 5-1. "Final Report for Design Applications of Rigidized Reusable Surface Insulation Thermal Protection System", March 1973, NAS9-12855 NASA/MSC.

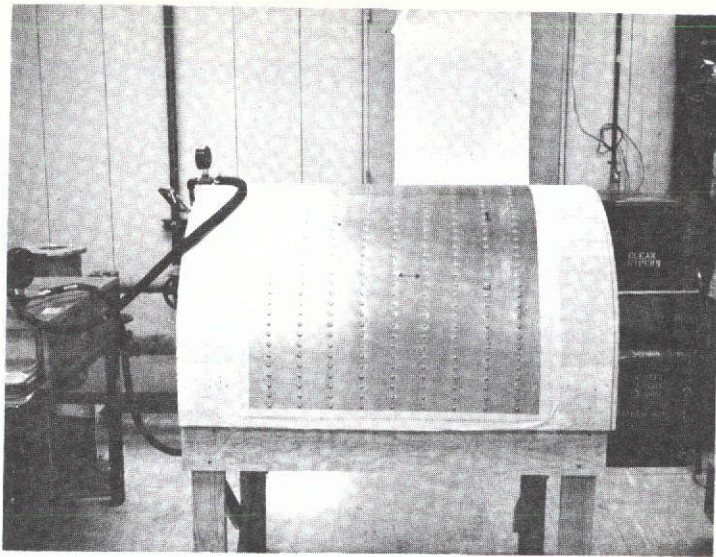


Figure 5-6. Simulated Structure

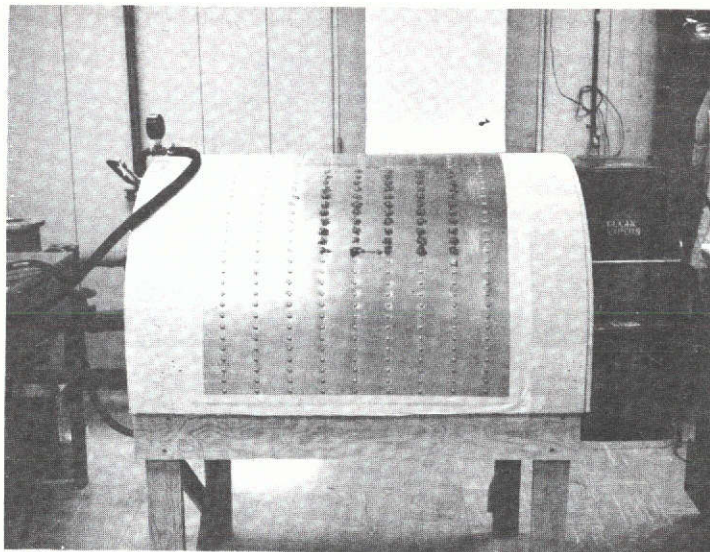


Figure 5-7. Adhesive Application To Rivet Heads

This page is reproduced at the back of the report by a different reproduction method to provide better detail.

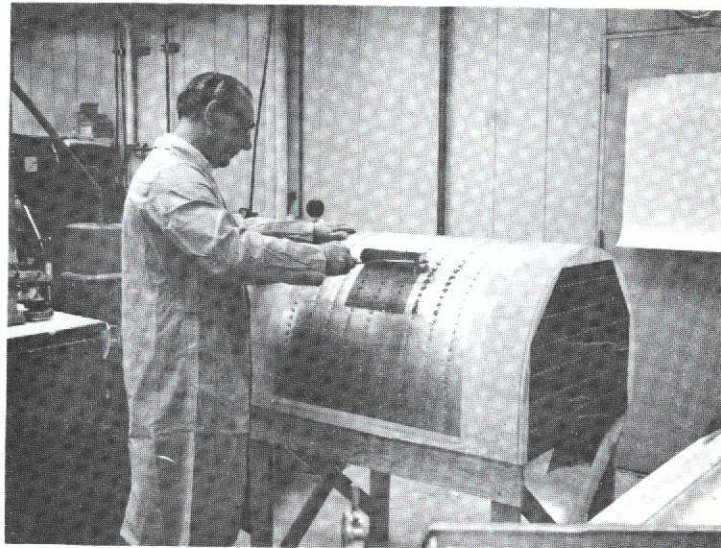


Figure 5-8. Adhesive Application

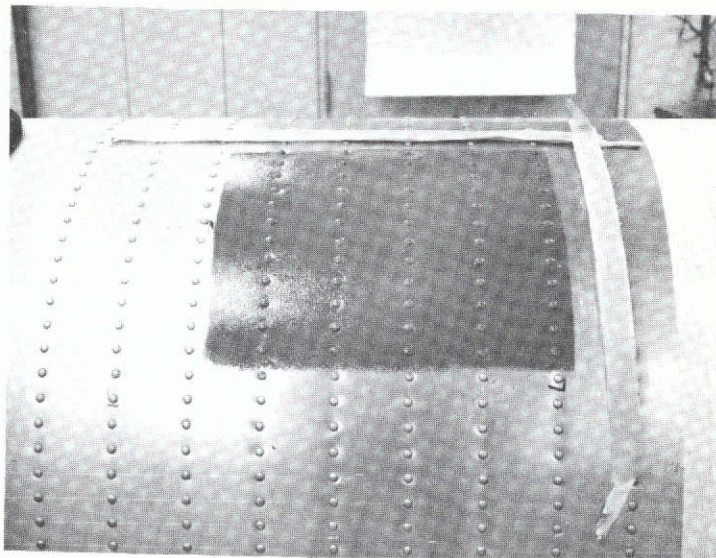


Figure 5-9. Applied Adhesive, Showing "Texture" Finish

This page is reproduced at the back of the report by a different reproduction method to provide better detail.



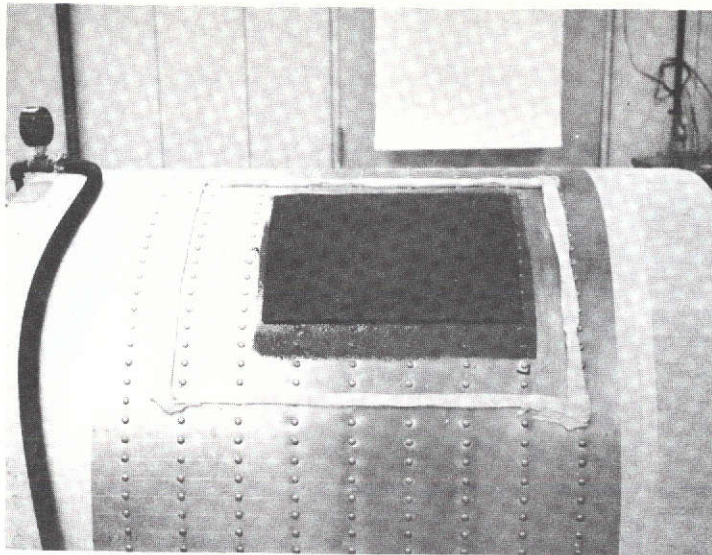


Figure 5-10. PD 200 Foam Applied To Adhesive

This page is reproduced at the back of the report by a different reproduction method to provide better detail.

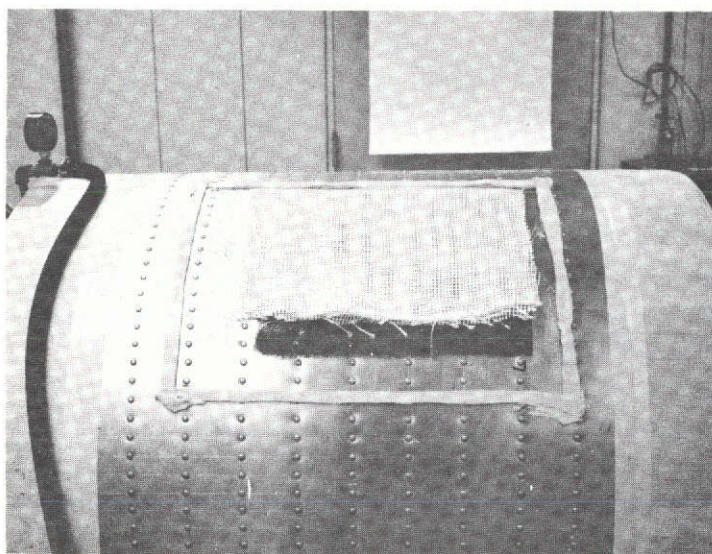


Figure 5-11. Application Of Vacuum "Bleeder" Material



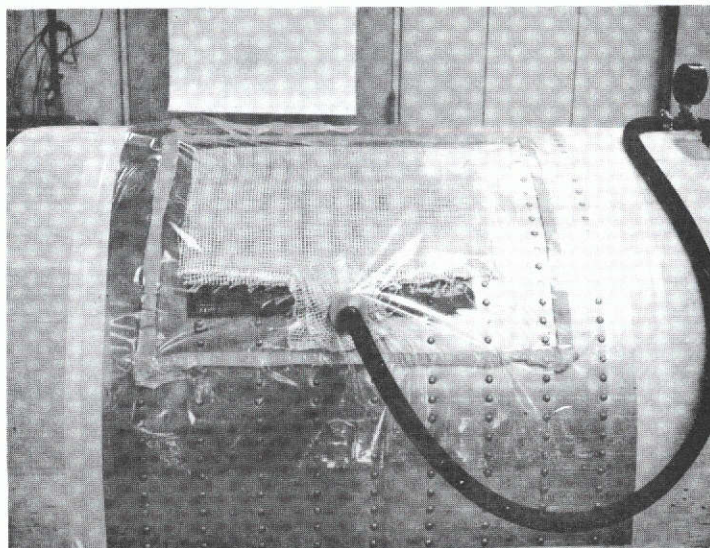


Figure 5-12. Completed Vacuum Bag Assembly

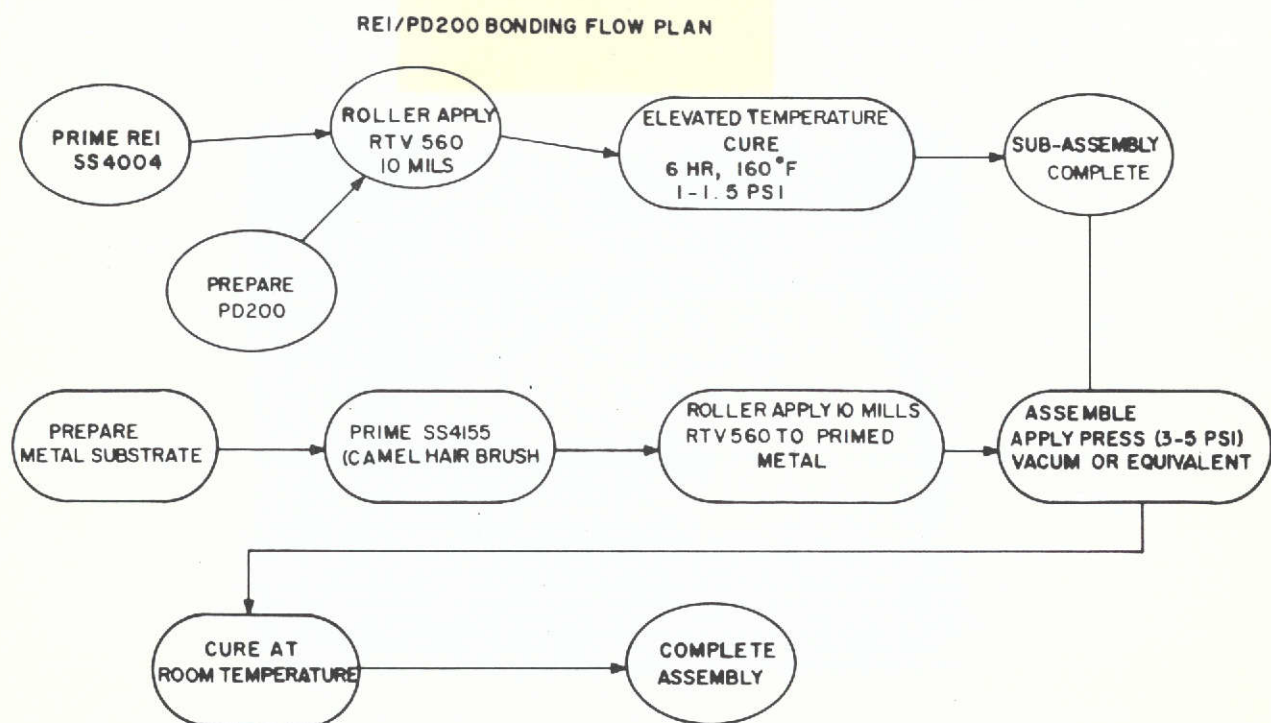


Figure 5-13. REI/PD 200 Bonding Flow Plan

This page is reproduced at the back of the report by a different reproduction method to provide better detail.

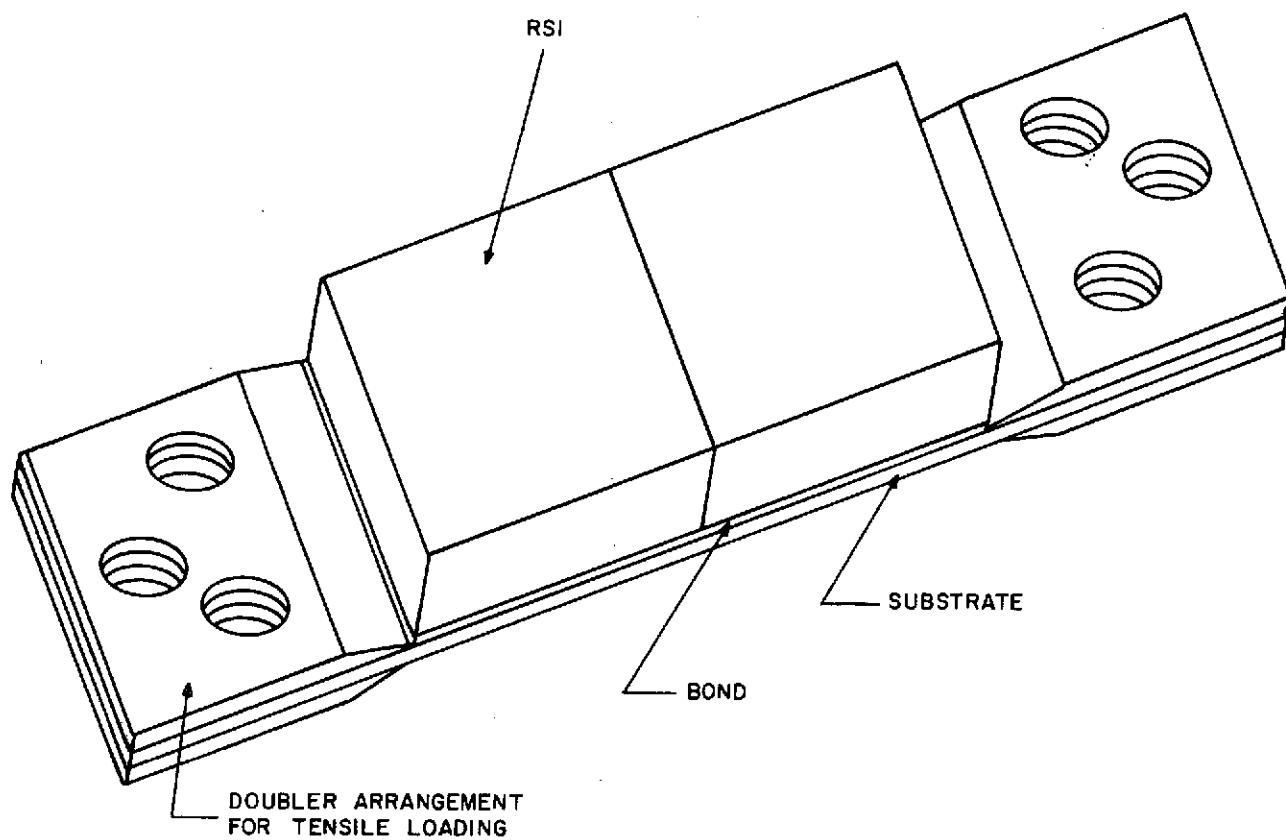


Figure 5-14. RSI Tensile Test Model

## APPENDIX A1

### PD 200 (BASE)

PD-200 (Base) has been characterized by GE-RES-D for use as an adhesive for re-entry vehicle application. It has also been used extensively in the production of GE Elastomeric Shield Materials (ESM).

It has excellent low temperature (155°K, -180°F) flexural properties and high thermal stability. The ultimate strength of PD-200 (Base) as a function of temperature is shown in Figure A1-1. Tensile and shear moduli values as a function of temperature are shown in Figure A1-2 where it is seen that the modulus is relatively constant over a temperature range from 255 to 478°K (0 to +400°F).

Below 172°K (-150°F), the modulus increases rapidly to the glass transition temperature of approximately 155°K (-180°F). The thermal stability of the cured elastomer is shown by the thermogravimetric analysis curve of Figure A1-3. It is seen that PD-200 (Base) does not begin to lose weight at a significant rate until around 867°K (1100°F); and is quite stable at 589-616°K (600 to 650°F), the maximum bondline temperature for a titanium structure.

The thermal expansion  $\Delta L/L_0$  is  $150 \times 10^{-6} \text{ } ^\circ\text{K}^{-1}$  from 200°K to 589°K (-100°F to 600°F). Its specific heat is 1.67 Joule/gm°K (0.4 Btu/lb°F) from 200°K to 589°K (-100°F to 600°F). The thermal conductivity is shown in Figure A1-4.

Long term stability of the material at 589°K (600°F) has been demonstrated under the SNAP-27 program where greater than  $13.8 \times 10^5 \text{ N/m}^2$  (200 psi) tensile shear strength was exhibited at 625°K (665°F) on specimens aged for 1341 hours (eight weeks) at 589°K (600°F).

Cure in deep sections has been achieved by strip bonding, i.e., by leaving gaps in the bond for air entry and volatiles removal. Removal of volatiles, however, has not been a problem in the bonding of porous, low density insulation materials.



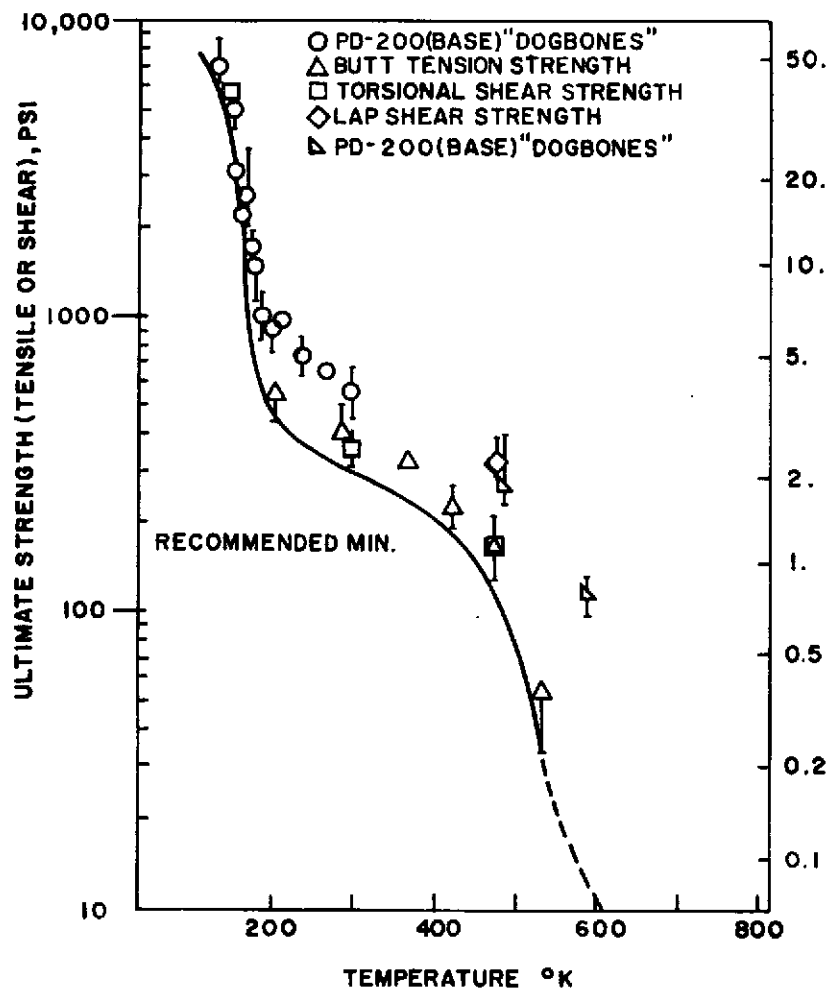


Figure A1-1. Ultimate Strength of PD-200 (Base)

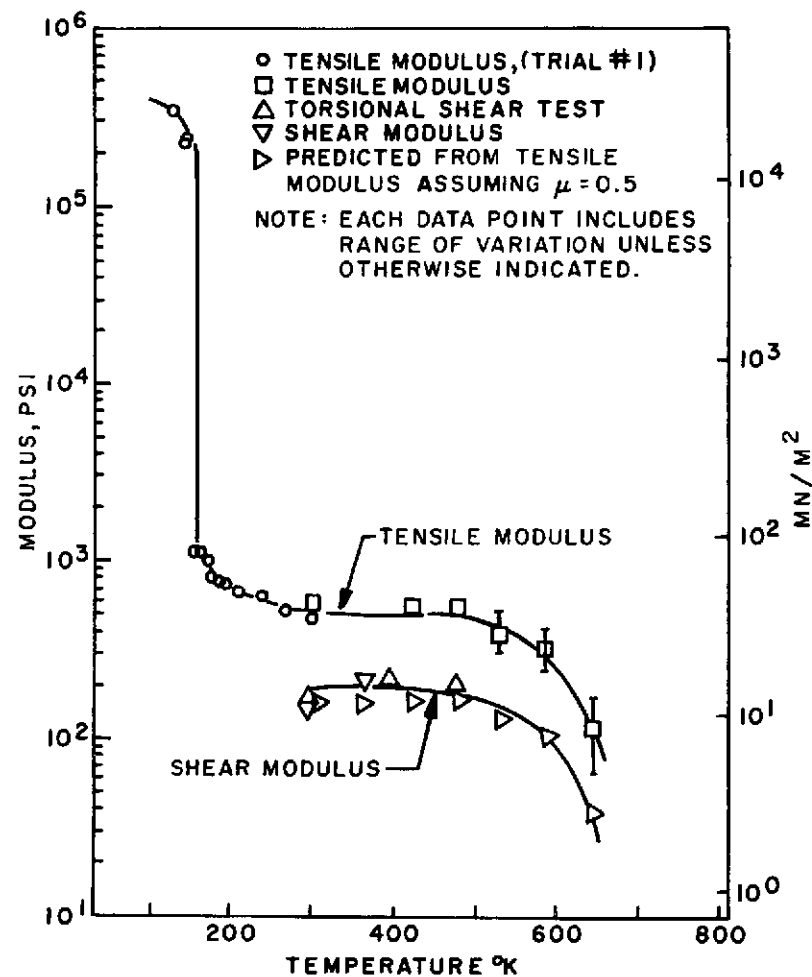


Figure A1-2. Elastic Moduli of PD-200 (Base)

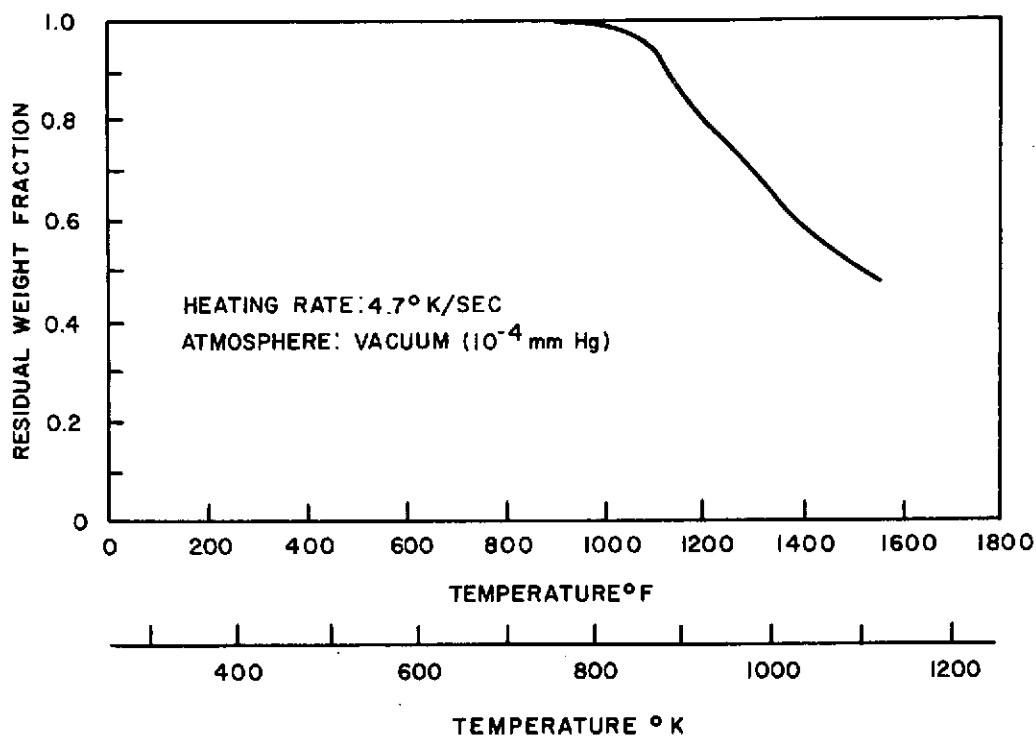


Figure A1-3. TGA Analysis of PD-200 (Base)

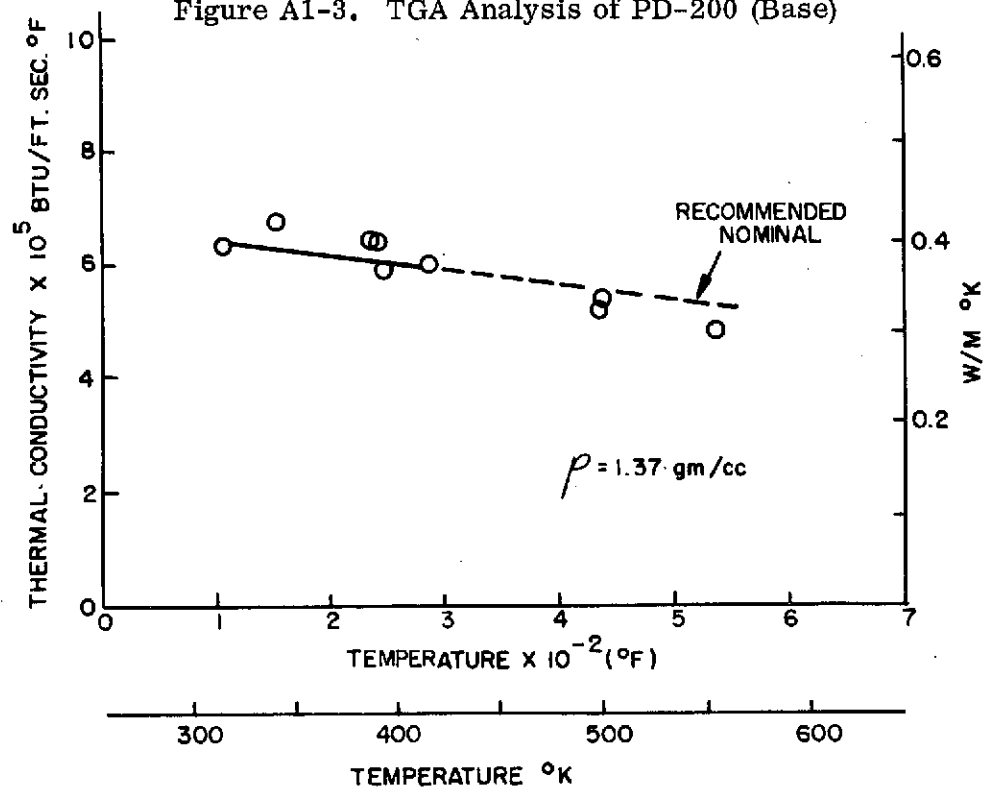


Figure A1-4. Thermal Conductivity of PD-200 (Base)

## APPENDIX A2

### PD 200 FOAM

PD-200 has been characterized by GE-RESO for use as a strain isolation foam system for space shuttle environment application. Its low temperature flexibility and high temperature stability are similar to the PD-200 (Base). Typical tensile and shear properties of PD-200 as a function of temperature before and after cycling are shown in Figures A2-1 and A2-2. The tensile and shear moduli values as a function of temperature are shown in Figures A2-3 and A2-4. The low temperature modulus data is shown in Figure A2-5. The thermal stability of the cured foam is indicated by the thermogravimetric (TGA) analysis curve of Figure A2-6.

The specific heat of PD-200 is shown in Figure A2-7, the thermal conductivity is shown in Figure A2-8, and the thermal expansion data is shown in Figure A2-9. Elevated temperature stability of the PD-200 foam has been demonstrated, and is indicated by the data presented in Table A2-1. As indicated in A1, the long term stability of the base material has been demonstrated in the SNAP-27 Program.

In contrast to PD-200 (Base) where cure in deep section requires the strip bonding approach, bonding of the PD-200 foam has not been a problem due to its porous nature, which allows removal of volatiles during the cure cycle.

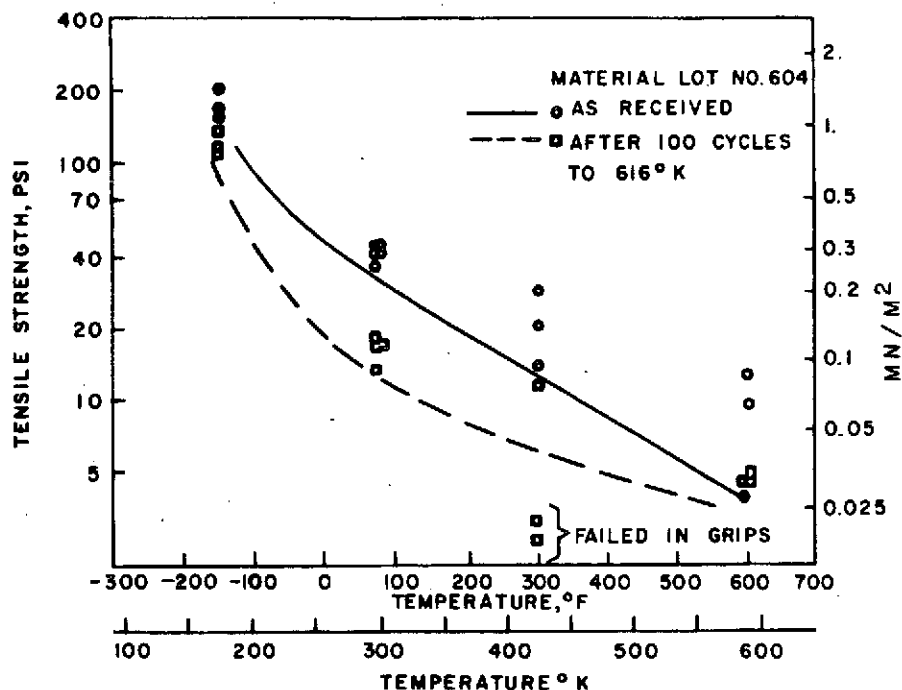


Figure A2-1. Tensile Strength of PD-200

Preceding page blank

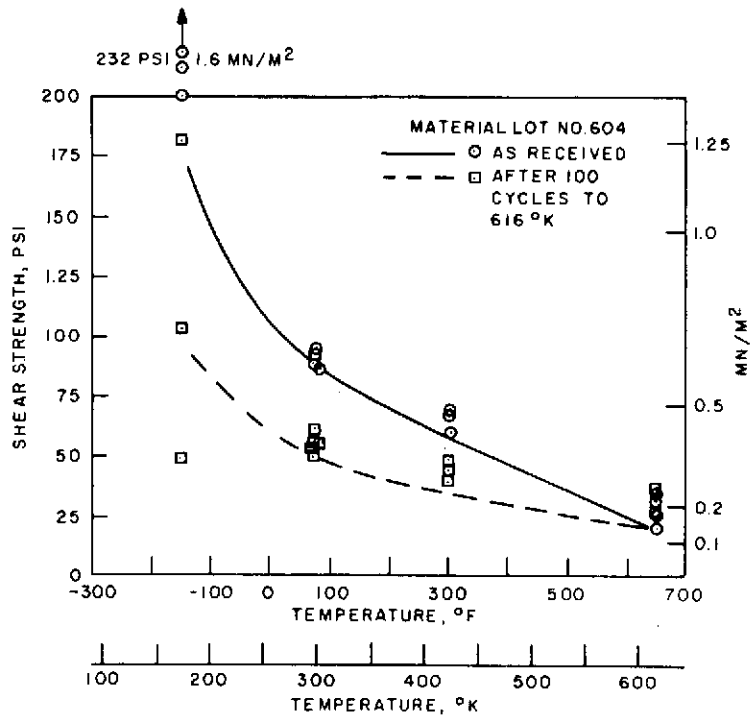


Figure A2-2. Shear Strength of PD-200

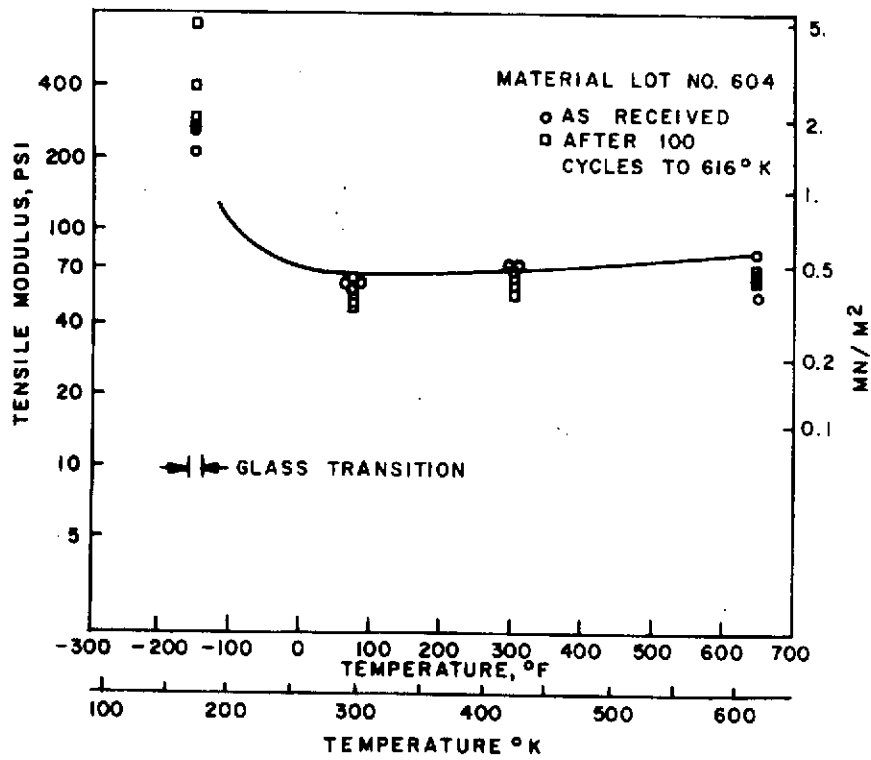


Figure A2-3. Tensile Modulus of PD-200

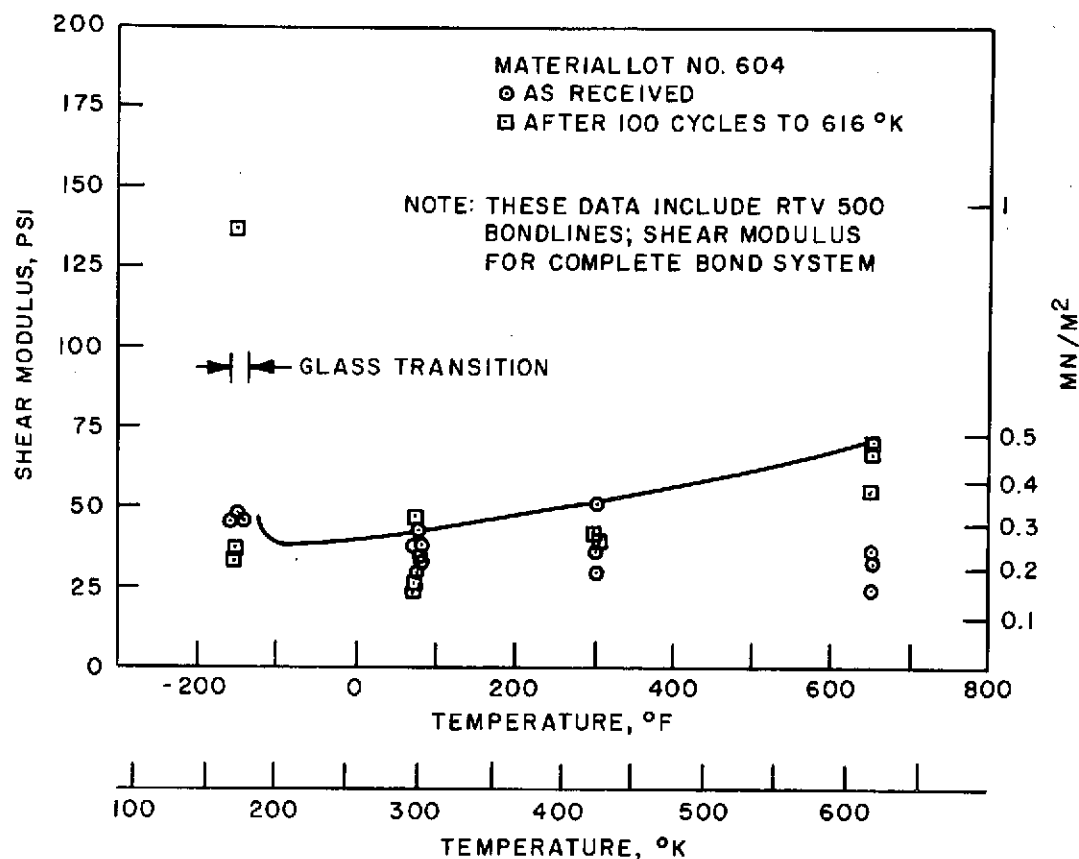


Figure A2-4. Shear Modulus of PD-200

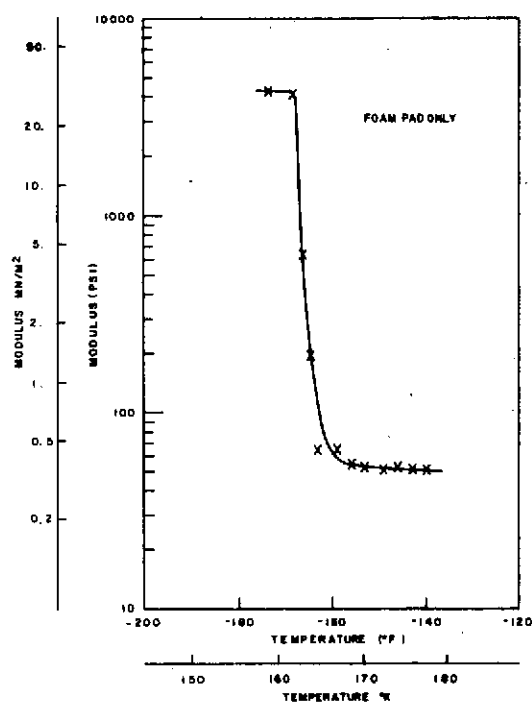


Figure A2-5. Low Temperature Modulus of PD-200

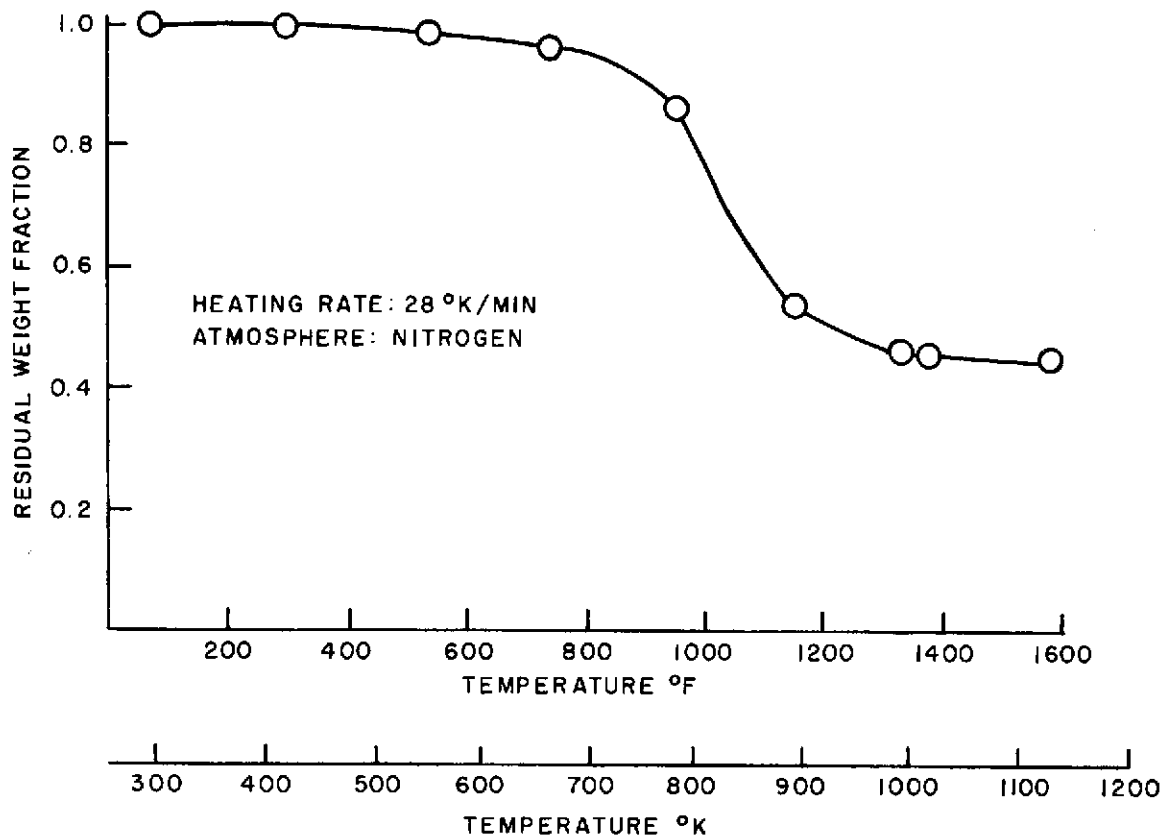


Figure A2-6. TGA of PD-200

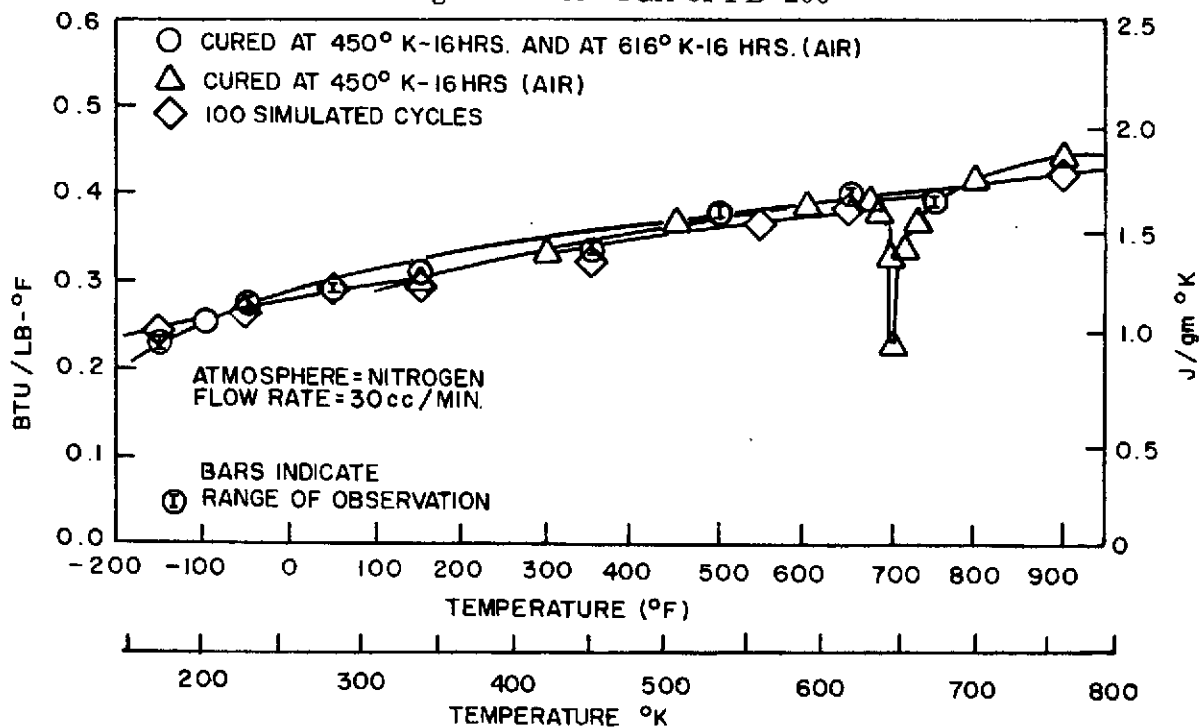


Figure A2-7. Specific Heat of PD-200

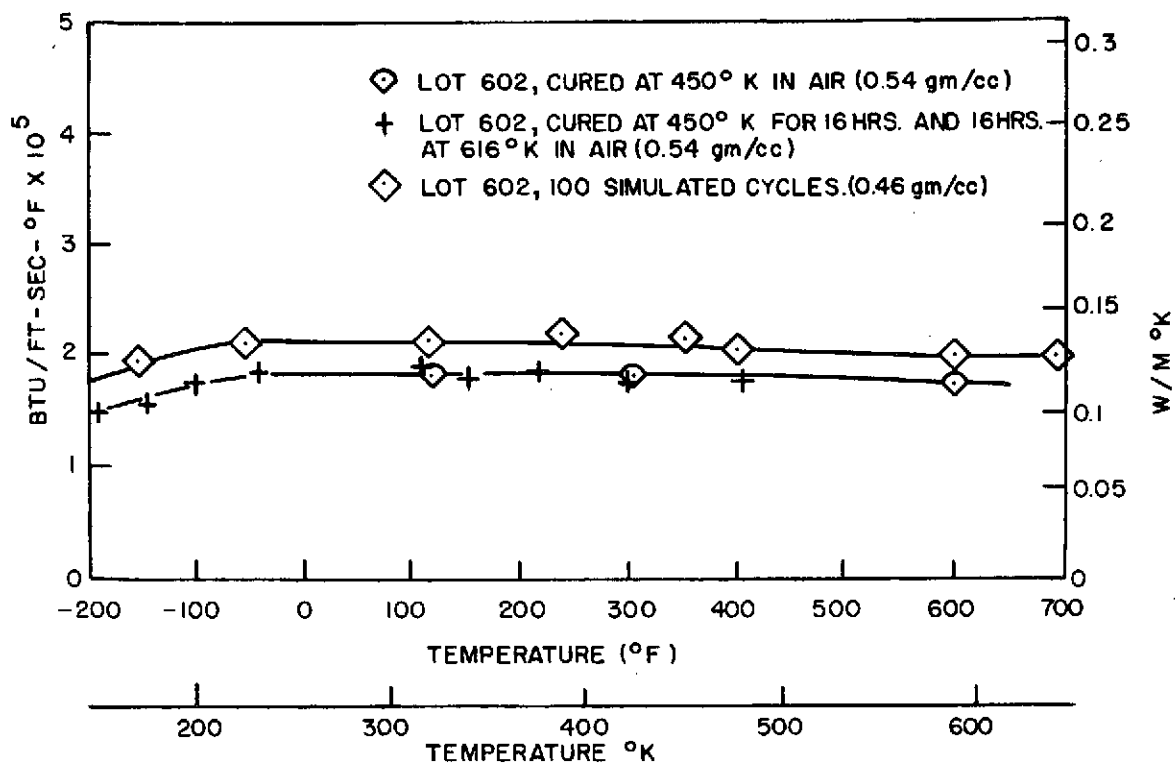


Figure A2-8. Thermal Conductivity of PD-200

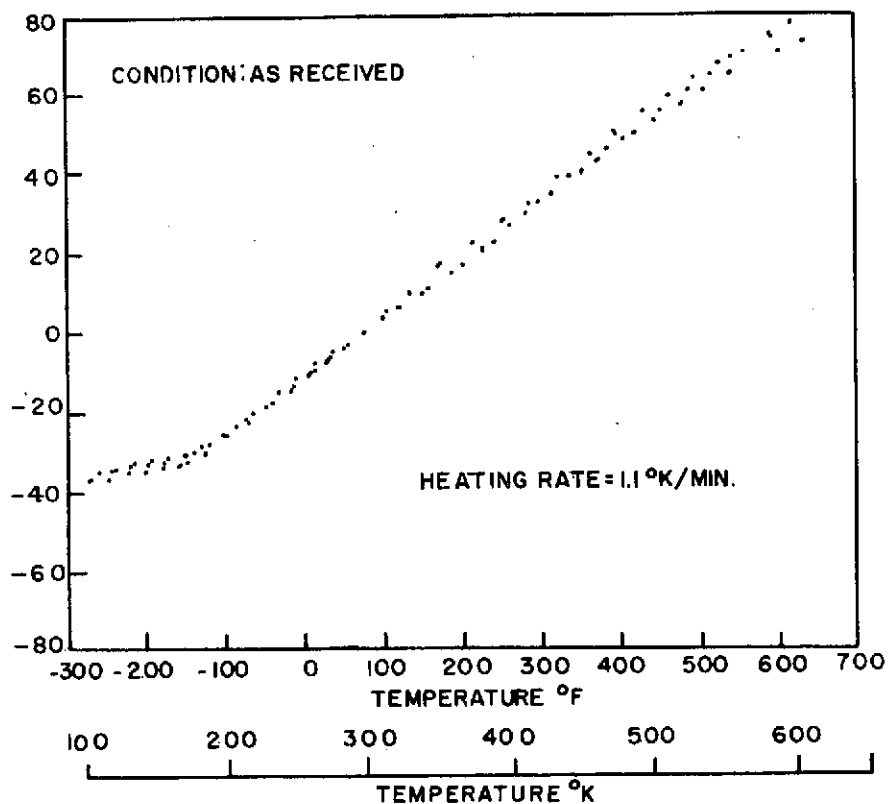


Figure A2-9. Thermal Expansion of PD-200

TABLE A2-1

## ROOM TEMPERATURE LAP SHEAR STRENGTH OF PD-200 ADHESIVE

AFTER 16 HOUR THERMAL SOAK EXPOSURES

(STRENGTH X  $10^3$  N/M<sup>2</sup>)

| Test Number  | Exposure Temperature °K |               |               |               |
|--------------|-------------------------|---------------|---------------|---------------|
|              | 297                     | 505           | 561           | 603           |
| 1            | 651.6                   | 462.6         | 339.9         | 232.4         |
| 2            | 574.3                   | 404.0         | 319.2         | 215.8         |
| 3            | 569.5                   | 482.6         | 362.0         | 219.2         |
| 4            | 580.5                   | 437.8         | 388.9         | 220.6         |
| 5            | 573.6                   | 428.8         | 288.2         | 224.8         |
| $\bar{X}$    | 590.2                   | 443.3         | 339.9         | 222.7         |
| S.D.         | 34.5                    | 30.3          | 38.6          | 6.2           |
| Failure Mode | All Cohensive           | All Cohensive | All Cohensive | All Cohensive |

Specimens: 25.4 x 25.4 mm lap joint  
 1.6 mm aluminum adherends  
 2.3 mm thick PD-200  
 RTV 560 bond ~.12 mm thick (both sides)



## APPENDIX A3

### REI-SILICA 9

REI-Silica 9 is a silica rigidized, near-random fiber insulative composite material with a nominal density of 0.14 gm/cc (9 pcf). It was developed for thermal protection of the Space Shuttle Orbiter. To maximize the reproducibility of properties and phase stability of the material, the Johns-Manville Code 108 high purity Microquartz<sup>®</sup> fibers are cleaned in a hydrochloric acid bath prior to composite fabrication. This bath, which removes surface contaminants from the fibers, has been shown to reduce the high temperature shrinkage and devitrification rates of both the fibers and rigidized composites (Ref. A3.1). The washed fibers are next dried and fired to 1367°K (2000°F) to increase their density and to stabilize them. This need for stabilization is caused by the extremely high surface free energy and low density of the Johns-Manville leached fibers.

Microquartz<sup>®</sup> fibers, because of their polar surface characteristics, can absorb up to 11 weight percent water, which is tightly bound to the fiber surfaces. This sheath of water, up to 300 molecules thick (Ref. A3.2), hinders adhesion of the rigidization agent during processing. To maximize wetting of the fiber by the silicone resin binder, the fibers are subjected to a gaseous phase treatment in which the water layer on the fibers is reacted with a halogenated silane. This reaction replaces the water with a high molecular weight polysiloxane coating that is chemically bound to the fiber surface and is chemically similar to the binder system.

The fibers are next slurried in a dilute trifunctional silicone resin/solvent solution. The mixed viscous slurry is then molded to a nominal fiber density of 0.12 gm/cc (7.2 pcf), the solvent removed by drying and the resin cured to 478°K (400°F).

The cured uncoated tiles are then thermally treated to pyrolyze the resin and achieve composite rigidization. This is followed with a firing cycle which results in sintering of the fiber/binder system and achievement of the required level of mechanical properties and density.

GE-RESID studies have shown that the silicone resin fabrication technique is superior to other binder systems, such as colloidal silica. This superiority results from surface energy effects which cause the organic binder solution to wet and coat the fiber surfaces as well as concentrating at fiber intersections. Thus, after resin pyrolysis and firing, the silica fibers are coated with an even higher purity silica sheath as well as being assembled in strong, but flexible truss networks. In fact, this approach provides the potential of maximizing structural margins-of-safety (from strength standpoint) and minimize TPS weights (minimized thermal conductivity). The high purity silica layer or sheath results in reduced crystallization rates

because devitrification is a surface nucleation phenomenon (Ref. A3.3). This later characteristic, in particular, offers the potential for helping to overcome the lot-to-lot variation in chemical purity of the Johns-Manville Microquartz® fibers.

#### References

- A3.1 H. E. Goldstein, M. Smith, D. Leiser, V. Katula, D. Stewart, "Silica Reuseable Surface Insulation Improvement Research", Presented at the NASA Ames Research Center Space Shuttle Symposium, November 1972.
- A3.2 R. C. Thuss, H. G. Thibault, and A. Hiltz, "The Utilization of Silica Based Surface Insulation for the Space Shuttle Thermal Protection System", presented at the National SAMPE Space Shuttle Material Conference, October 5-7, 1971.
- A3.3 W. Eitel, "The Physical Chemistry of the Silicates", University of Chicago Press, Chicago, Ill., 1954.